

AN INVESTIGATION OF POSSIBLE PHYTOPLANKTON SEEDING IN THE
STRAIT OF GEORGIA FROM NANOOSE BAY

By

Debby Ianson

B.Sc.E. Physics, Queens University, 1991

A THESIS SUBMITTED IN PARTIAL FULFILLMENT OF
THE REQUIREMENTS FOR THE DEGREE OF
MASTER OF SCIENCE

in

THE FACULTY OF GRADUATE STUDIES
DEPARTMENT OF PHYSICS
DEPARTMENT OF OCEANOGRAPHY

We accept this thesis as conforming
to the required standard

THE UNIVERSITY OF BRITISH COLUMBIA

January 1994

© Debby Ianson, 1994

In presenting this thesis in partial fulfilment of the requirements for an advanced degree at the University of British Columbia, I agree that the Library shall make it freely available for reference and study. I further agree that permission for extensive copying of this thesis for scholarly purposes may be granted by the head of my department or by his or her representatives. It is understood that copying or publication of this thesis for financial gain shall not be allowed without my written permission.

(Signature)

Department of Physics

The University of British Columbia
Vancouver, Canada

Date Jan 13 1994

Abstract

This thesis investigates the possibility of bays providing the seed population for the spring phytoplankton bloom to larger adjacent bodies of water via advective transport. The study area was Nanoose Bay, Vancouver Island and the adjacent region of the Strait of Georgia. In 1992 and 1993 data were collected 2-3 times weekly and a mooring with an array of 5 current meters was placed at the mouth of the bay during the 1992 study. Interannual variability was tremendous.

In 1992 seeding from Nanoose Bay was not possible as the net transport was into the bay at the surface and middle depths. The influence of the Fraser River seemed to dominate as low density water with high silicate concentrations was present at the surface and density profiles were generally well stratified. Although nutrients were not limiting and light availability appeared high, phytoplankton concentrations were low until March 5 when they began to increase and a bloom occurred. It is suggested that horizontal advection and flushing of the bay were responsible for suppressing a bloom prior to March 5 in 1992.

In 1993 phytoplankton concentrations were high inside the bay from the beginning of February onward. In the Strait no periods of high phytoplankton concentration occurred although there were two small increases which appear to be due to advective transport, although it is possible that the first was due to reduced wind mixing. It is suggested that seeding of the Strait from Nanoose Bay was possible in this year, although it is also possible that seeding occurred from other locations depending on time and conditions. The conservation equation for a scalar was used to investigate advective transport as balanced by biological sources and sinks. With no current measurements available in

1993, estimates were made from the above equation and compared to wind direction in the Strait and density changes at the mouth of the bay. In 1993 profiles were well mixed with respect to 1992 and overall salinity was higher. It is suggested that light was usually limiting to phytoplankton growth in the Strait due to vertical mixing throughout the study, while in the bay the depth of the water column limited vertical mixing thus allowing phytoplankton to bloom.

To continue experiments of this type it is suggested that daily sampling be done as temporal changes can occur quickly. As evidenced from the 1993 data, spatial resolution is also valuable. Current measurements are necessary and their absence in the 1993 data set was unfortunate. It is suggested that drogues may be useful for measuring currents. They could be used to attempt to track phytoplankton when concentrations begin to increase.

Table of Contents

Abstract	ii
List of Tables	vii
List of Figures	viii
Acknowledgements	x
1 Introduction	1
1.1 Introduction	1
1.1.1 Spring Bloom Dynamics	1
1.1.2 Seeding	1
1.2 Thesis Objectives	2
1.3 Sverdrup Critical Depth Theory	3
1.3.1 Critical Depth	4
1.4 Stratification and Mixing	5
1.4.1 Depth of the top layer	5
1.4.2 Mixing	7
1.5 Advection and Diffusion	8
1.5.1 Physical Forcing	10
1.6 Phytoplankton Ecology	11
1.6.1 Diatoms and Flagellates	12
1.6.2 Sources	13

1.6.3	Sinks	13
2	The Experiment	15
2.1	Nanoose Bay	15
2.2	Design	16
2.2.1	Sampling Timing and Locations	16
2.2.2	Sampling	18
2.2.3	Current and Wind	20
3	Results and Analysis	23
3.1	Current and Wind	23
3.1.1	Processing	24
3.1.2	Wind correlations between lighthouses and the mouth of Nanoose bay	33
3.1.3	Relationship between wind and current residuals	35
3.1.4	Advective exchange between Nanoose bay and the Strait of Georgia	41
3.1.5	Flushing and stability	43
3.1.6	Density changes and current direction	46
3.2	Density profiles	49
3.2.1	Mixed Depth	50
3.2.2	Density Gradients and Velocity Shear	51
3.2.3	Temporal changes	54
3.3	Critical Depth	59
3.3.1	Radiation data	59
3.3.2	Secchi disc depth and critical depth	60
3.4	Chlorophyll <i>a</i>	66
3.5	Species Composition	66

3.6	Nutrients	75
4	Discussion	83
4.1	Limitations to phytoplankton growth during the onset of the spring bloom	83
4.1.1	1992	84
4.1.2	1993	88
4.2	Seeding by advection	92
4.2.1	1992	93
4.2.2	1993	93
4.3	Summary	100
4.4	Suggestions for improving or continuing this experiment	101
Appendix A	Dominant genera in species composition	102
Bibliography		105

List of Tables

3.1	Tidal constituents used in the harmonic analysis.	29
3.2	Amplitudes (cm/s) of the stronger tidal constituents of the u current. . .	29
3.3	Maximum wind cross-correlations.	35
3.4	Angles for principal axis rotations for 1992 current and wind data. . . .	38
3.5	Maximum wind and current cross-correlations.	39
3.6	Velocity shear necessary for turbulence	54
4.1	Phytoplankton growth parameters determined from CTD profiles for NAN	
10.	86
A.1	Dominant genera with abundance for 1992.	103
A.2	Dominant genera with abundance for 1993.	104

List of Figures

2.1	Nanoose bay and the Strait of Georgia with locations of all sampling stations	17
3.1	Processed u current time series at NAN 20, 1992.	25
3.2	Processed v current time series at NAN 20, 1992.	26
3.3	Processed σ_t (kg/m^3) time series at NAN 20, 1992.	27
3.4	Filtered residual u current time series at NAN 20, 1992.	31
3.5	Filtered residual v current time series at NAN 20, 1992.	32
3.6	Wind time series for Ballenas Island lighthouse and Nanoose bay mooring.	34
3.7	Time series of the principal component of the wind for Ballenas Island lighthouse and 2 m currents.	40
3.8	Net transport plotted as a running integral with time.	42
3.9	A phytoplankton flushing index, $\frac{1}{t_2-t_1} \int_{t_1}^{t_2} u(t)dt$, as a function of t_1 for each depth.	45
3.10	Filtered σ_t (kg/m^3) time series shown with the flushing index at each depth.	47
3.11	σ_{t7} (kg/m^3), at NAN 20 from the mooring and CTD profiles.	48
3.12	Representative density profiles at NAN 10.	52
3.13	Density structure time series: for two favourable intervals.	57
3.14	Density structure time series: for two unfavourable intervals.	58
3.15	I_o and PAR as functions of time.	60
3.16	Secchi disc depth as a function of time for NAN 10, 20 and 30 in 1992. .	61
3.17	Secchi disc depth as a function of time for inside stations in 1993. . . .	62
3.18	Secchi disc depth as a function of time for outside stations in 1993. . . .	63

3.19	Critical depth as a function of time for NAN 10 and 30.	65
3.20	Chlorophylla as a function of time in 1992.	67
3.21	Chlorophylla as a function of time for the inside stations in 1993.	68
3.22	Chlorophylla as a function of time for the outside stations in 1993.	69
3.23	<i>Skeletonema costatum</i> , <i>Chaetoceros</i> spp. and <i>Thalassiosira</i> spp. counts for 1992.	70
3.24	<i>Skeletonema costatum</i> , <i>Chaetoceros</i> spp. and <i>Thalassiosira</i> spp. counts for 1992 before the onset of the spring bloom.	71
3.25	<i>Chaetoceros debilis</i> counts for 1993, inside stations.	72
3.26	<i>Chaetoceros debilis</i> counts for 1993, outside stations.	73
3.27	<i>Skeletonema costatum</i> and <i>Chaetoceros debilis</i> counts for 1993, NAN 10 and 30.	74
3.28	Time series of nitrate in 1992 for NAN 10, 20 and 30.	77
3.29	Time series of silicate in 1992 for NAN 10, 20 and 30.	78
3.30	Time series of nitrate concentrations in 1993, inside stations.	79
3.31	Time series of nitrate concentrations in 1993, outside stations.	80
3.32	Time series of phosphate concentrations in 1993, inside stations.	81
3.33	Time series of phosphate concentrations in 1993, outside stations.	82
4.1	1992 time series of phytoplankton concentration and factors possibly lim- iting its growth for stations NAN 10 and NAN 30.	85
4.2	1993 time series of phytoplankton concentration and factors possibly lim- iting its growth for stations NAN 10 and NAN 30.	90

Acknowledgements

Dr. Stephen Pond's name should be emblazoned on this page in large bold letters. I acknowledge not only the experimental expertise and solid academic guidance, but especially the enthusiasm and immense support that Dr. Pond has given me.

I acknowledge Dr. Paul LeBlond and Dr. Tim Parsons for their support and guidance. Thank-you Dr. Parsons for the idea behind this experiment and for introducing me to an entirely new world outside of physics.

I would like to thank Dr. Paul Harrison for the discussions of biological aspects during the preparation of this thesis.

I am of course also grateful for the financial support from Dr. Pond's NSERC grant and teaching assistantships in the Department of Physics.

Thanks to the officers and the crew of the *C.S.S. Vector* for their assistance with the mooring work.

I would like to acknowledge the personnel at C.F.B. Nanoose Bay for their excellent sampling work and for welcoming me on their base.

Thanks to Dr. Richard Thompson and I.O.S. for making the 1993 experiment possible by providing a boat.

I carry many fond memories of the field work. Thank-you Hugh MacLean, Heinz Heckl, Jonathan Nash and David Timothy for your excellent assistance and company. Special thanks to Heinz for teaching me how to properly tie knots.

I do not know where to begin in thanking those in the department who have helped me with all aspects of my work. I did manage to spread out and pester most labs in the department during this experiment. I thank you all in random order, Catriona, Rowan,

Victor, John, Kedong, Peter, Scott, Roger, Renee, Denis, Roy, Joe, and David.

I can not complete the acknowledgements without a very sentimental mention of my mom and my dad who seem implicitly involved. Relaxing did make it all possible.

Chapter 1

Introduction

1.1 Introduction

1.1.1 Spring Bloom Dynamics

Primary productivity is defined as the change in phytoplankton biomass per time (Parsons, Takahashi and Hargrave [22]). A large net increase in primary productivity constitutes a phytoplankton bloom.

Phytoplankton require light and nutrients to survive. The depth over which they are vertically mixed depends on the stratification of the water column and the forcing. During the winter, mixing is at a maximum due to strong winds and low fresh water input. Light is at a minimum. As a result phytoplankton travel deeper than the range where they receive enough light so that, on average, their respiration demands are exceeded by their photosynthetic production. At this time nutrients that have been mixed upward are abundant and not limiting to phytoplankton growth. Light availability increases and mixing decreases as spring approaches. When phytoplankton receive enough light averaged over their vertical journey in the water column they are able to utilize the rich nutrient supply. At this time the spring bloom occurs.

1.1.2 Seeding

There are two main ways in which a phytoplankton bloom can be seeded. It can be seeded *in situ* by phytoplankton present at that location or advectively by phytoplankton carried

from elsewhere. Advective transport occurs through wind-driven currents, tidal currents and density driven circulation. These influences also control mixing.

In a coastal situation some interesting possibilities exist. The depth of the water column can limit the depth to which phytoplankton are mixed. If an area is mixed to the bottom and the critical depth of light penetration (defined below) reaches this depth a bloom can occur simply because the water column is shallow enough. In deeper areas the vertical mixing may be greater (i.e. below the critical depth) and a bloom would not occur.

Some areas may also be more sheltered by topography or more stratified due to terrigenous fresh water input. Both cases would serve to reduce vertical mixing and therefore allow a bloom to occur earlier.

Thus both, mixing to a shallow bottom or limited mixing, should provide potential seeding areas for offshore waters. It is however also possible that flushing of a potential seeding area could prevent a bloom from occurring there even when nutrients and light are not limiting. If the time for a full volume exchange to occur is less than the generation time for phytoplankton growth, a bloom will not occur. Phytoplankton will be flushed out before they have a chance to multiply.

1.2 Thesis Objectives

The intention of this work was to investigate the possibility of a spring bloom in larger open bodies of water being seeded advectively by adjacent areas. Of specific interest was a seeding area that is shallow enough to be mixed to the bottom. For this reason an increase in primary productivity could occur earlier there, once the critical depth reached the bottom. The study area chosen was Nanoose Bay and the adjacent waters of the Strait of Georgia. Nanoose Bay is large and shallow making it an excellent potential seeding

area. The bay is also sheltered with respect to the Strait. In low wind conditions, when the bay is not mixed to the bottom, the mixed layer would be expected to be shallower than in the Strait. In this case the spring bloom would occur first in the bay, still making it a good potential seeding area. What follows is a list of data collected in the field, and what was intended to be done with each data set in order to address the proposed question.

1. Currents at 5 different depths and wind at the mouth of the bay were measured to provide information about advection.
2. Time series of chlorophyll *a* were measured at all stations to represent phytoplankton biomass.
3. Time series of nutrients were measured at all stations mainly to ensure that phytoplankton growth was not nutrient limited.
4. Time series of density profiles were taken at all stations to estimate the extent of vertical mixing and provide information about circulation.
5. The Secchi disc depth was measured at each station and daily total solar radiation measurements were made to calculate the critical depth as a time series.
6. Phytoplankton species composition were examined for all stations as a time series for a quantitative measure of phytoplankton concentration and a qualitative description and comparison of phytoplankton communities.

1.3 Sverdrup Critical Depth Theory

Sverdrup [28] proposed a theory using light and stratification as the limiting conditions to determine when a spring bloom would occur: A net increase in primary production

can happen once phytoplankton are not being mixed deeper than the critical depth of light penetration.

1.3.1 Critical Depth

The critical depth (D_c) is defined as the depth above which respiration demands are more than met by photosynthetic production of phytoplankton (Parsons, Takahashi and Hargrave [22]). It is dependent on the absorption and scattering of light by water and the total amount of photosynthetically available solar radiation (PAR) received at the surface of the ocean, which is a fraction of the total incoming solar radiation at the surface (I_o). The former is parameterized by k , the extinction coefficient of light in water. The critical depth is calculated from:

$$D_c = \frac{FI_o}{kI_c}(1 - e^{-kD_c}) \quad (1.1)$$

where k is estimated from the measured Secchi disc depth, D_s , as $1.7/D_s$ [22]. I_c is the compensation light intensity inherent to the definition of the critical depth. It is the average amount of radiation available integrated from the surface to D_c and is set depending on the ability of phytoplankton to photosynthesize at a minimum light level. The accepted range for I_c is 0.12 to 0.54 langley/hr [22]. Radiation in the 400-700 nm band is considered photosynthetically available. PAR is obtained from I_o using the factor F . The accepted value for F is 0.5 [22]. Reflectance of radiation by the sea surface particularly when the sun is at low angles is also considered to be accounted for by F . At 50° N the percentage of total PAR reflected varies from about 10% in February to 5% in April (Campbell and Aarup [2]).

1.4 Stratification and Mixing

The ocean is often considered as a two-layer system. It is defined in terms of density structure. Both layers have constant σ_t ; ($\sigma_t = \rho - 1000$, where ρ is the density of water at the *in situ* temperature and salinity and at the reference pressure of 1 atmosphere). The bottom is more dense than the top with a strong density gradient, the pycnocline, between. In coastal waters fresh water input often plays a major role in the stratification of the water column. Density structure is often much more complex than this simple two layer idealization. What is of interest in this problem is the depth to which plankton is mixed. It is often assumed to be the depth of the top layer.

1.4.1 Depth of the top layer

It is possible to calculate an equivalent thickness of the top layer from density profiles as described by Freeland and Farmer [9]. In this method two relevant physical quantities are conserved, the potential energy of the water column and the baroclinic first mode internal wave speed. These quantities are calculated from continuous density profiles and then set equal to the theoretical values for the two layer system. In this way the experimental density profile can be fit to a two layer structure. From this fit the depth of the upper layer and σ_t of the lower layer are estimated.

Potential Energy

Work is required to mix water of different densities. The potential energy of a water column is increased when denser water is mixed upwards. The potential energy parameter χ is defined by Freeland and Farmer [9] as:

$$\chi = \frac{1}{H^2} \int_0^H \sigma_t(z) z dz \quad (1.2)$$

where H is the total height of the water column, z is the depth (which is zero at the surface and increases downward) and $\sigma_i(z)$ is the density profile. This equation is easily integrated for the ideal case to obtain:

$$\chi = \frac{1}{2}(\sigma_1 h^2 + \sigma_2(H^2 - h^2))/H^2 \quad (1.3)$$

where the subscripts 1 and 2 denote the upper and lower layer respectively and h is the depth of the top layer. Freeland and Farmer [9] assume that σ_1 is the experimental σ_i at 2 m.

First Mode Internal Wave Speed

A stratified system provides the physical environment for many modes of internal oscillations. The barotropic mode is the basic one that would occur without the density structure simply due to the restoring force of gravity. The next highest mode is the one considered. Its restoring force includes the buoyancy forces associated with the variation of density with depth. To estimate the internal wave speed the partial differential equation for vertical oscillations is solved for its eigenvalues:

$$\frac{d^2 W_n}{dz^2} + \frac{W_n(z)N^2(z)}{c_n^2} = 0 \quad (1.4)$$

where $W_n(z)$ are amplitude distributions for the n eigenfunctions with phase speeds c_n . $N(z)$ is the Brunt Vaisala frequency:

$$N^2(z) = \frac{g}{\rho} \frac{d\rho}{dz} \quad (1.5)$$

N is the natural frequency of the water column giving an upper limit to vertical oscillations. A rigid lid boundary condition is implied at the surface. The solution to this problem is presented in LeBlond and Mysak [18]. In the ideal two layer case the internal wave speed is:

$$c_1^2 = \frac{g}{\rho_2}(\sigma_2 - \sigma_1) \frac{h(H - h)}{H} \quad (1.6)$$

Using the two equations 1.6 and 1.3 and equating each to the respective values c_1 and χ , as estimated directly from the density profiles, h and σ_2 can be calculated.

1.4.2 Mixing

Turbulent mixing may occur due to vertical shear of the horizontal velocity ($\frac{\partial U}{\partial z}$). Strong stratification inhibits turbulence through buoyancy forces. More energy and thus a greater velocity shear is required to move heavier parcels of water upwards. Richardson defined a non-dimensional index to quantify this effect:

$$R_i = \frac{N^2}{(\frac{\partial U}{\partial z})^2} \quad (1.7)$$

Note that N is the Brunt Vaisala frequency, as defined above, and is a measure of vertical stability in the water column. Theoretically if $R_i > 1/4$ everywhere in the fluid there is no turbulence, as shown by LeBlond and Mysak [18].

It is easily possible that the top layer, although it is called the mixed layer, may not be actively mixing. Velocity shear and even weak stratification within layers should also be considered. In most cases fitting the density profiles in and around Nanoose Bay to the two layer model was not appropriate. For example, the density structure was often such that there was a nearly constant small density gradient from the surface to the bottom. The question arises as to whether this is a well mixed situation. Where were phytoplankton in the water column? To attempt to answer this question a Richardson number of $1/4$ can be used along with N , estimated from the density profiles, to calculate a velocity shear in the vertical necessary for turbulence. The velocity shear can be compared to current data at the mouth of the bay to estimate whether or not active mixing is occurring.

1.5 Advection and Diffusion

To determine whether or not a bloom is seeded other than *in situ* an understanding of advection and diffusion is necessary. The general conservation equation for the rate of change of a scalar in a fluid is:

$$\frac{\partial C}{\partial t} = -\nabla \cdot \mathbf{u}C + \kappa \nabla^2 C + \Sigma(\text{Sources} + \text{Sinks}) \quad (1.8)$$

C is a scalar quantity of interest, \mathbf{u} is the vector current velocity and κ is the molecular diffusivity. This equation describes changes in C at a fixed location. It simply states that the change in C with time is due to the net amount of C that is advected, or is diffused, to or from that location and the sum of any sources and sinks present. C will be considered generally at this point as either concentration of phytoplankton biomass or as number of cells per volume.

The sources and sinks come from biological influences and are discussed in the last section of this chapter.

Molecular diffusion is driven by gradients of a scalar and is proportional to the diffusivity κ of that scalar. In general molecular diffusion is negligible compared to the other terms. Often the diffusivity κ is replaced by a much larger value using the Reynolds approach as in Pond and Pickard [23]. It is called the eddy diffusivity K. Doing so can make diffusive effects appreciable. The dispersion of phytoplankton has been fit to equations using a similar method by J. Cloern [4].

To understand the Reynolds approach both C and \mathbf{u} are split into mean and fluctuating parts. The fluctuating parts, \mathbf{u}' and C' , are turbulence terms. C and \mathbf{u} are substituted into equation 1.8, each as a sum of the the two parts and the equation is time averaged.

$$\langle \mathbf{u}C \rangle = \langle \mathbf{u} \rangle \langle C \rangle + \langle \mathbf{u}'C' \rangle \quad (1.9)$$

where $\langle \rangle$ indicates a time average. The Reynolds fluxes $\langle \mathbf{u}'C' \rangle$ are replaced by

assuming that they are directly related to the spatial gradients of the mean C as in Pond and Pickard [23].

$$\langle u'C' \rangle = -K \nabla \langle C \rangle \quad (1.10)$$

The proportionality constant is the eddy diffusivity. Thus fluctuating terms lead to turbulent diffusion. Note that the turbulent and molecular diffusive terms differ only by the factors K and κ respectively, K being much larger. The molecular diffusive fluxes are therefore negligible compared to the turbulent fluxes.

The difference between eddy and molecular diffusivity other than scales is that K is not isotropic as κ is. Eddy diffusivity is much smaller in the vertical as the length scale in this direction is much smaller than in the horizontal. It is assumed that the vertical region over which phytoplankton were sampled (the top 3 m) was uniform, thus making the vertical gradient in C zero. For this reason the vertical Reynolds flux term was neglected. It is recognized however that it may be important. Vertical eddy diffusion has been related to increases in phytoplankton concentration by Cloern [3] in San Francisco Bay. It is noted however that tidal currents are much stronger in San Francisco bay than in Nanoose bay. Also, vertical chlorophyll a gradients often exist (Harrison et. al. [13]) and can be related to many different processes, as in Cullen [6]. Such gradients however are often associated with a well stratified water column where phytoplankton with the ability to move dominate. During the sampling time diatoms were the dominant type of phytoplankton. Diatoms have no means of locomotion. It is therefore hoped that, at least in the upper part of the water column which was sampled, the approximation of zero vertical C gradient is reasonable in the sense that any associated error is much smaller than the horizontal advective effects.

For this work both turbulent and molecular diffusion will be assumed negligible compared to advective transport in equation 1.8. Advection usually dominates turbulent

diffusion in coastal situations (Hansen and Rattray [11]), with the exception of areas where strong tidal currents and thus intense mixing exist. Tidal currents at Nanoose bay are not strong. It is therefore assumed that turbulent diffusion is negligible compared to advection. Equation 1.8 then becomes:

$$\frac{\partial C}{\partial t} = -\nabla \cdot \mathbf{u}C + \Sigma(\text{Sources} + \text{Sinks}) \quad (1.11)$$

where C and \mathbf{u} are now mean quantities.

1.5.1 Physical Forcing

Material transport, or advection, can be driven by three main forces, wind, tides and horizontal density gradients.

In the case of tides, the forcing in the open ocean is due to the gravitational pull of the moon and the sun. Boundary conditions are produced by the progressive elevation changes at the entrances (Juan du Fuca and Johnstone Straits) to the Strait of Georgia that are responsible for the tides there. The result is mixed, but mainly semidiurnal tides, with a mean tidal range of 3m (Thompson [29]). The amplitudes of the tidal currents at the mouth of Nanoose bay are a few cm/sec.

Wind blowing at the surface of the ocean produces a stress which causes motion. The wind stress is a function of the square of wind speed, density of air and a non-linear drag coefficient. This stress is transferred downwards as a function of vertical eddy viscosity and vertical velocity shear, (Pond and Pickard [23]). Winds at the mouth of Nanoose bay typically range from 2 to 8 m/s. Surface currents driven by such wind speeds are expected to be within the range of a few to 10 cm/s or so. The currents measured were in this range and it was expected that wind would be mainly responsible for non-tidal currents.

Density driven circulation occurs due to pressure gradients created by horizontal

variation in density. The force due to density gradients is proportional to the $\int \frac{\partial \rho}{\partial x} dz$ and in the opposite direction to $\frac{\partial \rho}{\partial x}$. Local fresh water input is an effective means of creating strong horizontal variation in stratification and is essentially responsible for estuarine circulation. In estuarine circulation there is a surface flow away from a fresh water source. The addition of fresh water causes an increased surface elevation which has a horizontal gradient thus driving the surface layer away from the source. The stratification set up in such a system generally varies spatially such that the fresher surface layer becomes progressively more saline away from the source through entrainment. The density change can create horizontal density gradients which more than compensate for the forcing due to elevation changes. The net result at depth is for a density driven current to flow towards the fresh water source.

The fresh water input from the Fraser river influences stratification throughout the Strait of Georgia (Thompson [29]). It is the dominant feature especially in the summer during freshet. It was expected that it would have little influence on Nanoose during the winter-spring season given that the distance between Nanoose and the mouth of the Fraser is approximately 70 km (see figure 2.1) and they are on the opposite sides of the Strait. The residual circulation of the entire Strait is very complicated (Stacey, Pond, LeBlond, Freeland and Farmer [25]) however and certainly influenced currents at Nanoose Bay.

1.6 Phytoplankton Ecology

Phytoplankton ecology will be considered in terms of providing source and sink terms in equation 1.8. Specifically the $\Sigma(Sources + Sinks)$ term will be replaced by biological parameters.

1.6.1 Diatoms and Flagellates

The main types of phytoplankton found in and around Nanoose Bay are diatoms, dinoflagellates and nanoflagellates, (which include cryptomonads, haptophytes and chloromonads). Each has different strategies for survival which tend to make it dominant under different environmental conditions. Dinoflagellates and nanoflagellates have flagella and therefore some means of locomotion. Diatoms are truly free-floating. Their strategy for movement in the water column involves cellular processes that change their density with respect to the surrounding sea water. Ability to take up nutrients from the water also differs amongst classes (Harrison and Turpin [14]). Diatoms tend to dominate in high nutrient conditions where they are able to take up nutrients very quickly. In general the flagellates are more flexible in their ability to use nutrients.

During spring bloom conditions nutrient availability is high as nutrients have been mixed up during the winter and not used. As primary productivity increases, nutrients get depleted. Nutrient depletion is often coincident with increased stratification, as there is generally less wind and greater fresh water input and therefore less mixing during the spring and summer months than in the winter. Diatoms therefore usually dominate early in the year and make up the majority of phytoplankton biomass during the spring bloom. Conditions are perfect for them in terms of high nutrient availability and stronger mixing providing them with a means of locomotion. Flagellates dominate later when nutrients are depleted in the upper layer and waters are more stratified. In these conditions flagellates may be able to swim down to the nutricline (the nutrient gradient usually just below the nutrient deplete upper region) where they can utilize available nutrients or at least move through the water and enhance their intake of nutrients.

Diatoms made up the majority of the phytoplankton population in Nanoose bay during the sampling period with very few flagellates as expected. Samples tended to be

low in species diversity and typical of spring boom conditions in the Strait of Georgia (Harrison, Fulton, Taylor and Parsons [13]).

1.6.2 Sources

The most obvious source of phytoplankton comes from growth and cell division. In favourable conditions the generation time for cell division is temperature dependent. In the Strait of Georgia during the study period a reasonable doubling time would be 2 days (Parsons, Takahashi and Hargrave [22]).

A second possible source is over-wintering cysts. Many genera of phytoplankton are able to form dormant resting spores. They sink to the sediments and excyst when conditions, for example a rise in temperature and light, become favourable. A situation in which the water column is mixed to the bottom could provide an excellent means of introducing the excysted phytoplankton back into the euphotic zone.

1.6.3 Sinks

Sinks for phytoplankton are due mainly to being eaten and sinking out of the water column. Two types of grazing were considered, grazing by zooplankton and by benthos. Zooplankton have a threshold in concentration of phytoplankton for grazing (Parsons and LeBrasseur [19]). If very little food is present they would expend more energy hunting for food than they would consume. Typical grazing rates for zooplankton in the Strait of Georgia for the study period were used. In Nanoose Bay however benthic grazing appears to play a much more important role. The bay is an oyster bed and if it is well mixed the filter feeding bivalves are being continually supplied with food. The flushing time for Nanoose bay was compared with the filtering time by bivalves.

Phytoplankton will sink passively to the sediments if they are not buoyant enough.

Dead plankton can sink over 10 times faster than live (Parsons, Takahashi and Hargrave [22]). Two of the factors affecting buoyancy are nutrient enrichment and light.

Putting the sources and sinks together yields:

$$\Sigma(\text{Sources} + \text{Sinks}) = C(t)(\mu - b - z - s) \quad (1.12)$$

where μ is the specific growth rate of phytoplankton, b is the feeding rate of bivalves, z is the grazing rate of zooplankton and s is the sinking rate.

Rewriting equation 1.8 in its final form with all substitutions yields:

$$\frac{\partial C}{\partial t} = -\nabla \cdot \mathbf{u}C + C(t)(\mu - b - z - s) \quad (1.13)$$

Note also that, since water is an essentially incompressible fluid, $\nabla \cdot \mathbf{u}C$ can also be written as $\mathbf{u} \cdot \nabla C$, which is the form that will be used in Chapter 4.

Chapter 2

The Experiment

2.1 Nanoose Bay

The study area chosen to investigate the seeding of a spring bloom from shallow areas was Nanoose Bay, on the east coast of Vancouver Island. It seemed an ideal location due to its bathymetry and geography. The bay itself is quite large, about 2 square kilometres, is shallow, generally 25 metres deep, and is directly connected to the Strait of Georgia via a narrow (approximately 0.5 km) opening. There are extensive mud flats at the end of the bay and several small creeks that input a little fresh water mainly near the mouth. The bay itself is shallow enough to be mixed to the bottom during strong wind conditions typical of winter and early spring. In the case of calm weather, the bay is sheltered and becomes quite stratified, with a brackish layer on top and a shallow mixed layer. Regardless of wind conditions therefore, the extent of vertical mixing outside the bay is generally greater, allowing for an increase in primary productivity to occur first in the bay. Advective exchange between the bay and the adjacent Strait occurs through the narrows at the mouth of the bay. Currents here appear to be density driven, wind driven and tidal and are not strong. The tides are typical of the Strait of Georgia, mainly semidiurnal with the M_2 and the K_1 constituents dominating (Thompson [29]). The mean tidal range is just over 3m.

2.2 Design

2.2.1 Sampling Timing and Locations

Data collection was started near the end of January to ensure that any early increase in phytoplankton biomass was recognized, as well as to observe the phytoplankton community surviving in the water column through the winter. Once the spring bloom was clearly in full force the experiment ended. Originally the main criterion for sampling locations was to choose stations representative of both the inside and outside of the bay. The criteria evolved to include spatial resolution and thus more stations between inside and outside.

1992 was the first year that data were collected. Data collection began on January 27 (Julian day 27). The sampling scheme was very simple. Stations were: NAN 10 inside the bay, NAN 20 at the mouth, NAN 30 in the Strait, just west of the Winchelsea Islands (figure 2.1). The location of NAN 30 was chosen as it was convenient for the military crew at Nanoose to sample. It was thought to be a reasonable location to sample receiving waters of the bay during the winter as the prevailing winds at this time are typically from the south east, creating wind driven north westerly currents. I was fortunate to have personnel from Nanoose sample twice weekly during their own maneuvers. Sampling was done by myself once weekly in the UBC departmental boat, the *Tintannic*. Weekly sampling ended March 21 (Julian day 81), 1992 when there was a strong phytoplankton bloom in the Strait. At this time the Secchi disc depth at all stations was limited to 5m by the high numbers of phytoplankton. The mooring was recovered on April 9 (Julian day 100) at which time an additional water sample (chlorophyll, nutrients and species composition) was drawn at each station.

In 1993 the experiment was significantly altered. More spatial resolution was desired, especially at the mouth of the bay, so four new stations were added. Two stations were

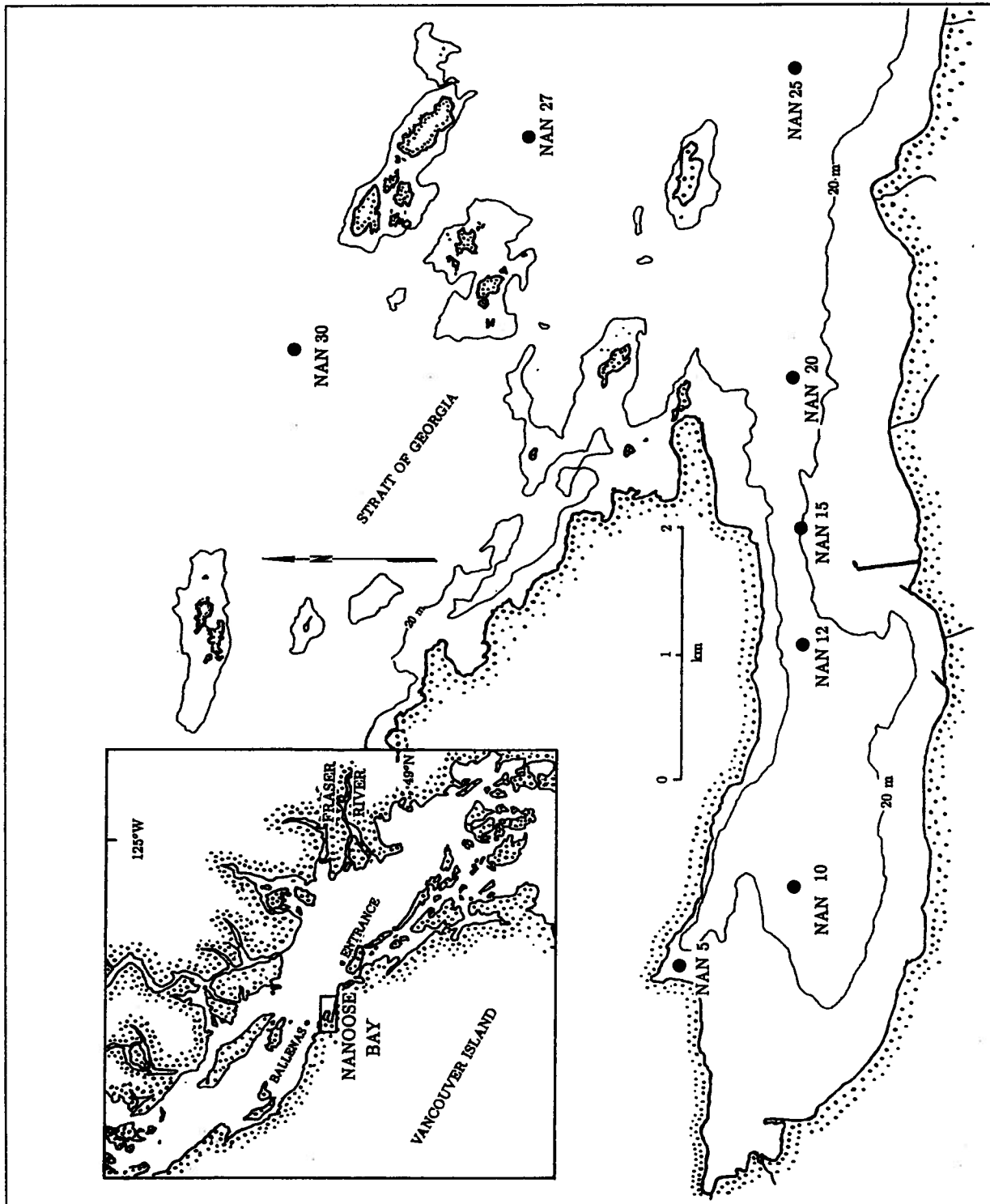


Figure 2.1: Nanoose bay and the Strait of Georgia with locations of all sampling stations

added between NAN 10 and 20 to create a line of stations at the mouth of the bay and two were added on the outside between NAN 20 and 30. It was hoped that horizontal chlorophyll *a* gradients could be estimated from this configuration. All stations are shown in figure 2.1. Chlorophyll measurements were taken in triplicate to make the record less noisy. On one occasion in 1992 triplicates were taken to give a measure of error in the sampling and it was found that chlorophyll *a* varied by over an order of magnitude between replicates at the same station. Clearly biological patchiness is a major consideration when taking discrete water samples from any location. An eighth station was added (NAN 5) in a shallow (several metres deep) cove in the bay. It was hoped that overwintering cysts could possibly be observed here as well as any early increases in primary productivity. Sampling was done twice weekly at all stations, weather permitting, in the Whaler 3 provided by the Institute of Ocean Sciences, Sidney, B.C. of Fisheries and Oceans, Canada. Three extra days of sampling at the original stations were done by the crew at Nanoose; they were unable to sample weekly. Sampling began on February 4 (Julian day 35) and ended on April 13 (Julian day 103). Strong south easterly winds during the first part of April suppressed a strong bloom in the Strait and caused sampling to continue later in the season than in 1992.

2.2.2 Sampling

At each station nutrients, chlorophyll and species composition were sampled. Density profiles and Secchi disc depth were also measured.

Water samples were drawn using a 3m integrated pipe sampler (see Sutherland [27]). The 3m water column was thoroughly mixed as it was emptied into a bucket. From this bucket, 100 ml were forced through a precombusted 2.5 cm diameter Whatman GF/F glass filter. The filtrate was collected in 30 ml polypropylene bottles for nutrient analysis. The filter and filtrate were put on ice and frozen as soon as possible to avoid bacterial

activity and enzymatic breakdown in the samples. Note that in 1993 three pipes were drawn at each station for chlorophyll triplicates although only one nutrient sample was taken. For species composition analysis a 60 ml glass jar was filled from the bucket and fixed with Lugol's iodine solution.

The chlorophyll analysis was done using the method described in Parsons, Maita and Lalli [20]. The filters were placed in 10 ml of 90% acetone solution and put in a sonification bath for 20 minutes to extract pigments and then stored for 24 hrs at 5 deg C. The chlorophyll *a* and phaeopigment concentrations were then measured fluorometrically using a Turner designs Model 10TM fluorometer. Fluorescence is converted to concentration using equations in Parsons, Maita and Lalli [20].

Nutrient analysis was done using a Technicon AutoanalyzerTM with a baseline of 3 ppt seawater. Nitrate, phosphate, ammonium and silicate were measured for the 1992 data. Only nitrate and phosphate were analyzed for the 1993 data as data from the previous year indicate that nutrients were high everywhere until phytoplankton concentrations increased and they were not at any time limiting to phytoplankton growth. Ammonium and silicate data were not directly used. Also ammonium concentrations were large enough to suspect contamination. Silicate concentrations are often used as a fresh water tracer and CTD data could be used for that.

Species composition analysis was done using an inverted microscope. Samples were settled for 24 hours in 10 ml and 25 ml Leitz settling chambers, the volume depending on abundance of phytoplankton. Identification was done to the genus level as it was sufficient in comparing phytoplankton communities. For reference and identification of diatoms Cupp [7] was used. All genera were noted for their presence and the most abundant was counted under 100X or 400X magnification depending on the size of phytoplankton. The percentage of the total number that the most abundant made up was also noted to provide an estimate of the relative composition of the different species present. In

addition three genera were always counted regardless of their abundance: *Chaetoceros* spp., *Thalassiosira* spp. and *Skeletonema costatum*. The presence of zooplankton, larvae or any other plankton was also noted.

Density profiles were taken using an S4 current meter as a CTD. The S4 meter that was used has an inductive conductivity sensor. For temperature measurements it has a platinum resistance thermometer which has the fast response time necessary for taking profiles. For depth measurements a strain gauge pressure sensor is used. Based on laboratory calibration checks the accuracy is ± 0.02 for temperature, ± 0.05 for salinity, and ± 0.05 for σ_t . After the correction for zero offset the depths should be accurate to ± 0.5 m or better. All casts were done to 20 m, which is nearly to the bottom at stations 10 through 15, and then to 40 m in 1993 at station 30 on the outside to observe the structure in the deeper water of the Strait. The S4 was set to sample continuously at 5 sec intervals before going out to sample and left running. All of the data were read off of the S4 afterwards and the useful segments, (i.e. when the S4 was in the water) were extracted from the record.

To measure the turbidity of the water, and thus calculate the extinction coefficient k , the Secchi disc depth was measured at each station. Solar radiation was measured using a pyranometer placed on a piling in Nanoose bay. The pyranometer was connected to a data logger inside a weather proof case. The data logger recorded 24 hr values of integrated solar radiation.

2.2.3 Current and Wind

On January 27 1992 a mooring was placed near the mouth of Nanoose bay at station NAN20 to measure the advective exchange in and out of the bay. It was equipped with 5 interocean S4 current meters and an Aanderra meteorological station. The location of the mooring was chosen to be just outside of the bay. The reason for its placement

was mainly to avoid possible difficulties with boat traffic entering the bay, especially log booms during storms. Advantages of its placement include measuring wind components that are blowing in the Strait as well as into the bay.

The S4 current meters were placed at 2, 4, 7, 12 and 20 m below the surface. It was expected that most variation in the currents would appear near the top of the water column as was found for wind driven responses in Peter Baker's work in Knight Inlet [1]. The current meters were therefore packed more closely near the surface. The S4s were set to record conductivity, temperature and a one minute vector averaged velocity every 10 minutes.

By laboratory calibration the accuracy is ± 0.02 for temperature and generally ± 0.2 for S and σ_t . Conductivity is measured by conductive sensors and because of the long immersion time some fouling is possible. Examination of the records suggests that the precision for the set of measurements is ± 0.1 for S and σ_t .

Currents are generally small at the mouth of Nanoose bay, typically a few cm/s and therefore difficult to measure. Mechanical devices, such as Aanderra current meters are prone to errors through friction, rotor pumping and alignment to surface wave trains, (see Kollstad and Hansen [16]). S4 current meters use magnetic induction to measure motion in the water. A magnetic field is set up and the motion of conductive seawater through it induces a voltage which is measured and recorded by the S4, (see Lawson et al. [17]). The S4 is capable of measuring smaller currents than mechanical current meters. The velocity is vector averaged so the results are unaffected by surface wave trains.

The wind data were taken by an Aanderra system on the Geodyne buoy of the mooring. Unfortunately it failed to record data for the first 40 days that it was deployed, which happened to be the portion of the record with stronger winds. To obtain a complete wind record lighthouse data were used from both Ballenas and Entrance Islands, on either side of Nanoose bay (figure 2.1). Correlations between both lighthouse records

and the Geodyne record were high and the Ballenas record was therefore used.

The meteorological station was equipped with an anemometer 4m above the water, a compass, and a thermometer to measure ambient temperature. Wind speed, direction and air temperature were recorded at 10 min. intervals. The reported ambient temperature was a suspicious 16 deg C throughout the entire experiment.

It was hoped that the non-tidal part of the currents could be correlated with the wind for the 1992 record and this correlation could be used to extrapolate 1993 currents from the the 1993 wind data. This approach proved to be more difficult than anticipated and the comparison is discussed in the next chapter.

Chapter 3

Results and Analysis

3.1 Current and Wind

All current data are from the mooring set at NAN 20 for the 1992 season. There is a 73 day record of current speed and direction as well as density for depths of 2, 4, 7, 12 and 20 m. Wind data came from three sources, the geodyne anemometer and Ballenas and Entrance Island lighthouses. All data were run through a sequence of processing which is described in the next section.

The current data were taken to measure the advective transport in and out of the bay as a function of time, and thus determine whether phytoplankton were traveling from the bay to the outside and possibly providing a seed population. Because current data were only taken in 1992, it was hoped to gain knowledge from these data to allow 1993 currents to be estimated. To do so, cross-correlations between the current and wind were done to estimate the contribution of the wind to the current. As wind data are readily available a relationship between wind and current would have allowed the extrapolation of current in 1993. It was however not possible to find such a relationship as is shown in section 3.1.3.

The time scales of interest are related to phytoplankton growth. To consider advection important to phytoplankton, fluctuations with periods less than their generation time were removed. The generation time during this experiment is assumed to be about 2 days (Parsons, Takahashi and Hargrave [22]), thus it was desired to remove energy with

frequencies greater than $1/2$ cpd from the current record. Harmonic analysis was used to take the energy at tidal frequencies out of the record. The main tidal constituents are semidiurnal and diurnal and thus of time scales less than phytoplankton growth. To remove remaining high frequency energy 25 hour averaging was done.

3.1.1 Processing

Currents

Raw data (velocity components, conductivity, and temperature) came directly from the S4 current meters. Velocity data were rotated to correct for the magnetic declination which is 22 degrees at Nanoose Bay. Possible spikes were then removed from the rotated files and averaging was done to make hourly values from the 10 minute samples, and thus remove high frequency noise. This processing was done using a window based average centred on the hour. In this case the highest and lowest values in each window were discarded and the remaining 5 values were averaged. Salinity and σ_t were calculated using the practical salinity scale and the international equation of state as in Pond and Pickard, [23]. After the binning and calculations, the S4 data were split into two files, one with Julian day, u and v and the other with Julian day, temperature, salinity and σ_t . Results are shown in figures 3.1 and 3.2 of the east-west (u) and north-south (v) current components, respectively. The σ_t series is shown in figure 3.3. Note that the density range shown at each depth is identical with the exception of the 2 m series which is shown over a larger range.

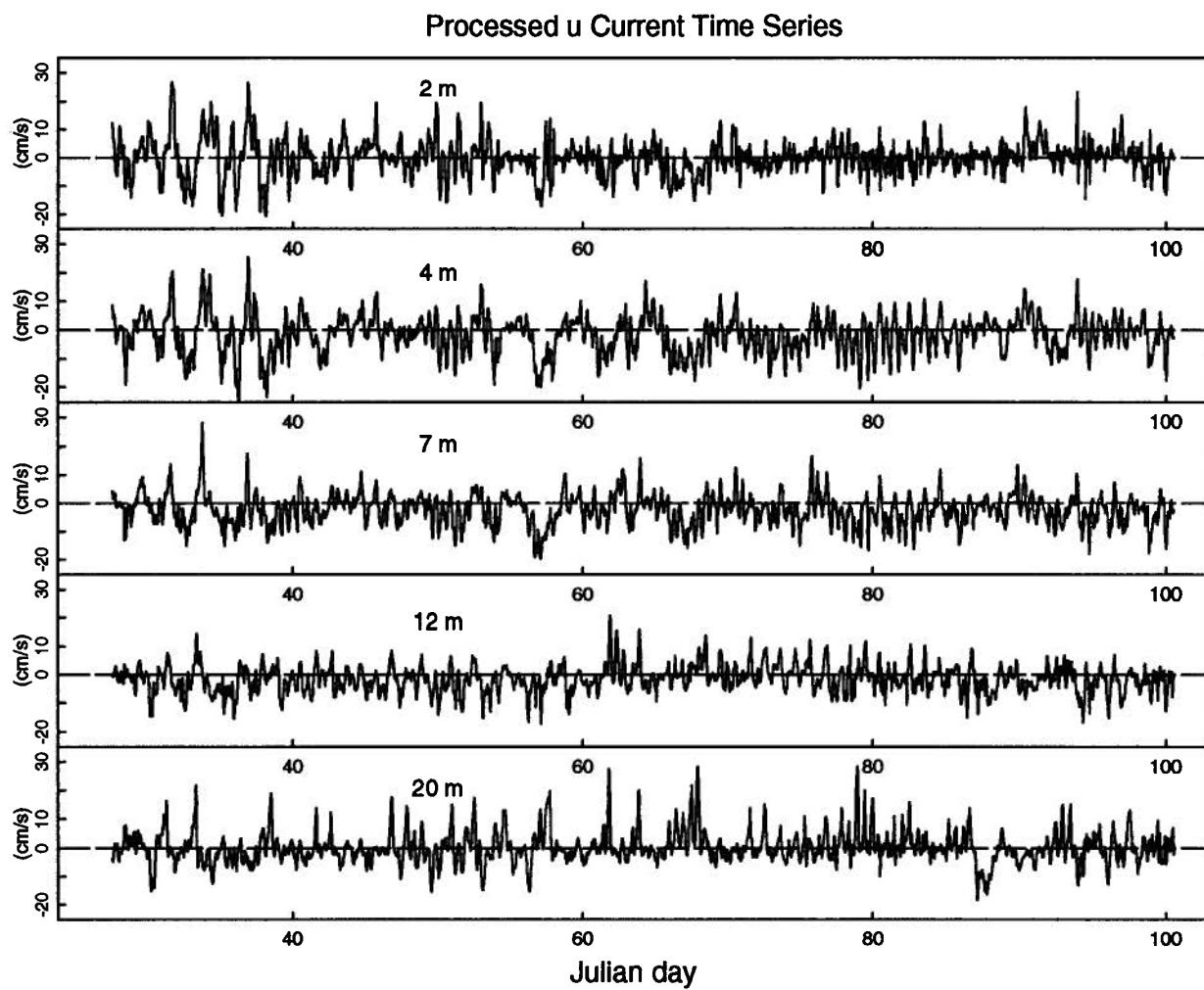


Figure 3.1: Processed u current time series at NAN 20, 1992.

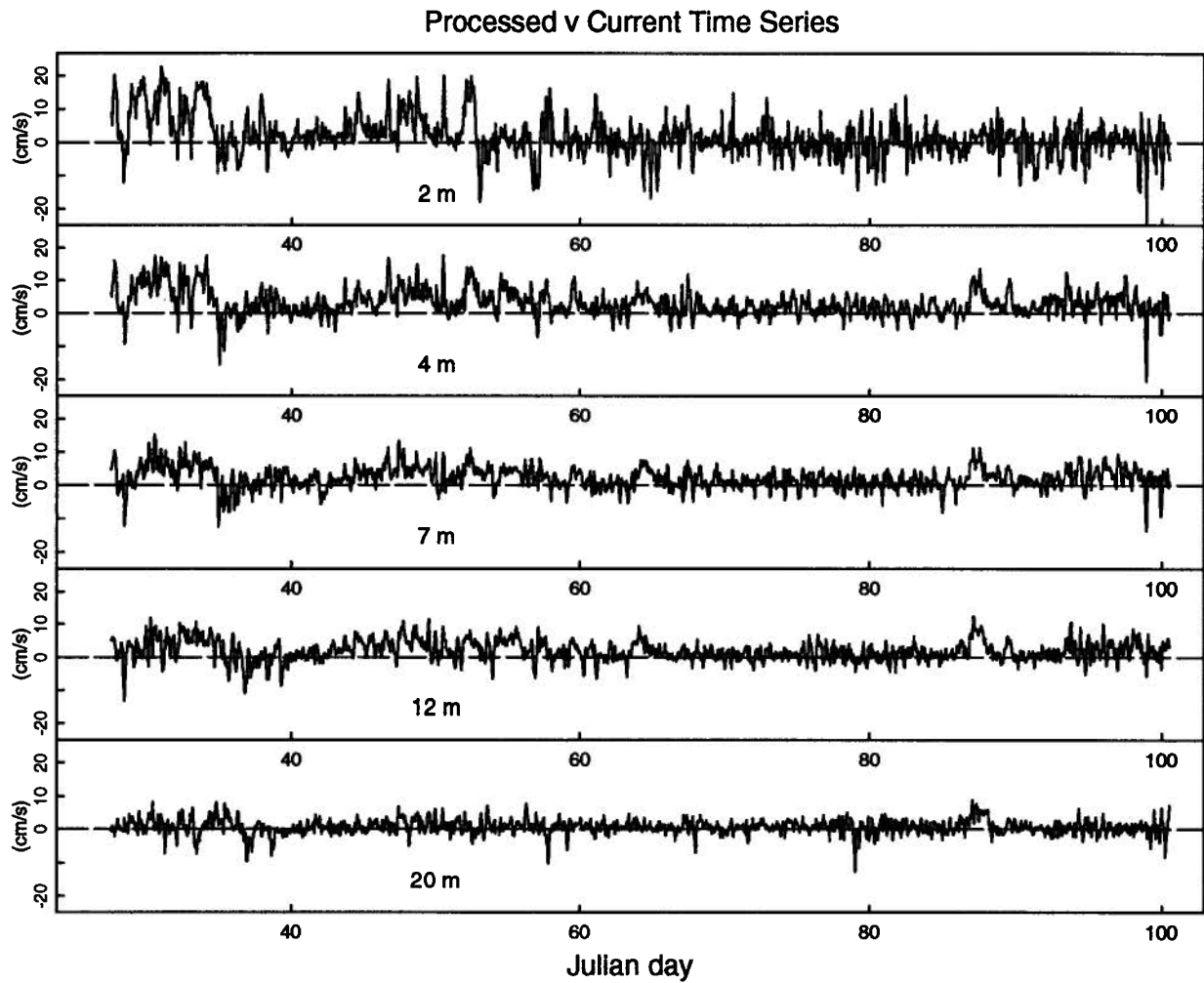


Figure 3.2: Processed v current time series at NAN 20, 1992.

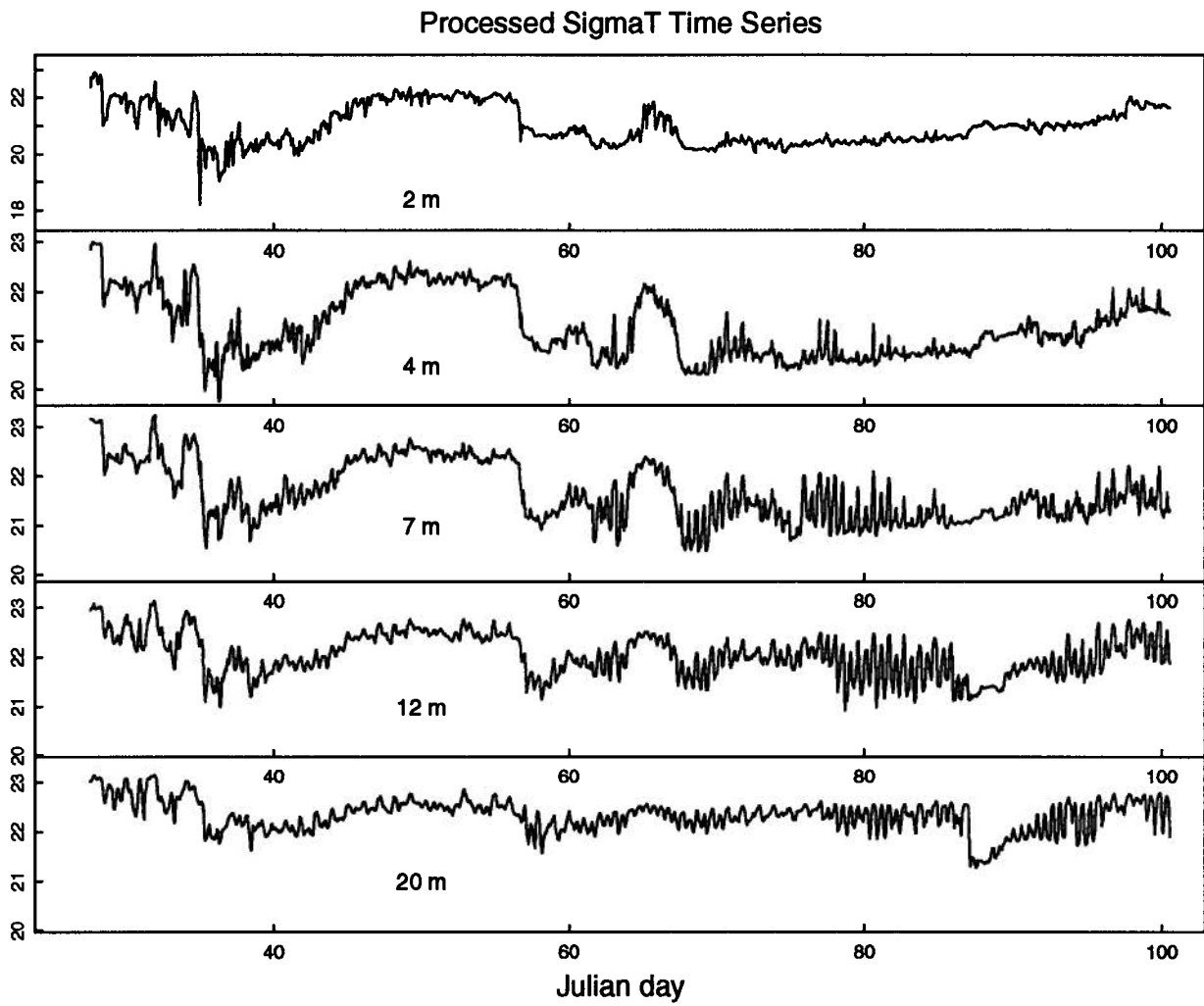


Figure 3.3: Processed σ_t (kg/m³) time series at NAN 20, 1992.

Harmonic Analysis

Fourier spectral analysis gives a frequency spectrum from a time series. The spectral level at a given frequency is a measure of the energy present in the record at that frequency. For the current data the frequency spectra are expected to have high amplitudes at the astronomical forcing frequencies responsible for tides. Therefore, amplitudes at the known forcing frequencies were calculated from these data and subtracted at each depth without doing a full spectral analysis. The calculation of the amplitudes of expected frequencies is known as harmonic analysis. Linear matrices were used to do the computation as the tidal constituents are orthogonal. The matrices are:

$$[A][T] = [D] \quad (3.1)$$

$[D]$ is the matrix of observed data and $[A]$ is the matrix of amplitudes to be solved for. $[T]$ is the matrix of known tidal constituents. It was expanded in terms of *sin* and *cos* functions with a first order polynomial added to represent the mean and the trend. The tidal constituents that were used in the analysis are shown in table 3.1 along with their respective periods. The matrix $[A]$ was found using standard matrix techniques as in Godin [10]. The method of singular value matrix decomposition used was that of Press et.al. [24]. The larger amplitudes in the *u* current direction determined in the analysis are shown in table 3.2 for all depths.

After $[A]$ was found, the tidal contribution was subtracted from the record at each depth, with the exception of the mean, the trend and the MS_f and M_m constituents. The resulting currents were used for all of the following analyses. They are referred to as residual currents.

Tide	Description	Period, (hours)
M_m	Lunar Monthly	661.3
MS_f	Lunar solar fortnightly	354.4
O_1	Principal lunar diurnal	25.82
K_1	Luni-solar diurnal	23.93
N_2	Large lunar elliptic	12.66
M_2	Principal lunar	12.42
S_2	Principal solar	12.00
MK_3	Lunar solar tridiurnal	8.18
M_4	Quadiurnal	6.12

Table 3.1: Tidal constituents used in the harmonic analysis.

Depth	Tidal constituent				
	MS_f	O_1	K_1	M_2	S_2
2	1.02	0.97	1.04	2.17	1.45
4	0.89	0.73	2.01	3.43	1.37
7	1.31	0.79	2.18	2.51	0.52
12	0.40	0.92	2.08	1.83	0.36
20	0.78	0.88	1.44	2.69	1.02

Table 3.2: Amplitudes (cm/s) of the stronger tidal constituents of the u current.

Smoothing

Harmonic analysis assumes that the amplitudes are independent of time and effectively calculates an average amplitude for each frequency. Amplitudes often vary with time however. As a result, high frequency energy may still be present after the estimated tidal constituents are subtracted. Also there may be noise still present in the record.

The residual current record was low-pass filtered to remove any such remaining high frequency energy. A moving 25 hour average was used. Current data were now smoothed, non-tidal, averaged hourly values. The results are shown in figures 3.4 and 3.5 for u and v respectively. Records were later gridded to 3 hourly values for cross-correlations with lighthouse winds.

Wind

Wind data were run through a similar processing sequence to the current data. A certain amount of formatting was first necessary to make all wind records compatible with current data and its software. Raw data were converted to standard units using calibration constants for the meteorological station. Wind direction was calculated from the mooring compass and the anemometer wind vane. This record was then formatted and time was added. The lighthouse data came from Environment Canada with wind speeds in knots, time in GMT and with the meteorological direction convention. Directions and time were adjusted and split into two files, one for each location. All times were in terms of decimal Julian day.

The next step for the anemometer data involved a process similar to the averaging done with the current records. The anemometer data was first hand edited to remove spikes that persisted over more than an hour (such as a two hour sudden wind of 140 m/s). Hourly values were then computed from the 10 minute record by discarding the

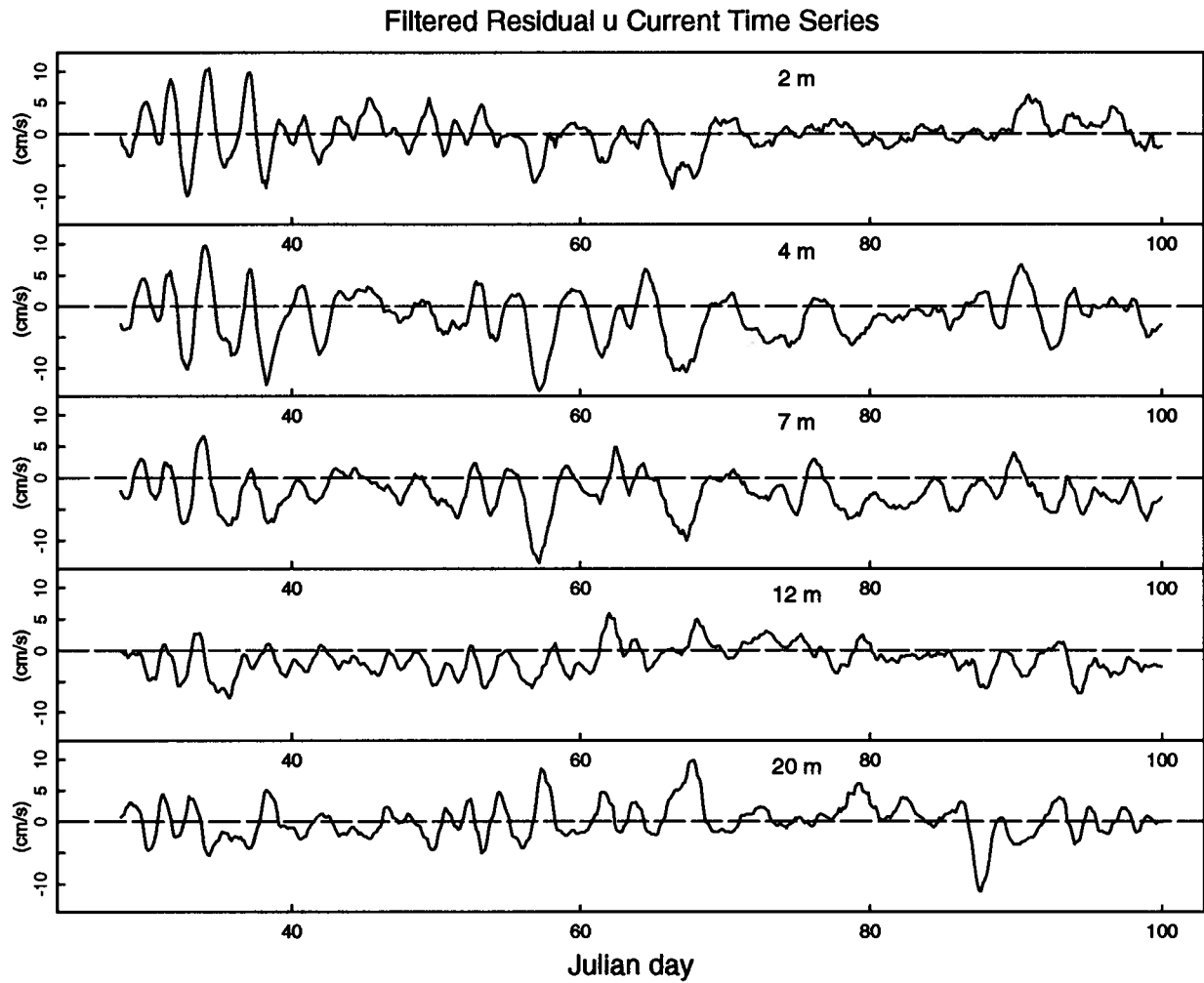


Figure 3.4: Filtered residual u current time series at NAN 20, 1992.

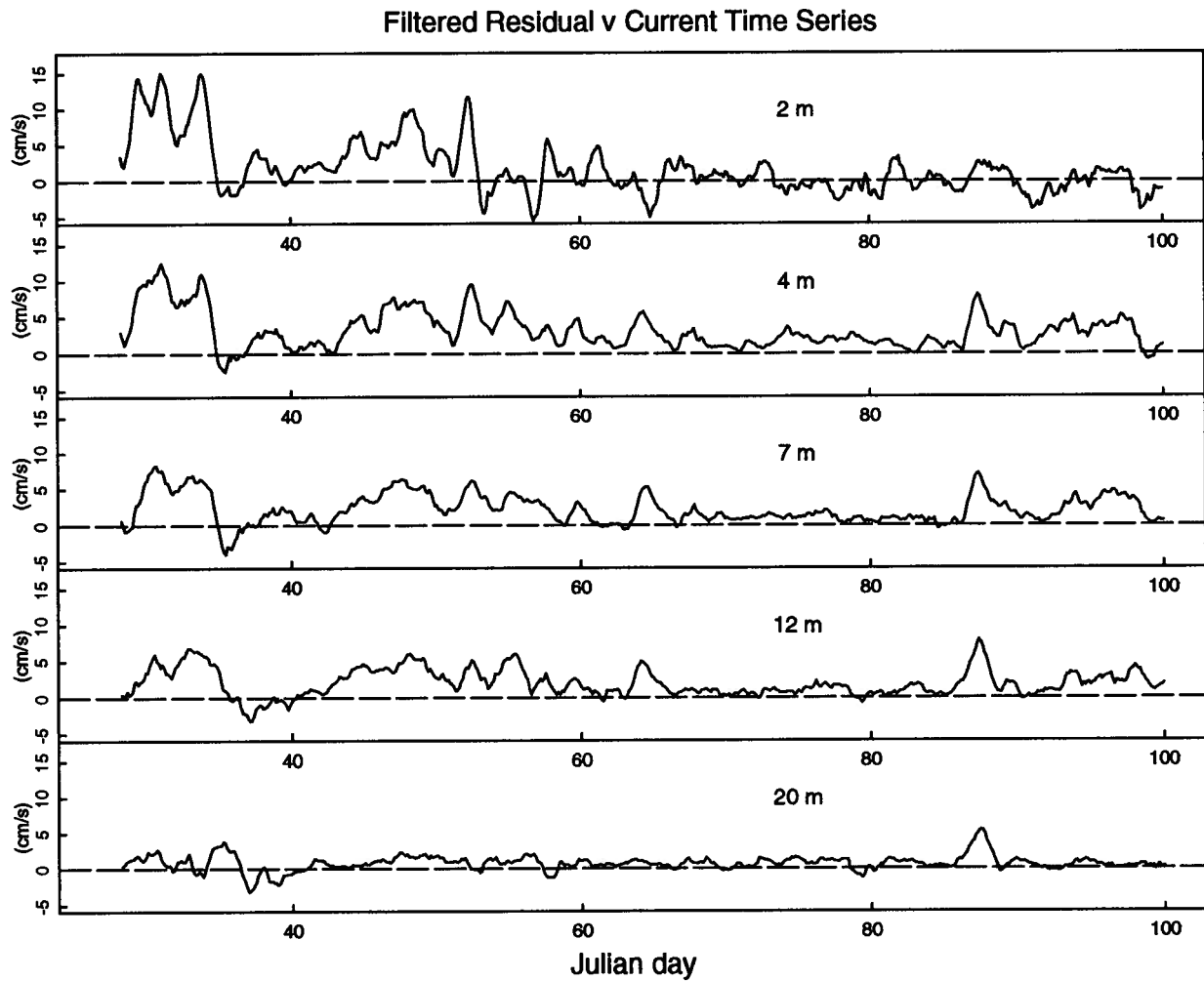


Figure 3.5: Filtered residual v current time series at NAN 20, 1992.

two highest and two lowest values in each window and averaging the remaining three. Two values were removed on either side instead of one as in the case of the current data because the anemometer record had much more high frequency noise. Unlike the S4 data, the velocities were not vector averaged. Wind speed was averaged while direction was taken as a spot reading. The 10 minute values were determined by averaging the resolved components of two consecutive readings on either side of the interval.

$$u = \frac{V_n}{2}(\sin\theta_n + \sin\theta_{n-1}) \quad (3.2)$$

$$v = \frac{V_n}{2}(\cos\theta_n + \cos\theta_{n-1}) \quad (3.3)$$

The angle θ is the true direction recorded as a spot reading and V is the average speed. The subscript n denotes the sample number. The determined east-west and north-south velocity components are u and v respectively.

The lighthouse data were manually recorded. The record had 3 hourly values with occasional missing blocks of data, as much as 36 hours. Where only one datum was missing it was added by linear interpolation. Where a large block was missing, it was replaced with zeros so that uniform time steps were maintained throughout the record. A complete time series was needed to do cross-correlations. Note, when records with a block of zeros were correlated with others, zeros were placed in the second record to match and thus not affect the correlation.

All of the wind records were gridded and filtered. A 25 hour running average was used for the hourly winds and similarly, the 3 hourly lighthouse data were averaged over 24 hours. All files were then gridded to 3 hourly values.

3.1.2 Wind correlations between lighthouses and the mouth of Nanoose bay

As mentioned, the anemometer only functioned for the last 30 days that it was deployed, from day 70 to day 100. Unfortunately during the missing part of the record the winds

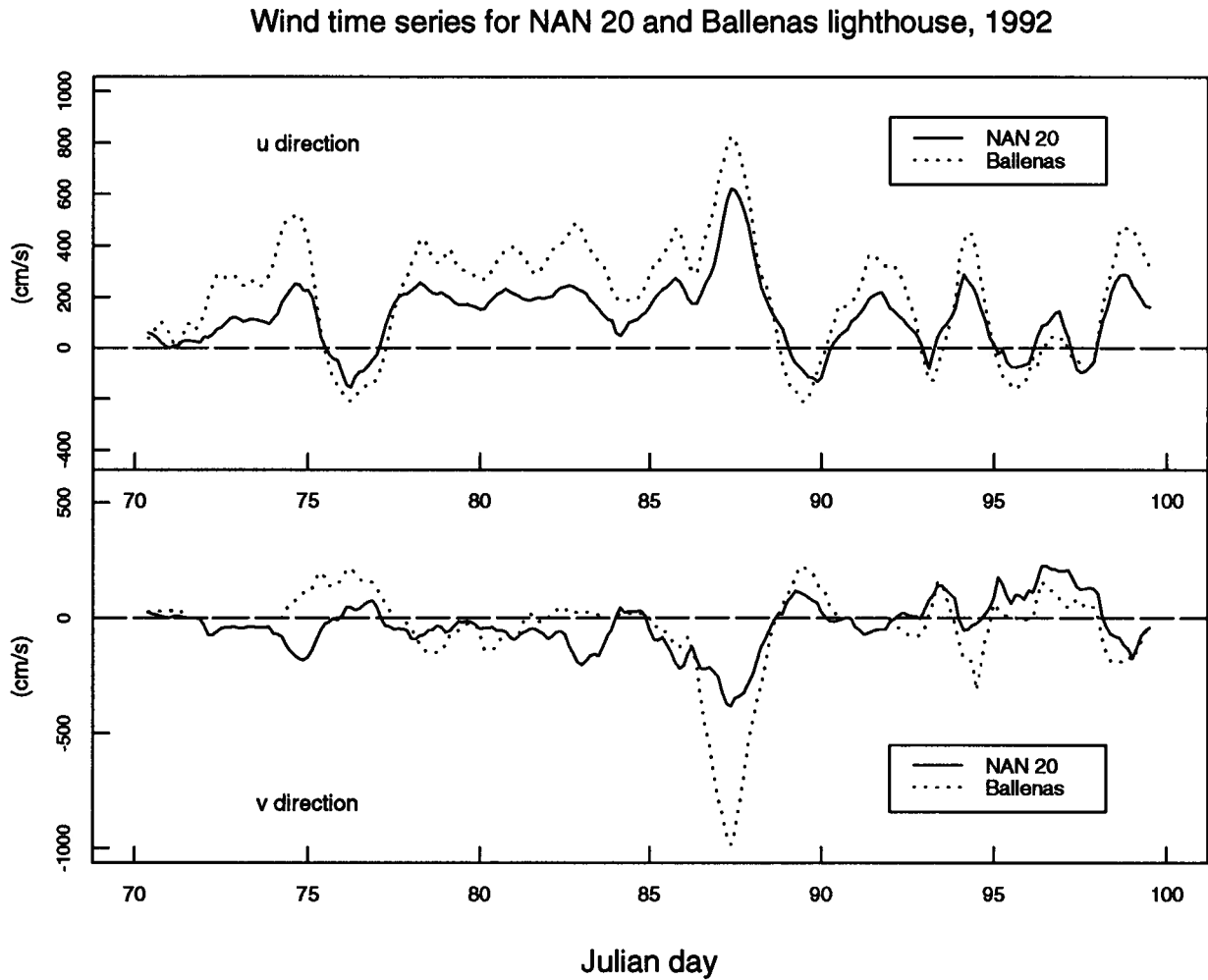


Figure 3.6: Wind time series for Ballenas Island lighthouse and Nanoose bay mooring.

and currents were the strongest. To replace the missing portion, wind data from Ballenas and Entrance lighthouses were examined. Lighthouse records also had the advantage of being available for the 1993 season; therefore any comparisons made with wind data would be uniform for both years.

Both Entrance and Ballenas islands displayed fairly high positive correlations with the anemometer data. Lagged cross-correlations were done using Splus software [26]. A 3 hour time step was used. The time series for both u and v components as well as the magnitude of the wind velocity between lighthouse and anemometer data were

First data set	Correlation	Time lag (hrs)	Second data set
Ballenas u	0.86	0	Entrance u
Ballenas v	0.79	0	Entrance v
Ballenas u	0.74	0	NAN 20 u
Ballenas v	0.54	0	NAN 20 v
Entrance u	0.69	0	NAN 20 u
Entrance v	0.62	0	NAN 20 v

Table 3.3: Maximum wind cross-correlations.

compared. The data were not rotated, thus u and v were east-west and north-south components respectively. Nanoose bay is oriented in an east-west direction, thus the u direction is of primary interest as it is in and out of the bay. In this direction the wind correlation was the highest with the Ballenas Island data. Ballenas wind data were therefore used throughout the rest of the analysis. Figure 3.6 shows the filtered Ballenas Island wind data with the filtered anemometer data over the 30 day time period for both u and v . Correlation values are shown in table 3.3. Note that the time periods are not uniform for all correlations. Ballenas and Entrance lighthouse records were correlated over days 27 to 100 to match the current record. Correlations with NAN 20 were over days 70 through 100, the length of the NAN 20 record. A positive time lag corresponds to the first data set leading the second.

3.1.3 Relationship between wind and current residuals

Once high frequency and tidal energy had been removed from the records a certain amount of low frequency energy remained. Much of the remaining energy was originally expected to be due to wind. If this were the case a correlation matrix would have been calculated so that 1993 currents could be extrapolated from 1993 wind data. The extrapolation would have been used to provide advective information for the 1993 analysis.

Cross-correlations of wind and current at different depths however did not yield strong

maxima at any time lag between the two records. As above Splus software [26] was used for all cross and auto-correlations. The records used in the analysis had gone through an identical sequence in processing with the exception of harmonic analysis.

First relationships between the Ballenas wind and currents at all depths separately for east-west and then north-south directions were investigated. The cross-correlations were low. Maxima in the u direction occurred for time lags between the two on the order of 10's of hours with negative and positive correlation values of less than 0.4. The time lags associated with these maxima were negative however, implying that the wind was lagging the current. In the v direction results were a little more as expected. The correlations were all positive and had maxima at time lags of 0 to +3 hours, with the exception of the 20 m current. The correlation values were not high however. The largest value was 0.32 at 4 m.

A correlation between the magnitude of the velocity at 2 m, where the influence of wind was expected to be the greatest, and the magnitude of the wind at Ballenas was equally poor. It had a very flat time lagged cross-correlation series with the maximum at 0 time lag. This poor correlation showed that when the wind was strong the current was not necessarily strong in any direction.

Although it appeared that wind and current were poorly related, the data were rotated to see if the correlations would improve. Contributions to the current by the wind need not be in the same direction as the wind. Also wind and current at the mouth of the bay (inside NAN 20) may not be in the same direction as at NAN 20. Wind in the Strait of Georgia obviously tends to blow northwest or southeast. Thus east-west and north-south components have roughly the same variance. Topographic effects could be funneling the wind and affecting its direction in and out of the bay. Observations in the field during the experiment support this idea. A wind from the southeast appeared to blow forcibly straight into the bay (westward) at the mouth. In a wind from the northwest the bay

was much more sheltered. Bathymetry could affect currents in the same manner. The location of the mooring at NAN 20 was also a consideration. Measured currents were probably affected by currents flowing up and down the Strait as NAN 20 is just beyond the mouth of the bay. To consider these possibilities principal axis rotations were done.

Principal axis rotations

A principal axis rotation rotates vector data such that the variance in the data is at a maximum along one axis, the principal axis, and a minimum along the other. The equation relating the variance in one coordinate system to the new one under a rotation of θ is:

$$\overline{u'v'} = \overline{uv}\cos 2\theta - \frac{1}{2}(\overline{u^2} - \overline{v^2})\sin 2\theta \quad (3.4)$$

The primes denote the rotated components and the overbars averages. To minimize the variance in one direction (and thus maximize the variance perpendicular to that) $\overline{u'v'}$ is set equal to zero yielding:

$$\theta = \frac{1}{2}\arctan\left(\frac{2\overline{uv}}{\overline{u^2} - \overline{v^2}}\right) \quad (3.5)$$

Here θ is the angle of rotation to put u , v data into its principal coordinate system. Angles were calculated and subsequent rotations done for all data. Results are shown in table 3.4. The ratio of the variance along the principal axis to the variance perpendicular to it after the rotation (equation 3.6) is also presented in the table.

$$\text{Variance ratio} = \left(\frac{\overline{u'^2}}{\overline{v'^2}}\right) \quad (3.6)$$

The ratio indicates how isotropic the record is. For a completely isotropic situation the variance ratio would be one.

As expected wind data from Ballenas had a strong principal axis in the northwest, southeast direction. Current data however were more isotropic with almost as much

Location	Angle	Variance ratio
Ballenas	-39deg	8.1
2 m current	81deg	1.8
4 m current	-32deg	1.3
7 m current	-26deg	2.2
12 m current	-43deg	3.3
20 m current	-7deg	5.9

Table 3.4: Angles for principal axis rotations for 1992 current and wind data.

variance along the calculated principal axis as along the perpendicular axis, with the exception of the 20 m data. The maximum currents at 20 m were in and out of the bay as expected within the channel due to bathymetry. Note that although the angles of rotation vary greatly amongst depths in the current data, they have little meaning due to the isotropic nature of the currents.

To fully investigate possible wind effects, cross-correlations were done between all possible combinations of the principal component of wind at Ballenas and current data at all depths. Also rotations were done of 2 m currents in 10 degree steps over 180 degrees and the resulting u was compared to the principal wind. In this way all possible rotations were considered. Note that the rotation is not sensitive to small changes in θ as the derivative of the \cos function with respect to θ is very small for small $d\theta$, thus 10 degree steps provided sufficient resolution.

The results confirmed the lack of correlation between wind and current at the mouth of Nanoose bay. The highest correlation values were found between the principal component of the wind and the north-south current components. The values were around 0.5 with no time lag (table 3.5). This correlation corresponds to a wind blowing to the north west causing a northerly flow. In the u direction however the maximum correlations occurred with negative time lags indicating that the current was leading the wind at those maxima. Values were around 0.4 as they were before the winds were rotated (table 3.5). With

First data set	Correlation	Time lag (hrs)	Second data set
Ballenas u	-0.27	-15	2 m u
Ballenas v	0.31	3	2 m v
Ballenas wind speed	0.39	-3	2 m current speed
Principal Ballenas	0.28	-9	2 m u
Principal Ballenas	0.52	0	2 m v
Principal Ballenas	0.41	-9	4 m u
Principal Ballenas	0.55	0	4 m v
Principal Ballenas	0.42	-6	7 m u
Principal Ballenas	0.52	0	7 m v
Principal Ballenas	-0.40	-30	12 m u
Principal Ballenas	0.53	0	12 m v
Principal Ballenas	-0.23	-21	20 m u
Principal Ballenas	-0.32	-33	20 m v

Table 3.5: Maximum wind and current cross-correlations.

the exception of the 12 and 20 m correlations, values were positive. Here the positive sign indicates that a wind blowing from the northwest is related to a current traveling westward into the bay. This result seems to indicate that there is no strong relationship between current and wind that can be found with cross-correlations. The time series of the principal component of the Ballenas wind with both components of the 2 m current are shown in figure 3.7.

The time-lagged auto-correlations of the north-south current components were very flat showing little periodicity with the exception of the current at 20 m. This current showed some periodicity in auto-correlations at roughly 2 and 4 days, although the amplitudes were low. These periods are often associated with weather fronts.

Cross-correlations are done in the time domain. It is recognized that a comparison between records in the frequency domain (coherence analysis) can provide a more complete relationship as destructive interference between signals that are not in phase may occur in the time domain. At this point a coherence analysis was not done as it appeared that it would not improve results sufficiently to provide a predictive relationship between

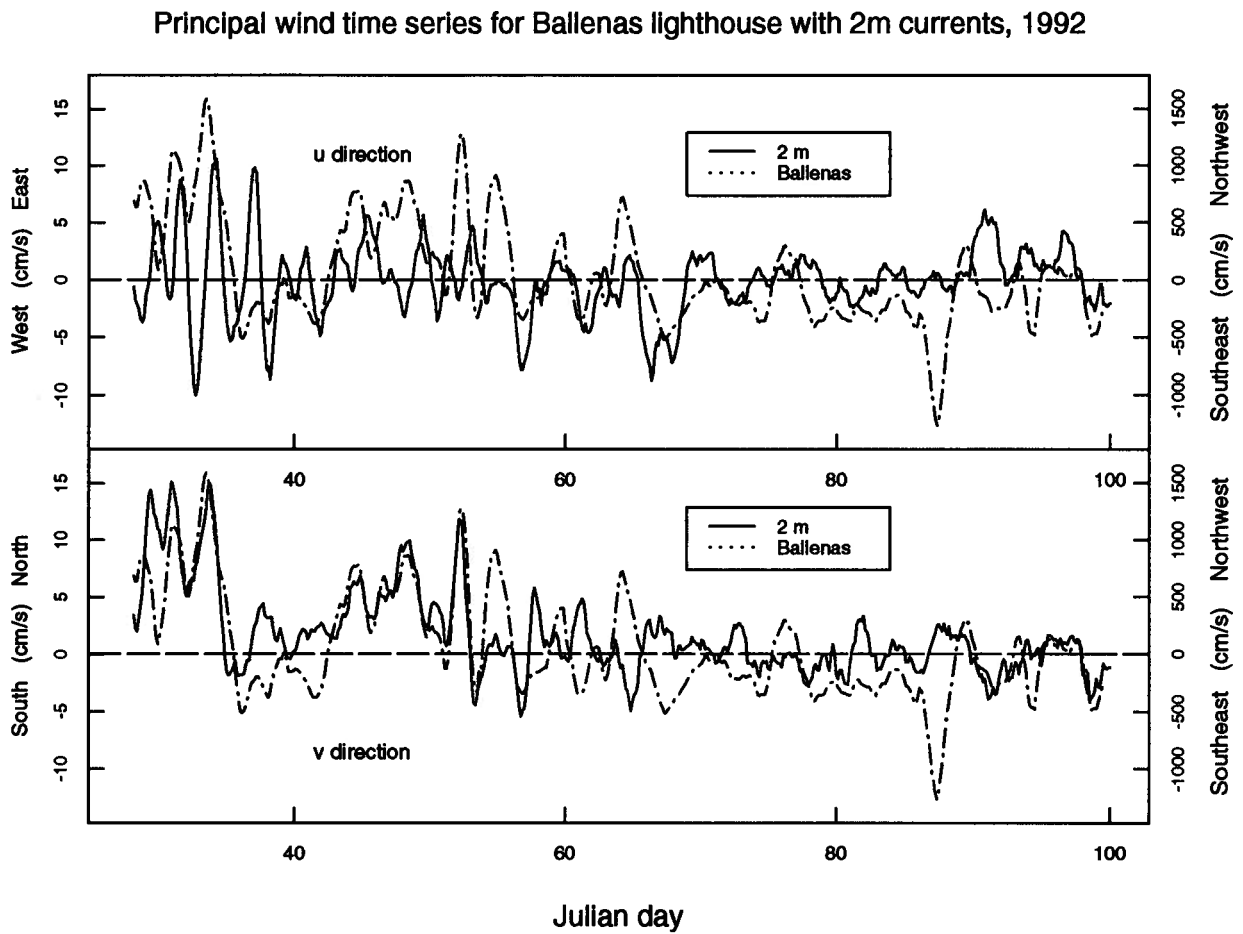


Figure 3.7: Time series of the principal component of the wind for Ballenas Island light-house and 2 m currents.

residual current and wind.

The conclusion of this investigation was that the near surface residual circulation in the Strait of Georgia is complicated. It could not be described only in terms local wind forcing. As a result an extrapolation of current data from wind data for the 1993 season was not possible.

For all following considerations involving current, the east-west component, essentially in and out of the bay, was used.

3.1.4 Advective exchange between Nanoose bay and the Strait of Georgia

The purpose of having an array of current meters at the mouth of Nanoose bay was to estimate advective exchange between the bay and the Strait. This estimate was done to determine if phytoplankton could be carried out of the bay and possibly seed the Strait. Thus the velocity in the advective term in equation 1.13 was provided. Also a flushing time for the bay was estimated to determine its potential for phytoplankton growth.

To get an overall picture of the net transport during the study period a running integral, $\int_0^t u(t)dt$ was calculated for the entire record at each depth. Here u is the residual velocity and dt is 1 hour.

$$Net\ transport(t) = \int_0^t u(t)dt \quad (3.7)$$

This running integral was then plotted against time and is shown in figure 3.8. It was also hoped that the net transport would yield information about the residual circulation.

The integral plotted against time is cumulative. It has units of length, shown as km in figure 3.8. This measure represents a volume flux when multiplied by the cross sectional area perpendicular to the current direction spanning the mouth of the bay.

The most notable feature in figure 3.8 is that the net transport at 4, 7 and 12 m is into the bay. At 2 and 20 m fluctuations add over time to yield a net transport near

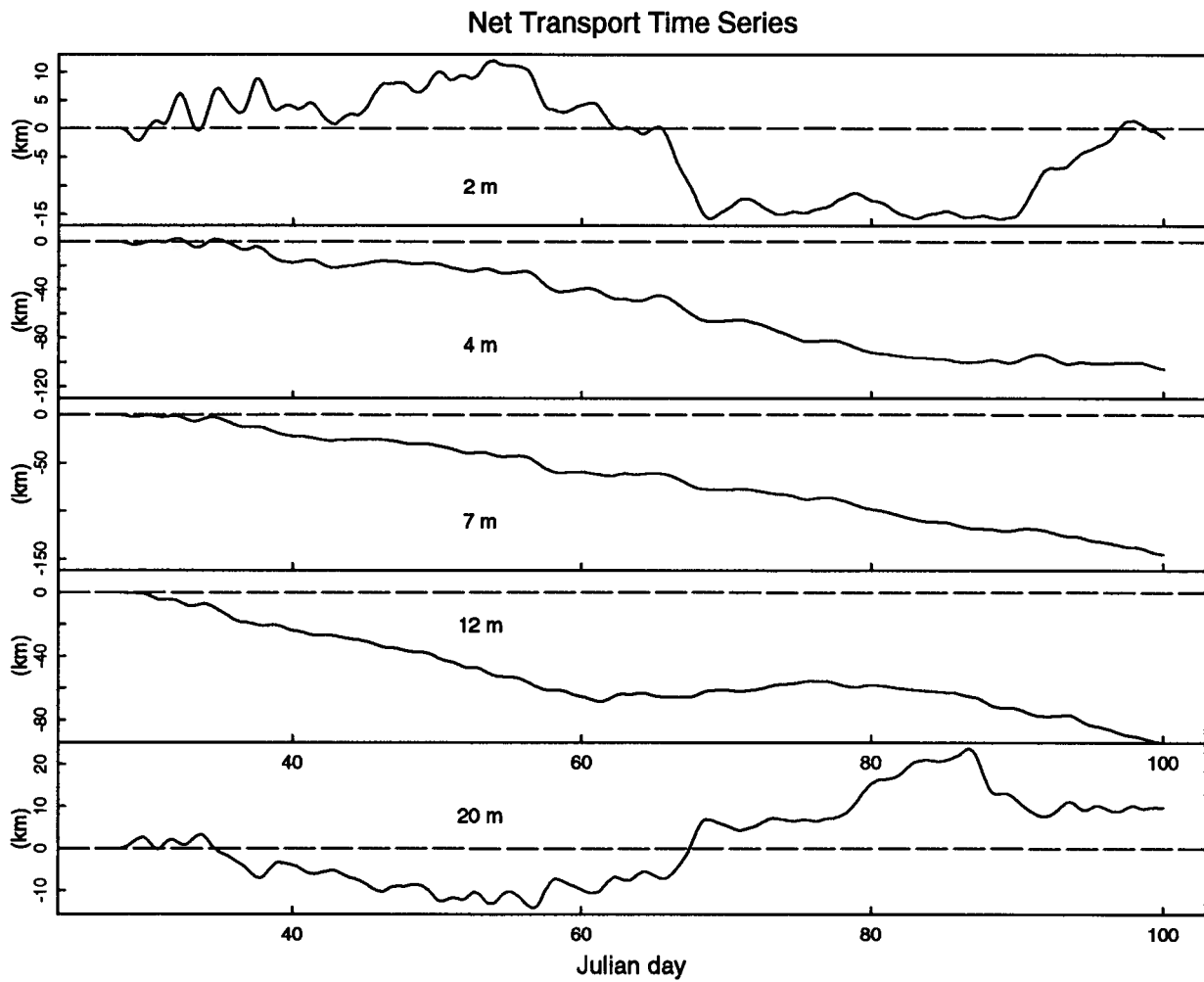


Figure 3.8: Net transport plotted as a running integral with time. The positive direction is eastward (out of the bay) and the negative direction is westward.

zero, although at different times during the record there was appreciable transport in both directions. Note the much smaller length scales on the y axis at 2 and 20 m. At 2 m it seems that wind and other effects cause fluctuations that cancel one another. At 4, 7 and 12 m however it appears that the residual circulation was generally into the bay. The density time series suggests that water flowing inwards tends to be less saline. The possible relationship between current direction and density changes with time is investigated in section 3.1.6.

When net transport at all depths was added together mass continuity was not obeyed as the data show net inward transport. The array of current meters obviously did not measure all transport in and out of the bay, probably because the array was not deep enough. There must be transport out and it is assumed to be at depth, although it is generally not seen at 20 m. There were however several periods of strong inflow at the middle depths where outflow was seen at 20 m, for example around day 56 and again around day 68. This outflow at 20 m can best be seen in fig 3.9 which is discussed in the next section. The depth of the shallowest part of the mouth of the bay is 20 m, however the mooring was located in 50 m of water. To account for water coming out of the bay it is suggested that deeper water in the bay is often more dense than water outside at the same depth. The dense water moves over the 20 m sill and then sinks down as it flows out because it is more dense than the surrounding water and thus is not detected at the mooring. Secondly, it is possible that there is cross-channel variation in the current. This variation may also account for some of the outflow that is not observed in the mass balance at the mooring location.

3.1.5 Flushing and stability

The running integral $\int_0^t u(t)dt$ vs. time shows that transport in one direction is often maintained over a time period long enough for several or more km to pass consecutively.

Using the length of the bay and scaling by a width factor ($\frac{W_{mouth}}{W_{bay}}$) to account for stronger flow through the narrows, a distance of 5 km was determined to be a reasonable for one complete flushing. For each depth in figure 3.8 a $\Delta \int_0^t u(t)dt$ of 5 km or more therefore represents a flushing of the layer at that depth.

Using this distance as a limit, an index was determined. If the bay is flushed in a time scale faster than the generation time of phytoplankton, an increase in primary productivity will not occur in the bay. The index also shows the direction of advection, in or out of the bay, in each layer during the flushing event.

This index was calculated by using a running integral as in the case of the net transport. The integral starts at t_1 and continues adding $u(t)dt$ until t_2 , when the distance of 5 km is reached or just exceeded. The index was then calculated by dividing the integral (5 km or greater) by the time interval that it was calculated over as follows.

$$Flushing\ Index = \frac{1}{t_2 - t_1} \int_{t_1}^{t_2} u(t)dt \quad (3.8)$$

It was calculated as a function of t_1 . Once the sum of $u(t)dt$ added to 5 km and an index was calculated, the integral was set back to zero and restarted from $t_1 + dt$. Therefore for each time in the record there is a corresponding index. Note that the index is associated with the beginning of the time interval, thus it indicates flushing for the time period immediately following it.

A large flushing index corresponds to a complete exchange in a short time interval and an unfavourable period for phytoplankton growth. A small index indicates a long time interval for exchange and thus a favourable period for phytoplankton growth. A negative flushing index corresponds to inflow so that seeding of the outside waters from the bay is not possible. Such trapping of phytoplankton could allow a bloom in the bay which could be a source for seeding sometime later.

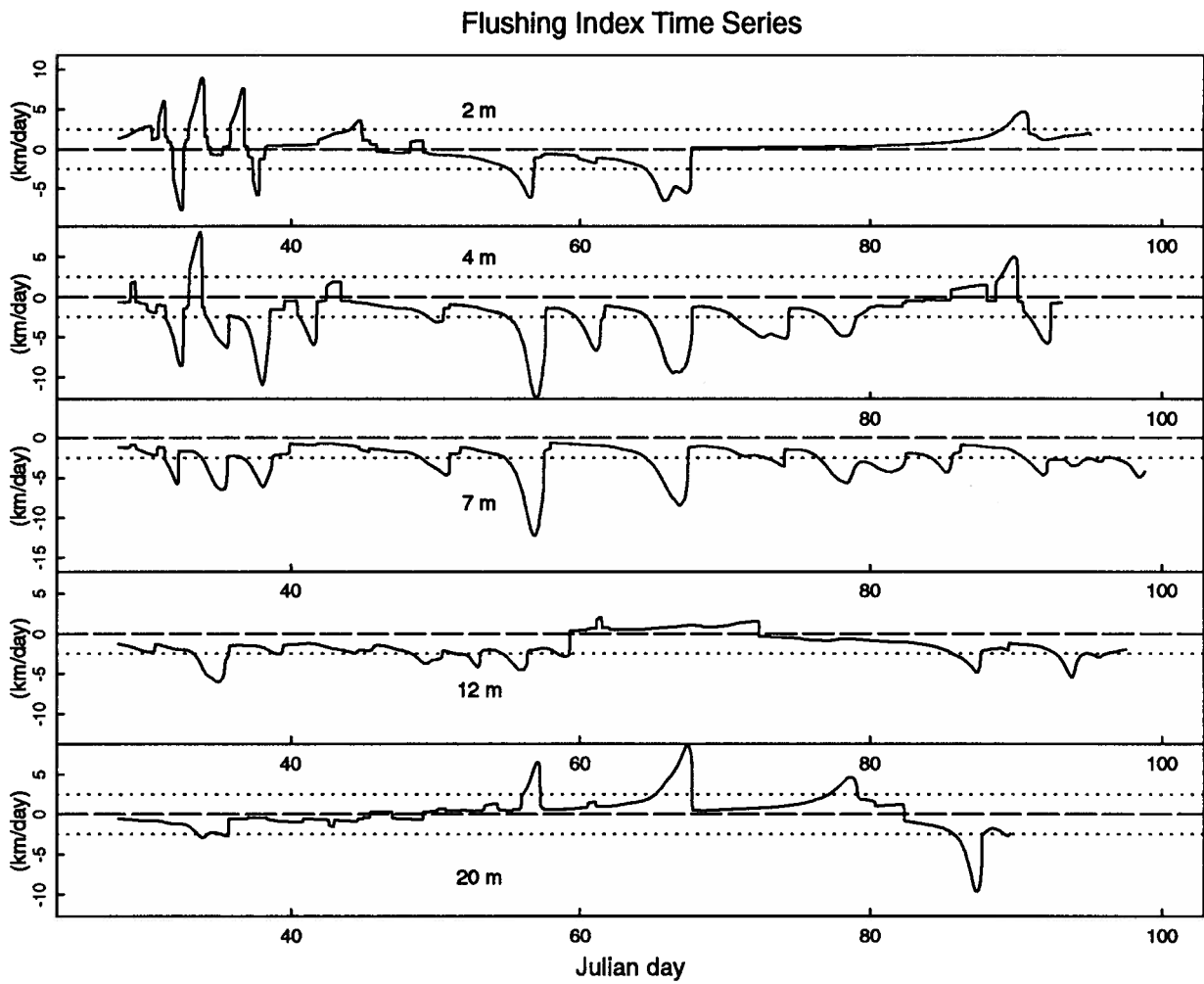


Figure 3.9: A phytoplankton flushing index, $\frac{1}{t_2 - t_1} \int_{t_1}^{t_2} u(t) dt$, as a function of t_1 for each depth.

Figure 3.9 shows the flushing index as a function of time for each depth. The index has units of velocity and was calculated in km/day. Considering the doubling time of phytoplankton to be around 2 days, a flushing index with the magnitude of 2.5 km/day provides a ceiling for phytoplankton growth. This ceiling is shown in figure 3.9. Although at depths of 4 and 7 m there was generally an appreciable constant inflow, at 2 m, which is where plankton was sampled, there were four periods which appear to be favourable for phytoplankton growth. The periods are; days 38 through 43, days 45 through 56, days 57 through 64 and days 68 through 89. Note that during two of the four time intervals (the first and the last) defined by the 2 m index, transport was out of the bay. During the middle two intervals transport is into the bay and these periods are subsequently terminated by high negative flushing indices. Note that the 4 m flushing index indicates a favourable period over days 45 through 55 and relatively favourable over days 68 through 89 (although during the latter period the index creeps below the -2.5 km/day ceiling on two occasions and is of the opposite sign of the 2 m index).

The index quickly indicates ranges of flushing times. The integral is only assigned to a time when enough water has passed at that depth to cause one complete exchange. Therefore each $(t_2 - t_1)$ is a flushing time. The plots in figure 3.9 show that under this analysis the bay can be flushed in a time scale of the order of days. Near the beginning of the record the index reaches its maximum at 2 m suggesting that a volume exchange can occur in as little as one day in the upper layer. During the period beginning at day 70 however $(t_2 - t_1)$ becomes several weeks.

3.1.6 Density changes and current direction

The predominant inflow in the middle layers at the mooring prompted an examination of the density of the incoming water. The assumption was that it was lower density brackish water, which is ultimately from the Fraser River, that was flowing in. The density time

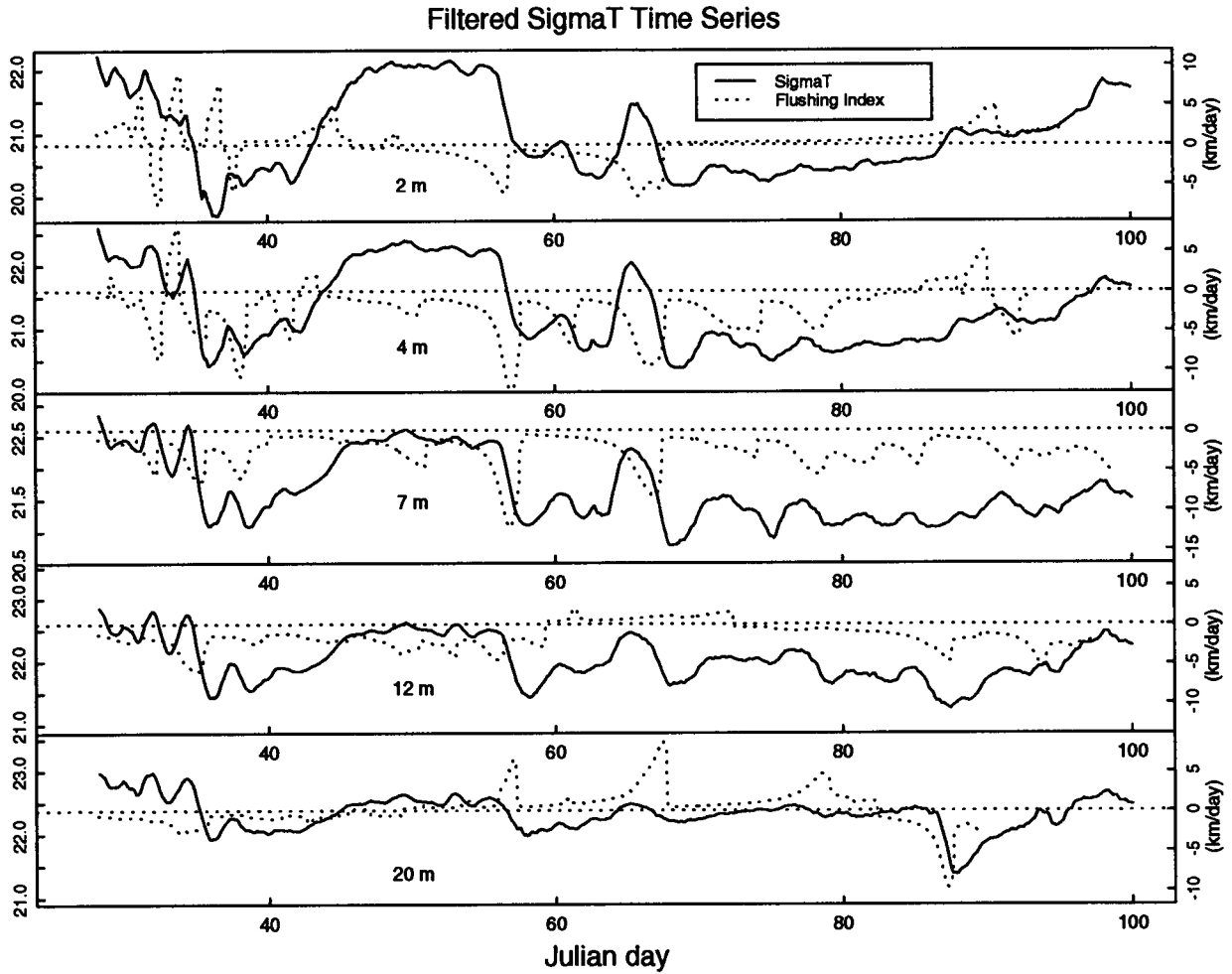


Figure 3.10: Filtered σ_t (kg/m^3) time series shown with the flushing index at each depth.

series at the mooring confirmed this assumption.

Filtered σ_t at each depth is shown in figure 3.10 with the flushing index to indicate the direction of appreciable volume transport. During periods of strong inflow the change in density with time often was negative. After an appreciable inflow the water at a given depth was less dense. Examples are seen around days 36, 56 and 69 particularly at 4 and 7 m. Likewise, during outflows the density change with time was often positive, although positive changes in σ_t also occurred during periods of little or no outflow, (for example the large increase in σ_t around day 42).

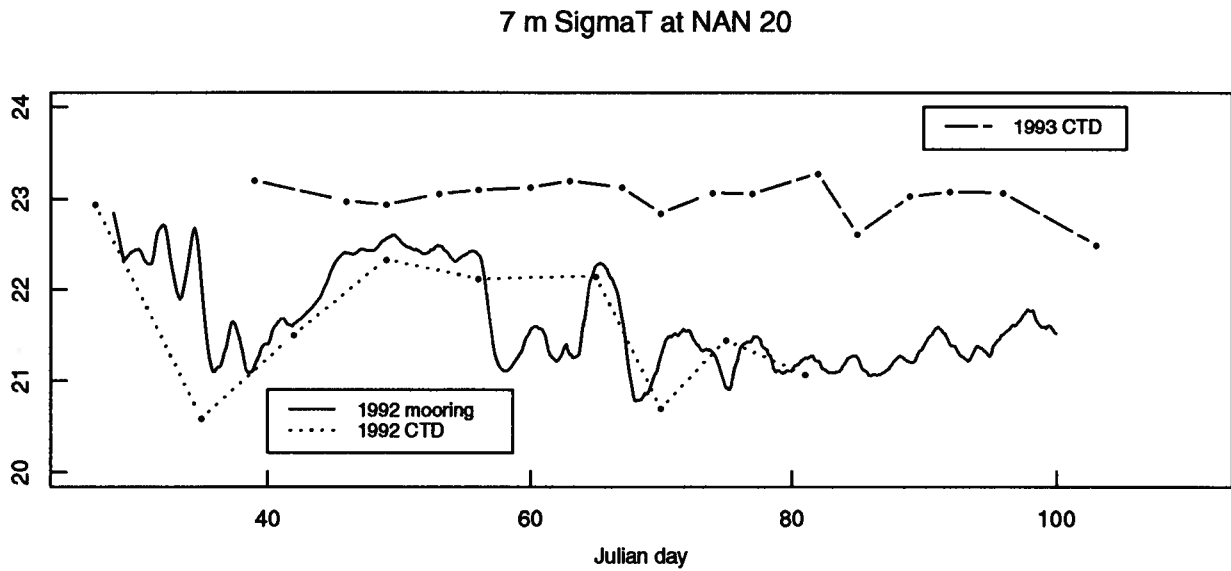


Figure 3.11: σ_{t7} (kg/m^3), at NAN 20 from the mooring and CTD profiles.

As no current data were measured in 1993 and no relationship between current and wind was found to allow an extrapolation for 1993 currents, it was desired to find a means of indicating at least the probable current direction with no direct measurement. To do so, the density time series at 7 m was chosen. Its signal was strong while having less high frequency noise than the 2 and 4 m time series. The signal to noise ratio became important as in 1993 only spot σ_{t7} values were available via CTD casts, instead of a comparatively continuous record as in 1992.

A comparison between σ_{t7} at the mooring and the flushing index (see figure 3.10) showed that during the 1992 season large volume transports into the bay were correlated with decreasing σ_{t7} .

In 1993 therefore, although density profiles are much different than in 1992, the change in σ_{t7} with time was used to suggest current direction. Figure 3.11 shows σ_{t7} as a function of time for both 1992 and 1993 with the continuous density time series from the mooring. Note that the CTD spot measurements are indicated by points (which were simply joined by a straight line). The 1992 CTD data follow the 7 m mooring record

well. CTD measurements such as on day 35, which do not lie on the mooring curve are due to the fact that the mooring data has been smoothed by 25 hour averaging. It is recognized however that the information between CTD measurements is unknown. Note the period between day 59 and 64 in 1992. The CTD data do not show the drop in σ_t that the mooring does. In 1993 however the sampling interval was half of that of 1992 so there is higher temporal resolution. Figure 3.11 also shows the large difference in σ_t between years. Fluctuations appear to be much smaller in 1993 and overall σ_t higher.

3.2 Density profiles

Vertical density profiles were sampled using an S4 current meter as a CTD. These profiles provided snapshots in time of density structure for each day that sampling was done at each station.

Estimating the extent of vertical mixing in the water column is essential in evaluating growth conditions and understanding why a bloom may occur in some places and not in others. Different locations can be compared in terms of their growth potential. One can also determine whether or not the depth of the bay limits the vertical mixing of phytoplankton and thus allows a bloom to occur earlier at that location.

Initially the mixed depth was estimated from each profile to represent the extent of vertical mixing for phytoplankton. The mixed depth approach proved inadequate given the data set. Instead some parameters were developed from the time series of density profiles to indicate the degree of mixing of the water column and thus potential increases in phytoplankton concentration. The different methods used in this analysis, successful and not, are presented in the following sections.

3.2.1 Mixed Depth

Originally the intention of measuring density structure was to allow estimation of the mixed layer depth. Given this estimate along with the critical depth, the Sverdrup criterion for a spring bloom could be considered.

In viewing the density profiles on different days it was realized that the mixed depth was not always obvious. Profiles were usually much more complex than two fairly homogeneous water masses with a large density gradient separating them. Density structure differed radically depending on day and location. An objective means of determining the mixed depth for all profiles was desired, which led to the use of the Freeland and Farmer approach [9] as described in Chapter 1. Density profiles were integrated and differentiated to provide measures of both the potential energy and the buoyancy frequency as in equations 1.3 and 1.5 respectively. Buoyancy frequency profiles were then used to solve for the eigenvalues in equation 1.4 through a series of iterative integration (deYoung [30]) and thus obtain the first mode internal wave speed. Both up and down casts were used and the results of each were averaged. Although the approach provided a uniform method to look at all types of profiles, it failed in addressing the pertinent question: where were phytoplankton in the water column?

For many profiles the two-layer fit was inappropriate to the given density structure. Where a solution was possible, internal wave speeds were in the range of 10 to 20 cm/s and potential energy parameter (χ) was around 10 to 12 kg/m³. Three very different representative profiles are presented in figure 3.12 with the results of the mixed depth calculation and a discussion as to why or why not they may represent the depth to which phytoplankton are mixed. All are from NAN 10, the station inside the bay.

Results were reasonable for the April 6, 1993 profile shown in figure 3.12. The approach predicts a mixed depth of 9.5 m, which is a bit larger than an intuitive evaluation

of about 8 m. This type of profile was the exception within the entire data set. The following two structures are representative of those that occur more often.

The second example was taken on February 11, 1992. The surface layer in this case is quite stratified. Mixing would be inhibited and if this profile were to persist over time, phytoplankton could be confined near the surface. The model fits the profile to a structure such that the top layer is 1.8 m and σ_2 is 22.0 kg/m^3 when σ_1 is from 1.5 m instead of from 2 m. Note that σ_1 was changed so that the equations could be solved and the profile fit to the model. The estimated mixed depth is consistent with phytoplankton being kept near the surface.

A third profile from March 4, 1993 indicates a uniformly stratified situation. The two-layer model fails in this case yielding a non-real value for h , the thickness of the upper layer. The failure could be interpreted as mixed to the bottom in a single layer. This interpretation would imply that phytoplankton were mixed at least to the bottom of the cast, which may be the case. There is still a small uniform density gradient however which could be enough to prevent turbulent mixing. The vertical shear of the horizontal velocity necessary for turbulence was considered to determine whether or not phytoplankton were being mixed throughout. This consideration is the topic of the next section.

3.2.2 Density Gradients and Velocity Shear

In determining the depth to which phytoplankton are mixed, results of the two layer model may be questionable or ambiguous. Density gradients still exist within the region that is assumed to be well mixed. The Richardson number, as defined in equation 1.7, was used to estimate the velocity shear necessary for turbulent mixing to occur given the density gradient from the experimental profile. R_i greater than $1/4$ is required everywhere in the fluid to ensure laminar flow. The velocity shear calculated using this

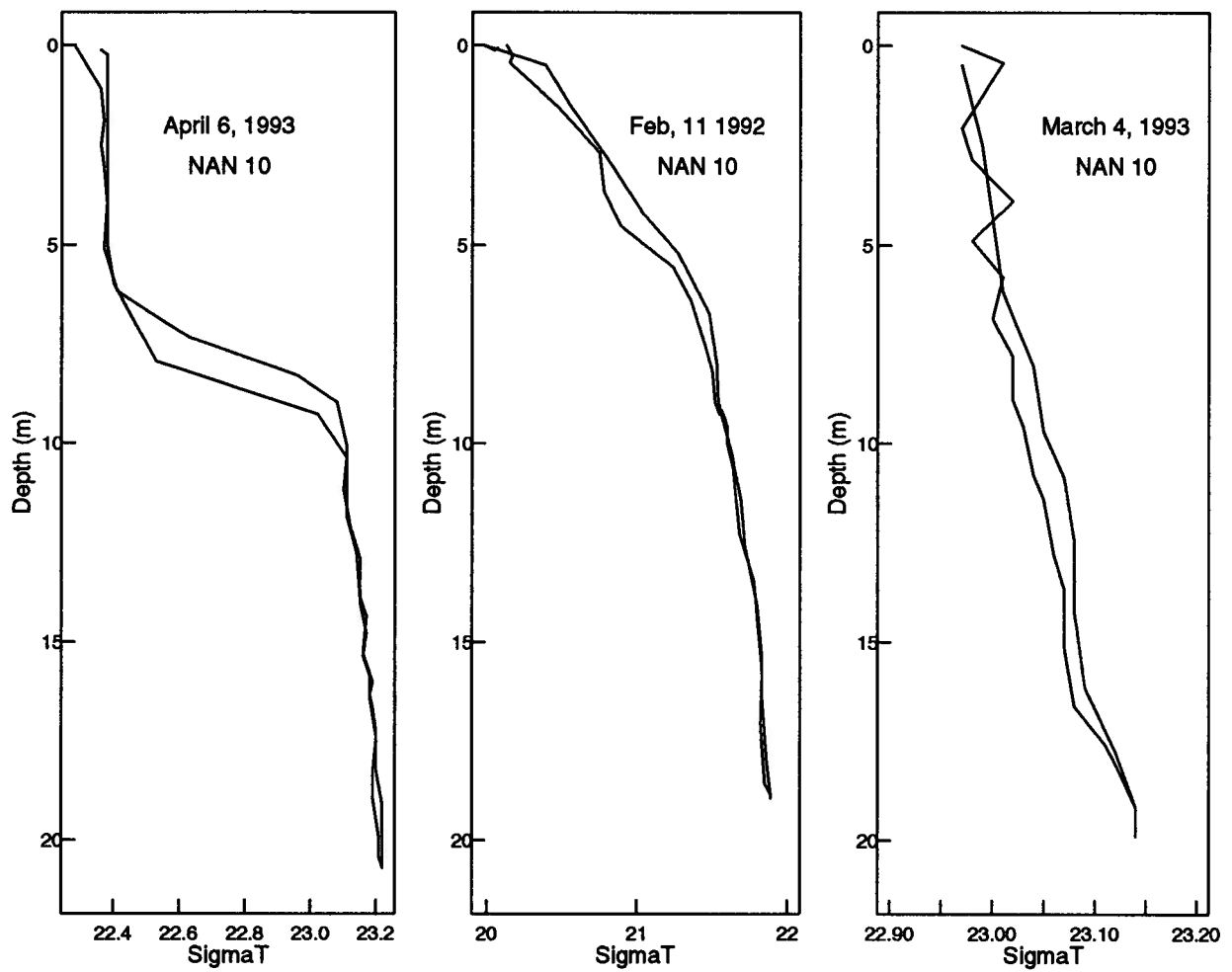


Figure 3.12: Representative density profiles at NAN 10. Note that both the up and the down casts are shown.

number therefore represents a lower limit necessary to ensure that phytoplankton are not being mixed over the region in question. Since $\frac{dU}{dz}$ occurs as a square in the Richardson number, only the magnitude will be considered. If the true velocity shear is greater than that calculated, then turbulent mixing is occurring.

An upper limit for the true velocity shear was set by comparing the raw hourly velocity measurements from the mooring data at 2 and 4 m. During the first two weeks of the record where the variance was higher, $\frac{dU}{dz}$ ranged from 0-7 cm/s/m, but was less than or equal to 1 cm/s/m approximately 70% of the time. In the latter part of the record (day 70 onward) $\frac{dU}{dz}$ ranged from 0-3 cm/s/m, and was less than or equal to 1 cm/s/m over 80% of the time. Velocity shear between 4 and 7 m was generally smaller by a factor of two. The limit in velocity shear determined to be reasonable in the study area at this time was set at 1 cm/s/m. Thus it will be assumed that any structure associated with a $\frac{dU}{dz}$ necessary for turbulence that is greater than 1cm/s/m is not being mixed. Note that this limit is only used where the uncertainty in the estimation of the density gradient allows. The uncertainty was determined by simply estimating the maximum and minimum gradient from the data subjectively. This estimate was made by using any scatter or noise in the cast as well as differences due to reproducibility between the up and down casts.

The resulting velocity shears (necessary for $R_i=1/4$) for different profiles are shown in table 3.6. Note that the $\frac{dU}{dz}$ presented in the table was calculated over the estimated mixed layer depth which is also shown in the table. Profiles that were apparently mixed to the bottom of the cast are listed in the table with B for the mixed depth. All casts except at NAN 30 in 1993 were done to about 20 m, depending on line angle. On some occasions casts are 1 or 2 m shallower where it was difficult to maintain position. In 1993 NAN 30 casts were done to 40 m. Where weather did not permit sampling, dashed lines are shown in the table. Only the results for the NAN 10 profiles that are presented in

this chapter along with the results for stations 20 and 30 on the corresponding days for comparison are shown. These results represent the overall range.

		NAN 10		NAN 20		NAN 30	
J day	h (m)	$\frac{dU}{dz}$ (cm/s/m)	h (m)	$\frac{dU}{dz}$ (cm/s/m)	h (m)	$\frac{dU}{dz}$ (cm/s/m)	
1992							
Feb 4	35	3.4 33 \pm 5	4.0	28 \pm 5	–	–	
Feb 11	42	1.6 12 \pm 3	4.1	4.0 \pm 0.5	4.3	12 \pm 4	
Feb 18	49	2.3 20 \pm 4	3.8	10 \pm 2	7.1	4 \pm 1	
Feb 25	56	<1 30 \pm 5	4.3	22 \pm 4	11	7 \pm 2	
1993							
Feb 22	53	B 2 \pm 2	B	2 \pm 1	B	1 \pm 1	
Feb 25	56	B <1 \pm 0.5	B	<1 \pm 0.5	B	1 \pm 1	
March 1	60	B 2 \pm 1	B	2 \pm 1	–	—	
March 4	63	B 2 \pm 1	12	2 \pm 1	B	1 \pm 1	
April 6	96	9.7 1.0 \pm 0.5	6.7	<1.0 \pm 0.5	19.8	2 \pm 1	

Table 3.6: Values of dU/dz are calculated from the Richardson number ($R_i=1/4$) using experimental density profiles to determine the Brunt Vaisala frequency.

3.2.3 Temporal changes

The full approach considering the density structure in terms of necessary velocity shear was still inadequate in predicting favourable enough situations for the occurrence of a spring bloom. For example, in the 1992 data set each density profile was stratified enough to suggest that a bloom should occur throughout the study period under the above analysis. Nutrients were certainly not limiting, and given the vertical structure, light was not limiting either. In 1993 profiles often had small density gradients that were constant to the bottom of the cast (see table 3.6). Velocity shears required for turbulent mixing were generally as low as the 1 cm/s/m limit within uncertainty and thus assumed to be well mixed. In 1992 phytoplankton concentrations were low however, and in 1993 they were high in the bay throughout the study.

The profiles are spot measurements. Nothing is known about the temporal variability. Time scales necessary for phytoplankton to reproduce must be considered. To include this variability the time series of the profiles at a given location were examined. Two general parameters were used to do so. First the change in the mean density gradient over the entire profile with respect to time was calculated.

$$P_1 = \frac{\Delta}{\Delta t} \left(\frac{\Delta \sigma_t}{\Delta z} \right) \quad (3.9)$$

Note that as z is depth positive downward, the more stratified the water column becomes the more positive $\frac{\Delta}{\Delta t} \left(\frac{\Delta \sigma_t}{\Delta z} \right)$ is. Second the change in σ_t at 20m (the lower limit of most casts) with respect to time was considered.

$$P_2 = \frac{\Delta}{\Delta t} (\sigma_{t20}) \quad (3.10)$$

The change in density gradient showed whether a structure was becoming more or less stable through change in overall stratification. A non-negative value of $\frac{\Delta}{\Delta t} \left(\frac{\Delta \sigma_t}{\Delta z} \right)$ was therefore considered a necessary stability criterion for non-mixing conditions.

The density at 20 m was used to indicate whether or not the same water mass was present. A large change in σ_{t20} would indicate new water and thus unfavourable growth conditions. The magnitude of $\frac{\Delta}{\Delta t} (\sigma_{t20})$ was required to be less than an upper limit for a bloom to be possible. The upper limit was set at $0.05 \text{ kg/m}^3/\text{day}$ using the 1992 results. This limit was determined using profiles from NAN 20, the location of the mooring, so that direct comparison with the mooring record would be possible. Profiles were chosen over a time period in which stratification increased and also when a large increase in phytoplankton concentration was observed. The time period used was day 70 through 75. The change in σ_{t20} is thought to correspond to an increase in stratification as opposed to a new water mass. The change could also be due to a slow exchange of water. Note that the sign of $\frac{\Delta}{\Delta t} (\sigma_{t20})$ was positive, while water at the surface became slightly less

dense (see figure 3.10). The current data show that volume transport at this time was very low (less than 10% of the bay's volume per day) and the σ_t time series show little variation.

Both of these parameters were required to indicate conditions necessary for a bloom to occur. Profiles from two favourable growth periods under this analysis are shown in figure 3.13. They are representative of the respective years that they were taken. In 1992 vertical structure in the bay was generally stratified while in 1993 profiles tended to be mixed and more saline throughout. Both situations in figure 3.13 however were stable with time. The 1992 example shows profiles spanning 7 days starting on February 18 (day 49). The net stratification increases during the period with the addition of brackish water at the surface while there is little change in structure below 4m. The second plot however indicates a very different situation that is favourable considering temporal variability of the two parameters defined above. The structure appears to be well mixed throughout the period spanning 4 days beginning on February 25 (day 56), 1993. There was a slight positive change in net stratification with time and $\frac{\Delta}{\Delta t}(\sigma_{t20})$ was essentially zero.

Figure 3.14 shows two very different poor growth periods inside the bay under this criterion. The first period suggests mixing while the second suggests flushing. The 1992 profiles are separated in time by one week. The earlier profile from February 4, (day 35) is well stratified with a large $\frac{\Delta\sigma_t}{\Delta z}$. One week later the density structure changed considerably. It is mixed with respect to the first and there is a large change in the density of the water at the bottom of the cast. It is much less dense. The second example from 1993 is also from the inside of the bay. Here the time between casts is only 3 days beginning on February 22 (day 53), 1993. In this case the change in net stratification is small but still negative. There is a change in σ_{t20} however as the water in the bay becomes more dense throughout the water column.

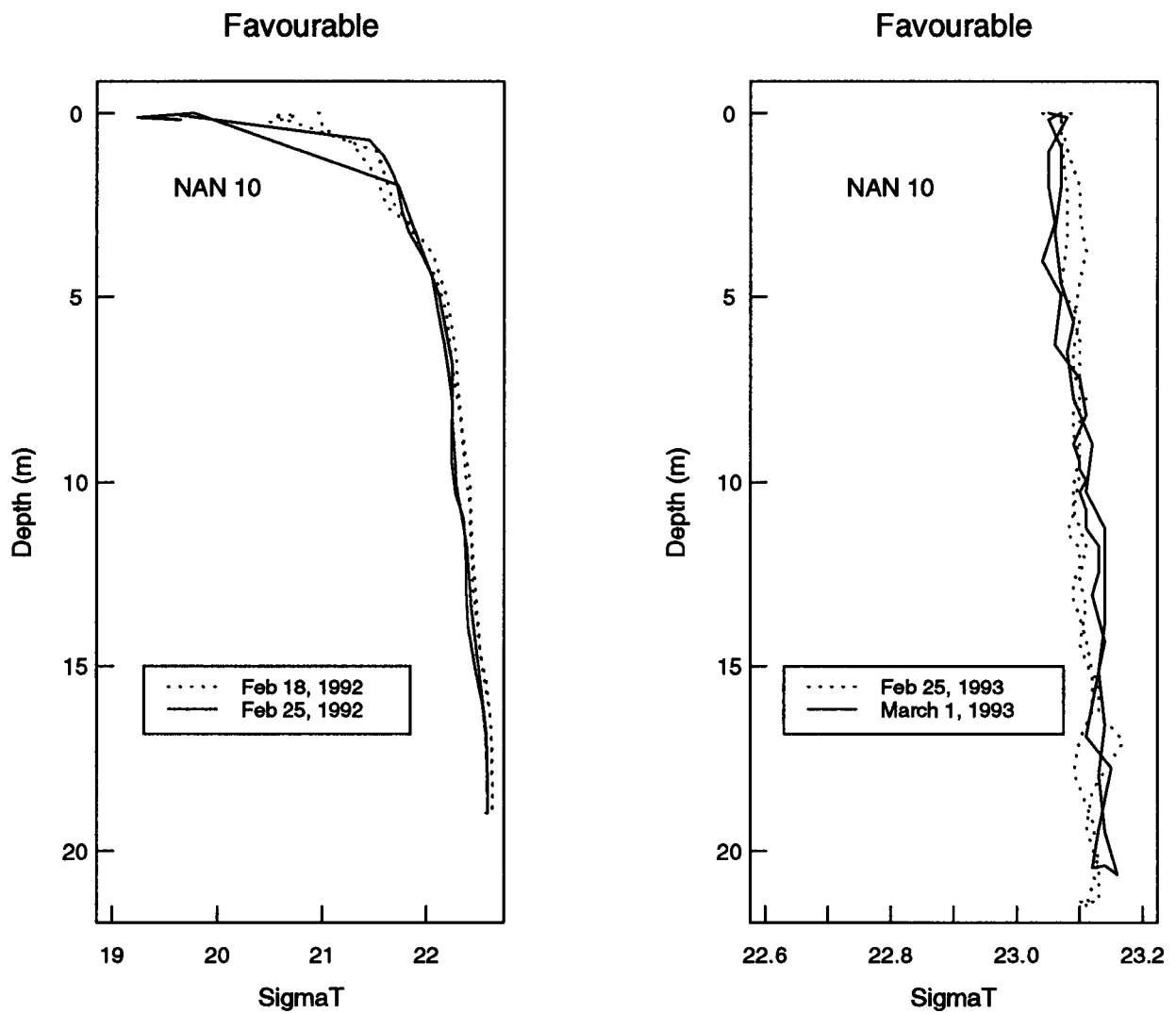


Figure 3.13: Density structure time series: for two favourable intervals.

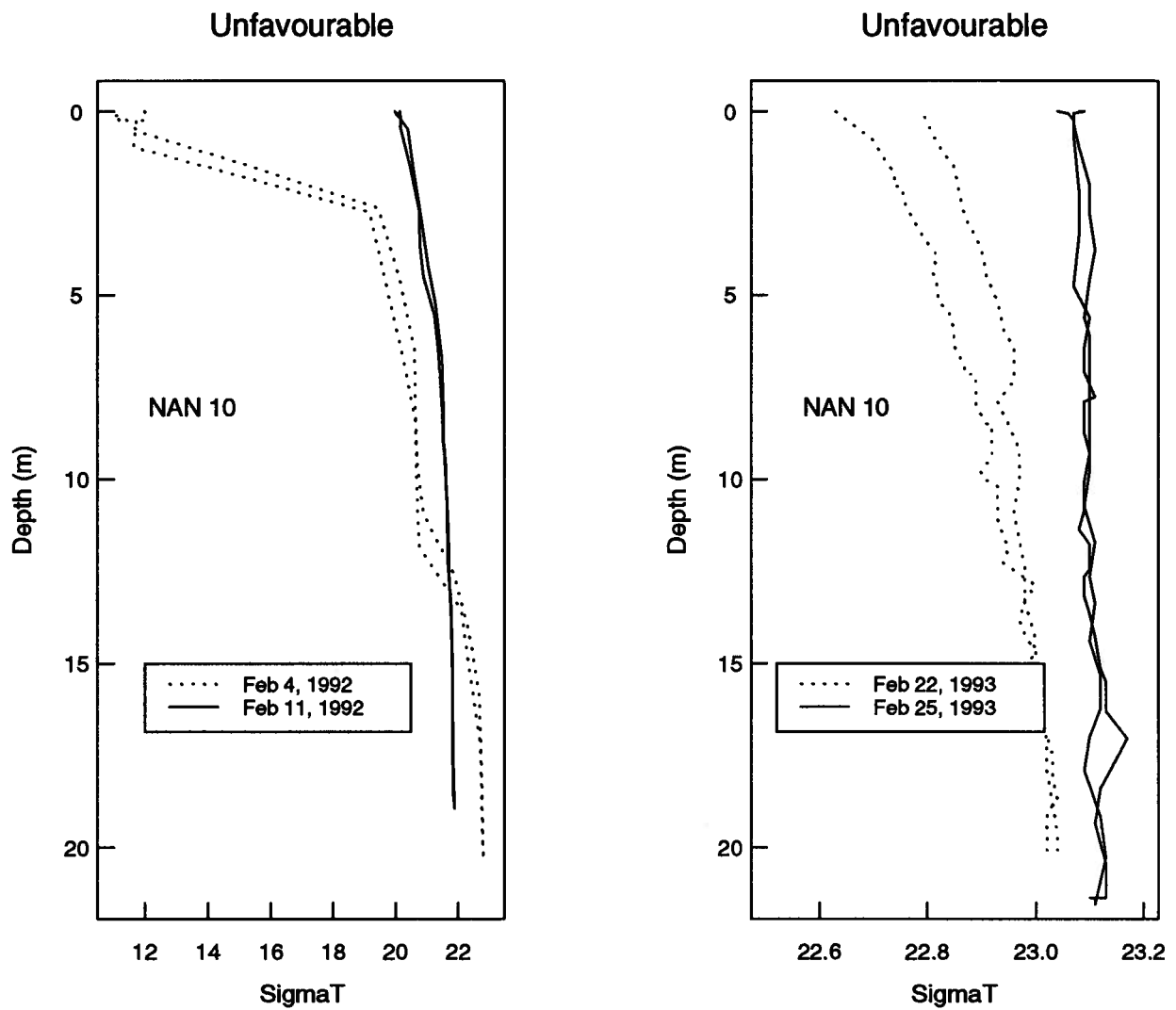


Figure 3.14: Density structure time series: for two unfavourable intervals.

The flushing index defined by the volume exchange as measured by current meters supports this method and agreement between the two is discussed in the next chapter. Although nothing is known about variation during the time between profiles, these parameters successfully form a minimum requirement for phytoplankton growth. The 1992 data are easily supported using the current data at the mooring when profiles were only taken once weekly. In 1993, when there are no current data, profiles were done twice weekly yielding a temporal resolution that is of the same order as the generation time for phytoplankton. The use of the two parameters therefore seems reasonable.

Using these criteria blooms within Nanoose bay were predicted, which is the subject of much of the following chapter.

3.3 Critical Depth

Critical depths, as described in chapter one, were estimated to measure light limitation to phytoplankton growth. Two sets of data were used; Secchi disc depth and solar radiation.

3.3.1 Radiation data

In 1992 there were some difficulties with condensation developing inside the bulb of the pyranometer. Condensation affected measurements by scattering some of the incoming light so that it was not detected. As a result there was a two week section in the study period in which a second pyranometer was also used. To scale the measurements and make them compatible over the entire record two calibrations were done between instruments, one in which both functioned with dry bulbs and one in which only one had condensation. It was found that condensation caused roughly 10% of the light not to be detected. In 1993 the use of dry desiccant in the pyranometers was perfected and no such problems occurred.

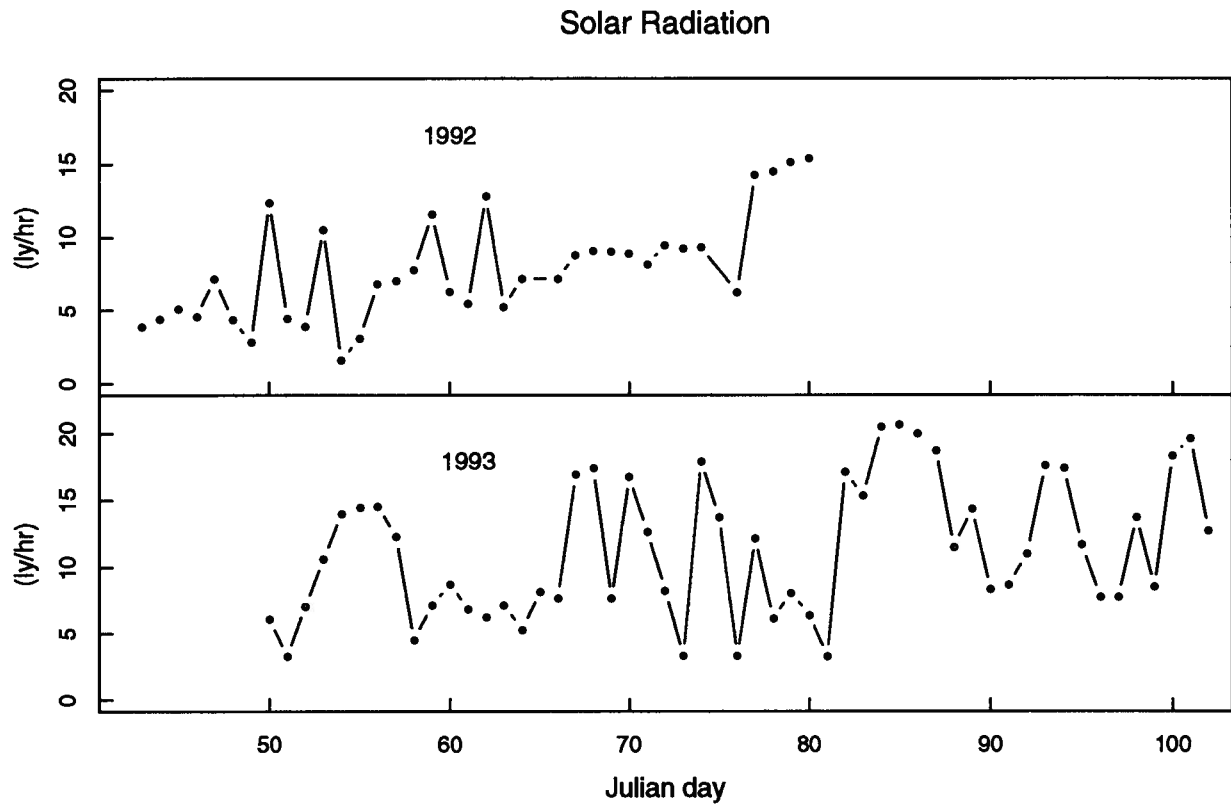


Figure 3.15: I_o and PAR as functions of time.

Radiation was directly measured in mV and converted to standard units of langley/hr using the instrument calibration. The time series of I_o , which are 24 hr integrated values, is shown in figure 3.15 for both the 1992 and 1993 data.

3.3.2 Secchi disc depth and critical depth

Secchi disc depths were measured at all stations. The 1992 results are shown in figure 3.16 and the 1993 results in figures 3.17 and 3.18. Decreases in Secchi depth generally coincide with either an increase in phytoplankton concentration or a period of rainfall in which terrigenous runoff is present. Both phytoplankton and terrigenous particles absorb and scatter light decreasing visibility.

Secchi disc depths and radiation measurements were combined to calculate the critical

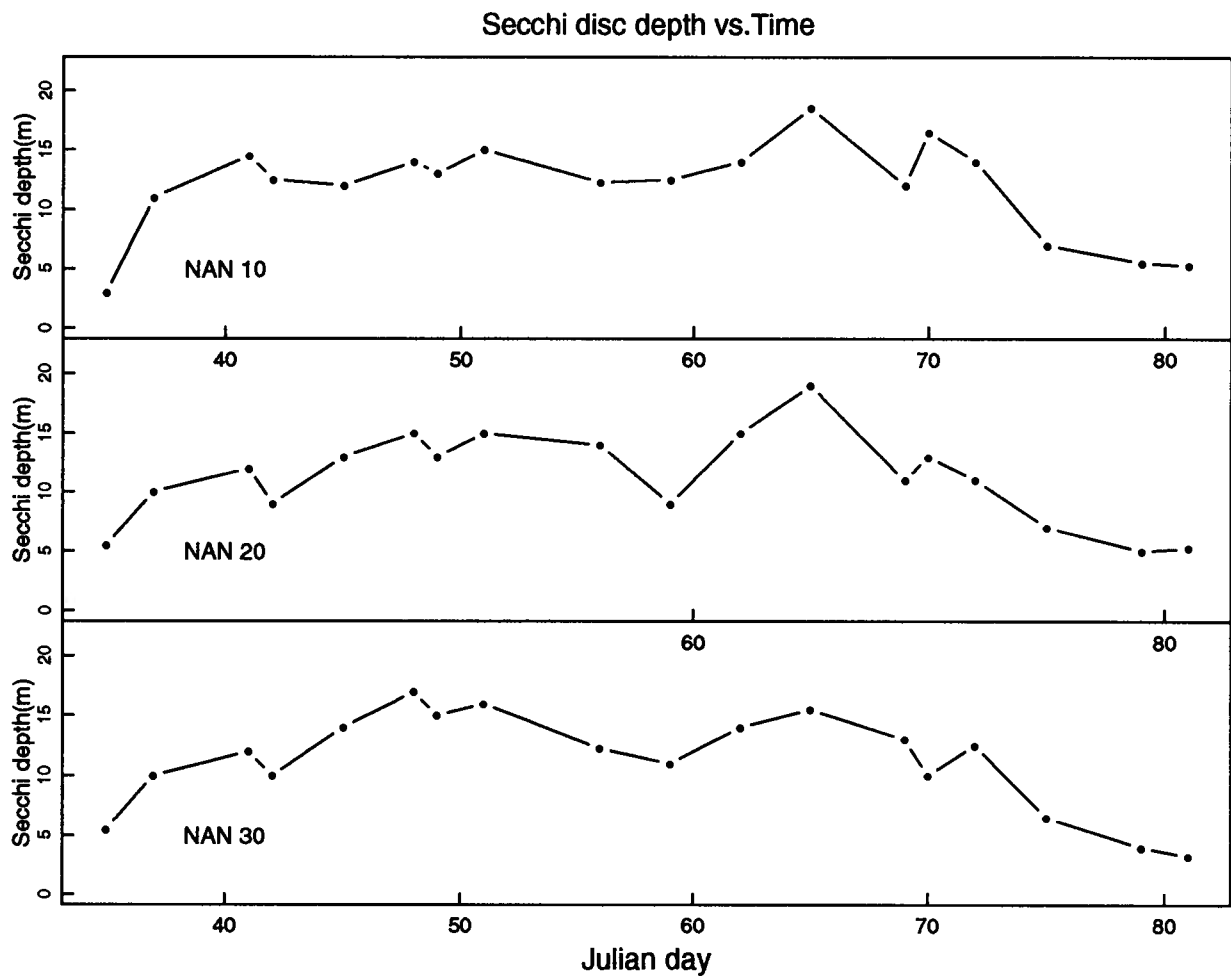


Figure 3.16: Secchi disc depth as a function of time for NAN 10, 20 and 30 in 1992.

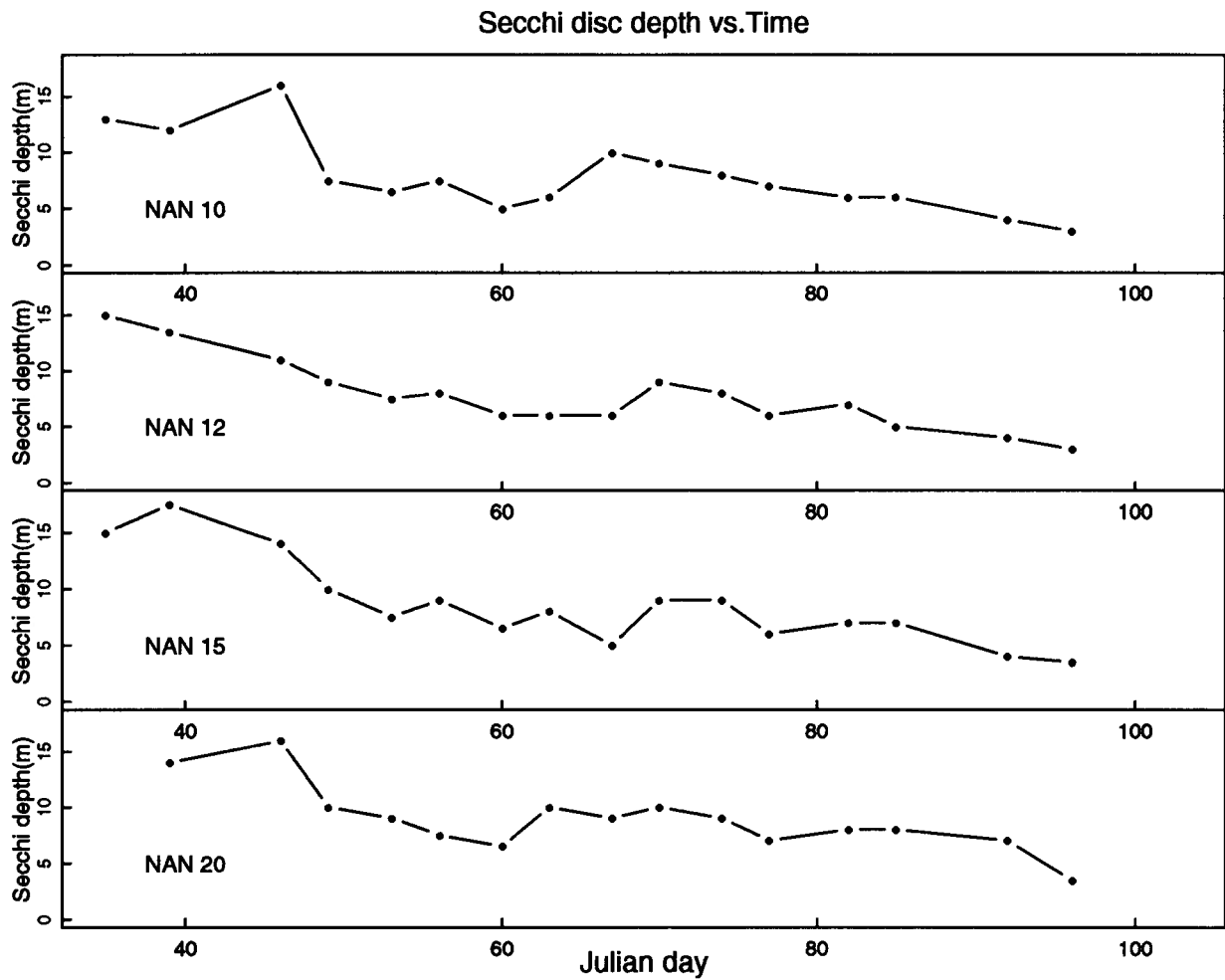


Figure 3.17: Secchi disc depth as a function of time for inside stations in 1993.

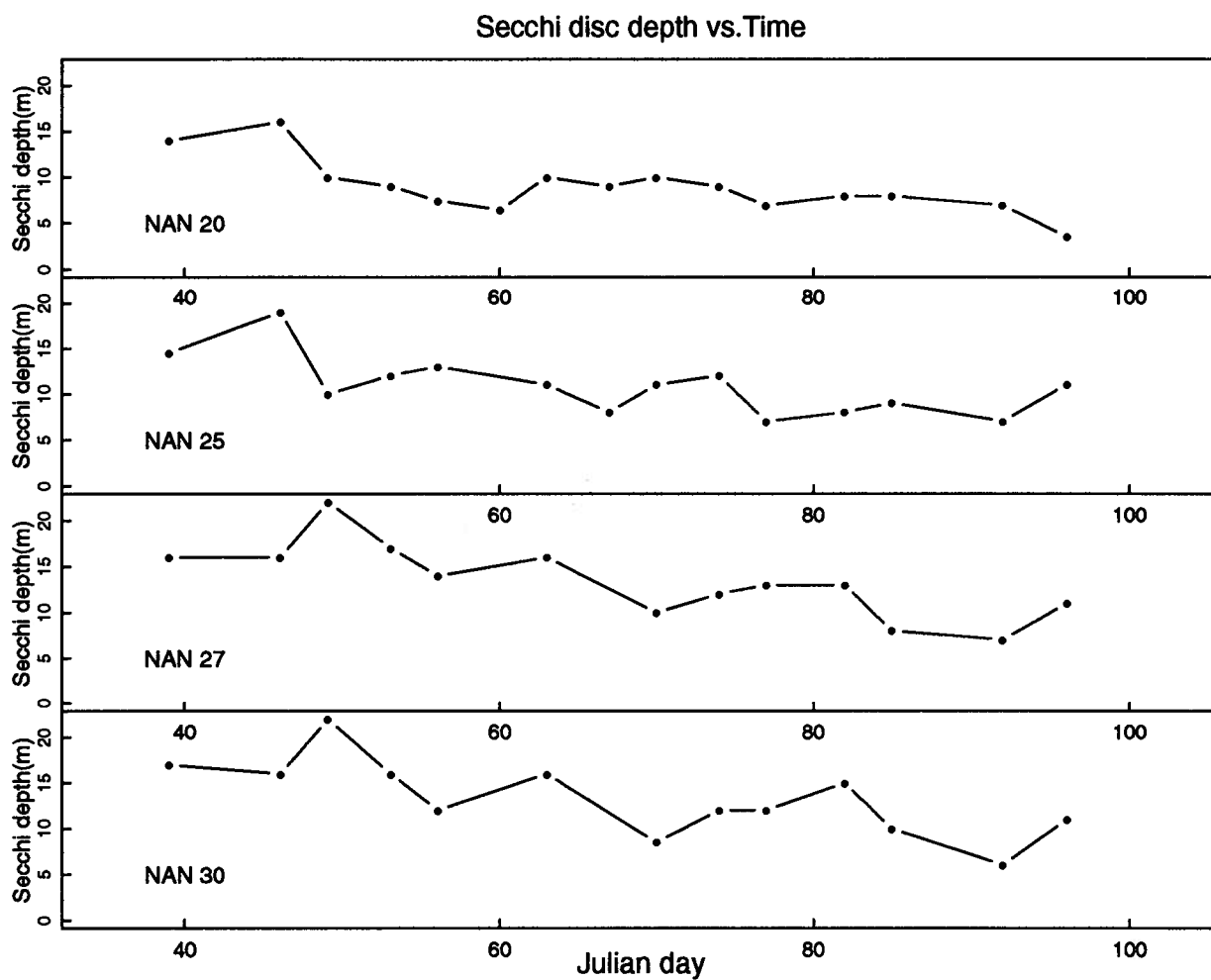


Figure 3.18: Secchi disc depth as a function of time for outside stations in 1993.

depth using equation 1.1. Critical depths were calculated at two day intervals, the time scale chosen to match that of phytoplankton growth. A running two day average of I_o was computed from the daily values. To determine 2 day Secchi disc depths a cubic spline was calculated from the Secchi time series. A spline was used because the data were not uniformly spaced. Results of the critical depth calculation are shown in figure 3.19. Only stations 10 and 30 are presented for each year. They will be used to represent critical depths inside and outside of the bay respectively.

A minimum critical depth was estimated. Thus the value for I_c which was used to calculate D_c was the upper limit, 0.54 langley/hr, of its range. Also the extinction coefficient (k) as determined from the Secchi disc depth was increased by a factor of 2 as suggested by Dr. T. Parsons (pers. comm.). The defined extinction coefficient corresponds to blue light ($\lambda = 450$ nm). Photosynthetically available radiation is made up of the 400-700 nm band and has a much higher k as radiation with longer wavelengths is absorbed in much shorter distances in water. Increasing k by a factor of 2 decreases D_c by a factor of 2. The minimum critical depths were still large and generally suggest that light was not limiting given estimates of vertical mixing. The choice of I_c was probably too large. The range of I_c for different types of phytoplankton has been investigated by Falkowski [8]. He found that I_c varied by over four orders of magnitude for different types of phytoplankton in a laboratory experiment. The most efficient users of light (and thus those with corresponding minimum I_c values) were diatoms. He used two diatoms, *Skeletonema costatum* and *Ditylum brightwelli*, both of which were observed in and around Nanoose bay. These results suggest that the I_c used here was definitely too large.

Although it was not possible to determine an absolute D_c with certainty, the minimum critical depth shown here should provide a true relative measure.

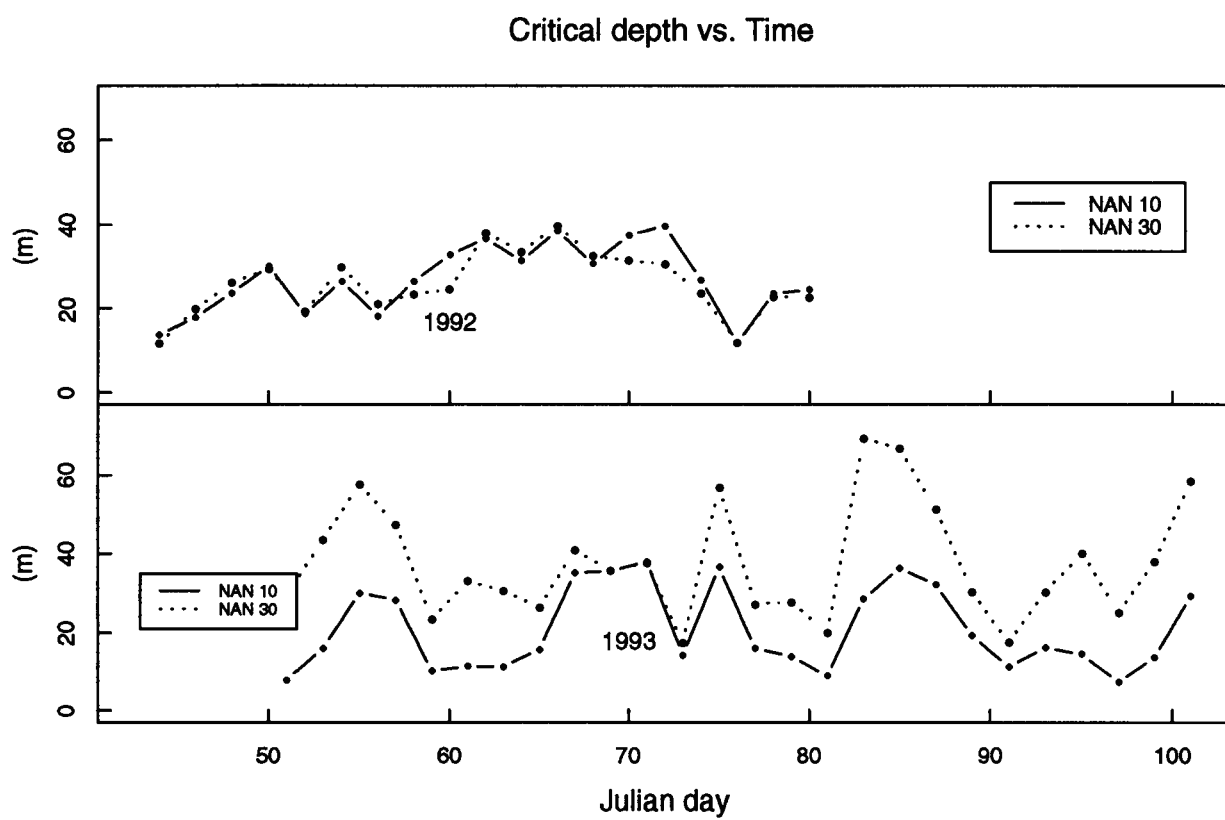


Figure 3.19: Critical depth as a function of time for NAN 10 and 30.

3.4 Chlorophyll *a*

In 1992 chlorophyll *a* was measured on each sampling day and location and is shown in figure 3.20. Results are noisy mainly due to biological patchiness. Note at NAN 30 on day 81 measurements were done in triplicate and results varied by over an order of magnitude. When a large increase in chlorophyll *a* concentration around day 75 was observed, it was not possible to determine whether it happened at one location any earlier than the others. These data are too noisy and do not have high enough temporal resolution to be useful in this problem.

In 1993, triplicate chlorophyll *a* measurements were taken at each station to improve the signal to noise ratio. The three samples were averaged to produce the plots shown in figures 3.21 and 3.22. The standard error was calculated for each point and suggests that all values have a fractional uncertainty of about 40%.

3.5 Species Composition

Species composition analysis was done to the genus level for each sampling date and location. Originally this analysis was done to back up the chlorophyll *a* data as a measure of primary production and also to ensure that the same types of phytoplankton were present at each location. Species within the seed population must bloom in the areas that they seed.

Counts of phytoplankton were found to have a higher signal to noise ratio than chlorophyll *a* data in 1992, where only one chlorophyll sample was drawn per location and time. The small increase in phytoplankton over days 45 through 56 at NAN 10, seen most strongly in *Thalassiosira* spp., is not seen at all in the chlorophyll data. For this reason phytoplankton cell counts were used in 1992 to represent *C* in equation 1.13.

A table listing the dominant genera (species where possible) with its concentration

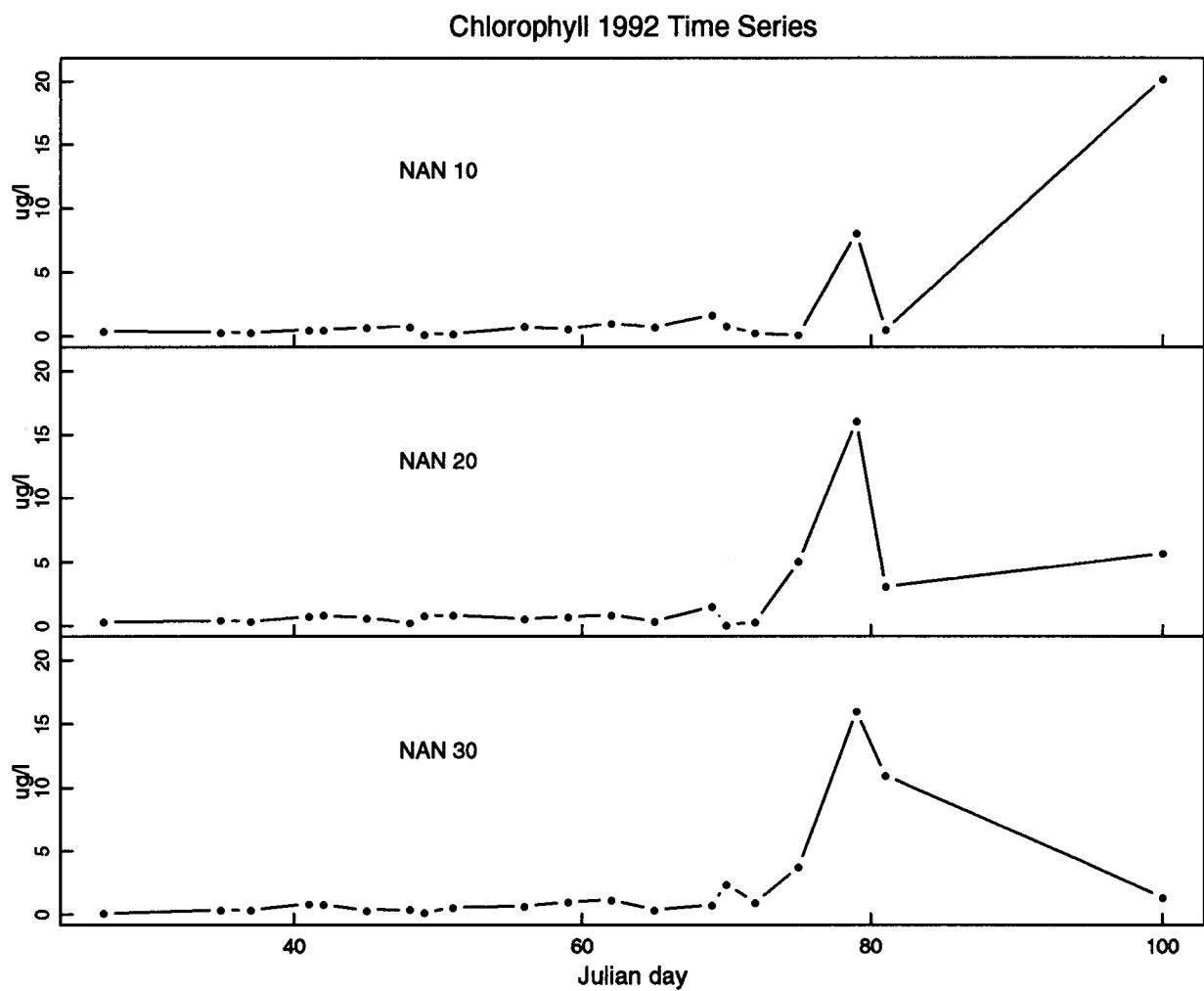


Figure 3.20: Chlorophyll *a* as a function of time in 1992.

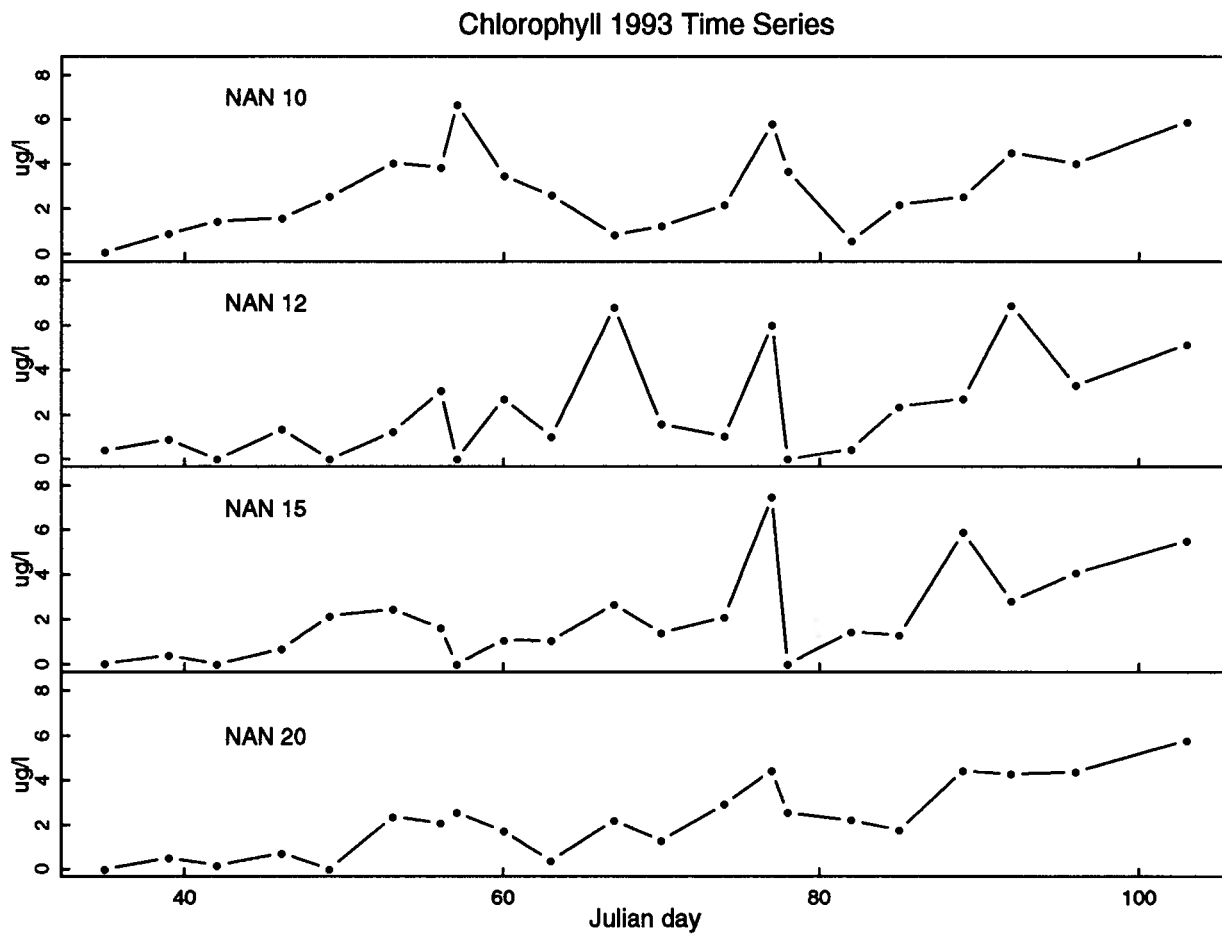


Figure 3.21: Chlorophylla as a function of time for the inside stations in 1993.

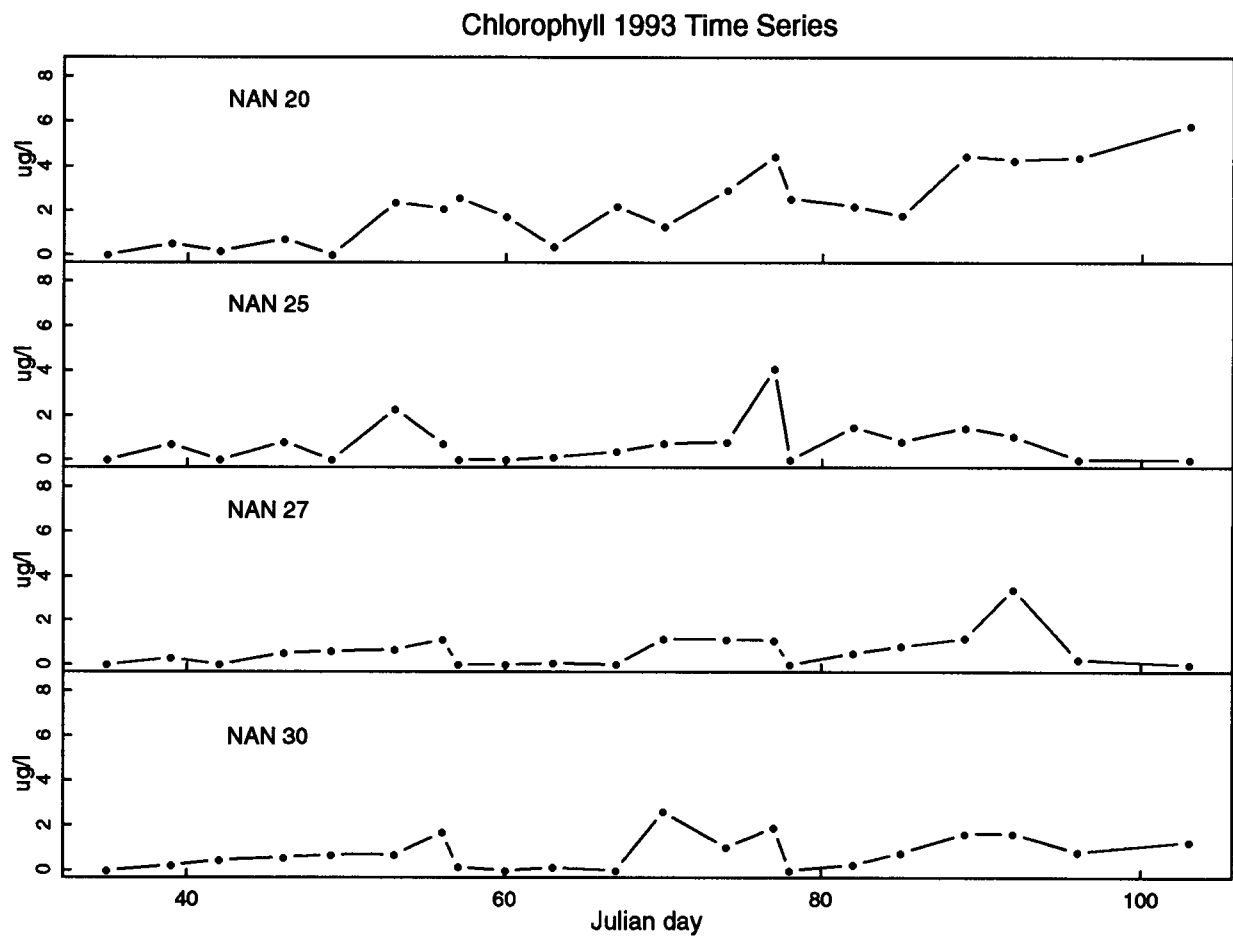


Figure 3.22: Chlorophylla as a function of time for the outside stations in 1993.

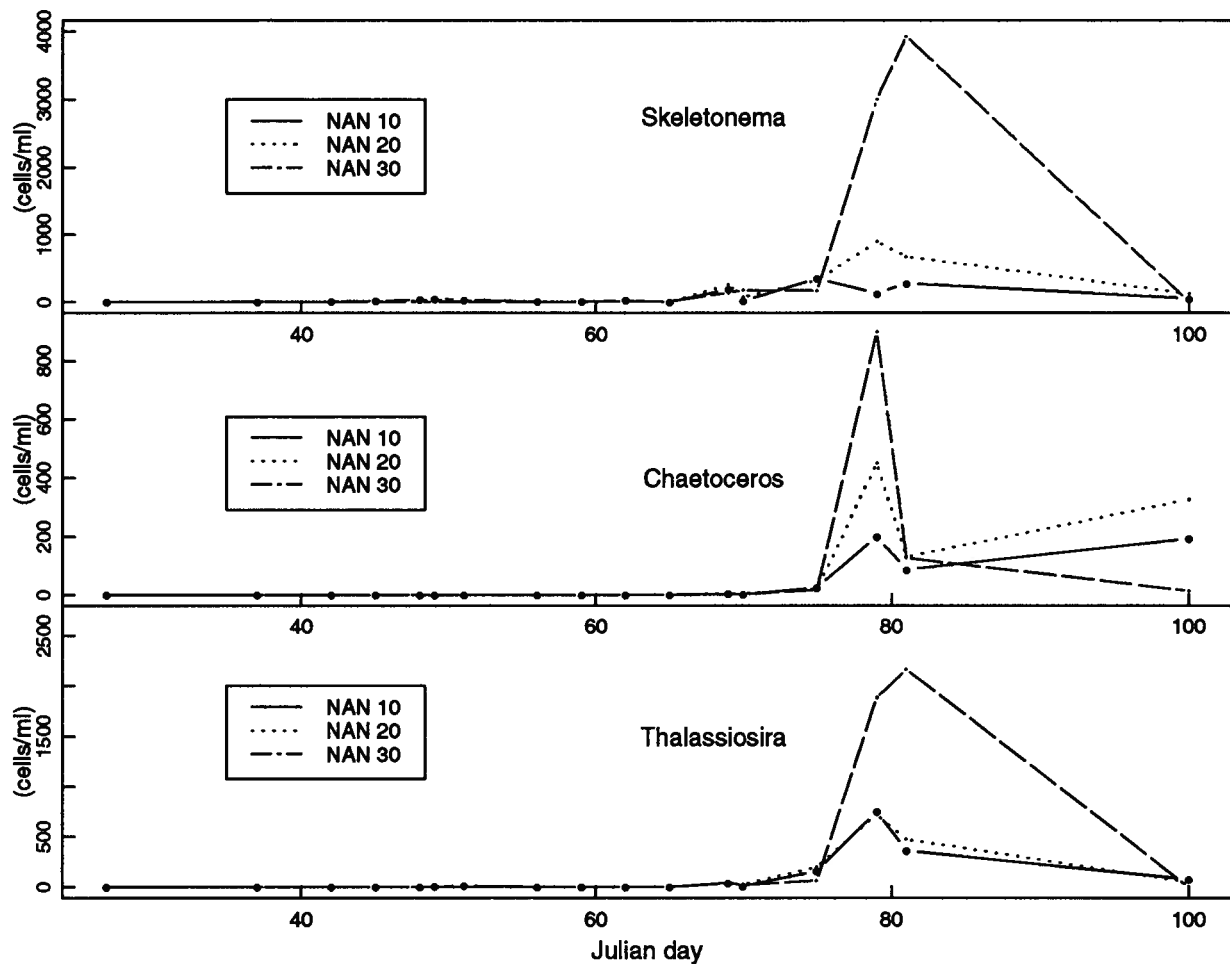


Figure 3.23: *Skeletonema costatum*, *Chaetoceros* spp. and *Thalassiosira* spp. counts for 1992.

for each sample counted is presented in the Appendix.

The 1992 full time series of *Skeletonema costatum*, *Chaetoceros* spp. and *Thalassiosira* spp. counts are shown in figure 3.23. A plot is done for each genus and stations 10 20 and 30 are shown together on each plot. The concentrations of each genus behaved in a similar manner at each station. Numbers were low, (0-10/ml) until around day 70 when they began to climb steeply. There was however a slight increase around day 50 inside the bay and at the mouth (NAN 10 and 20). Figure 3.24 shows this increase by contracting the axes to look at only day 35 through 70, the time period before the full

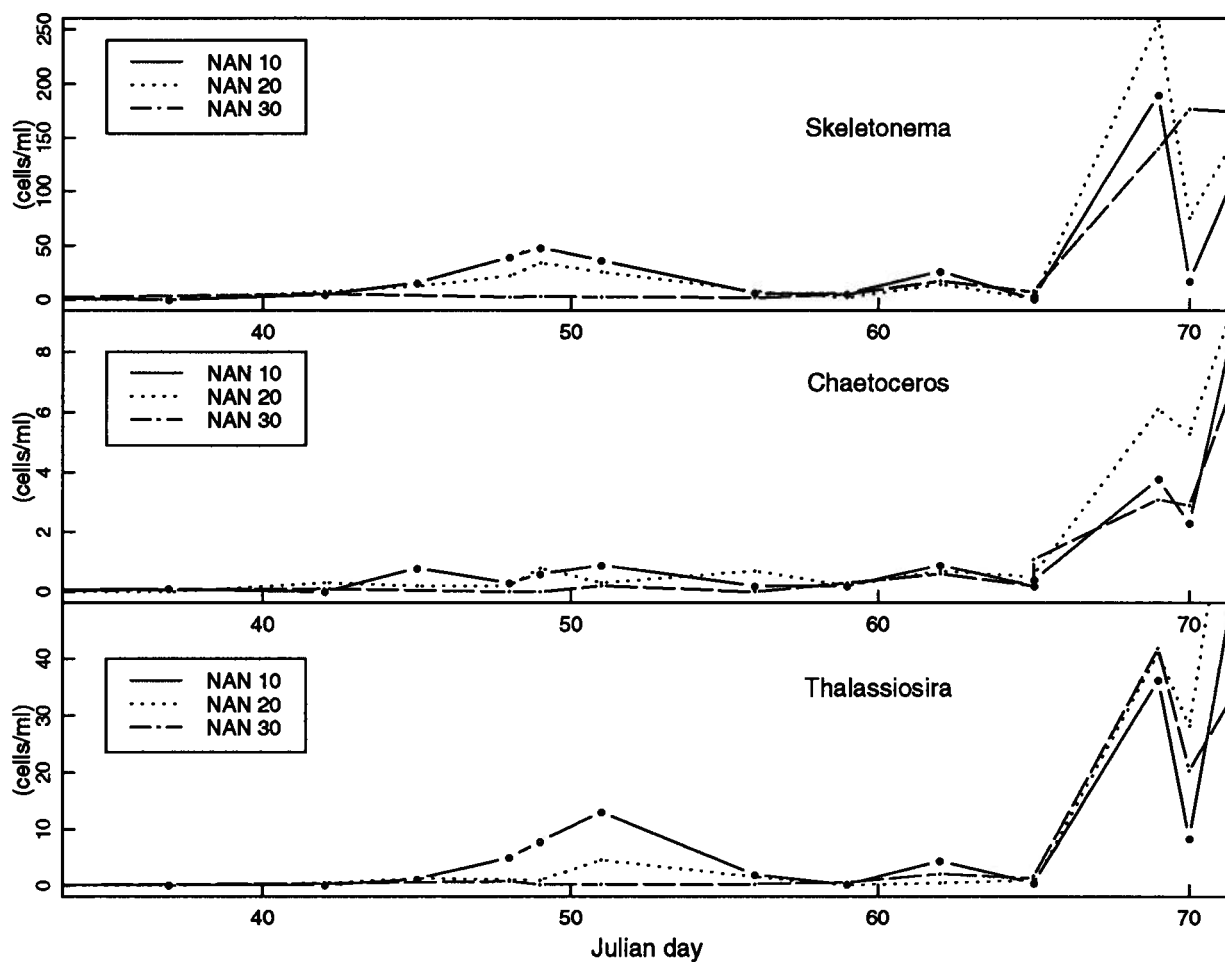


Figure 3.24: *Skeletonema costatum*, *Chaetoceros* spp. and *Thalassiosira* spp. counts for 1992 before the onset of the spring bloom.

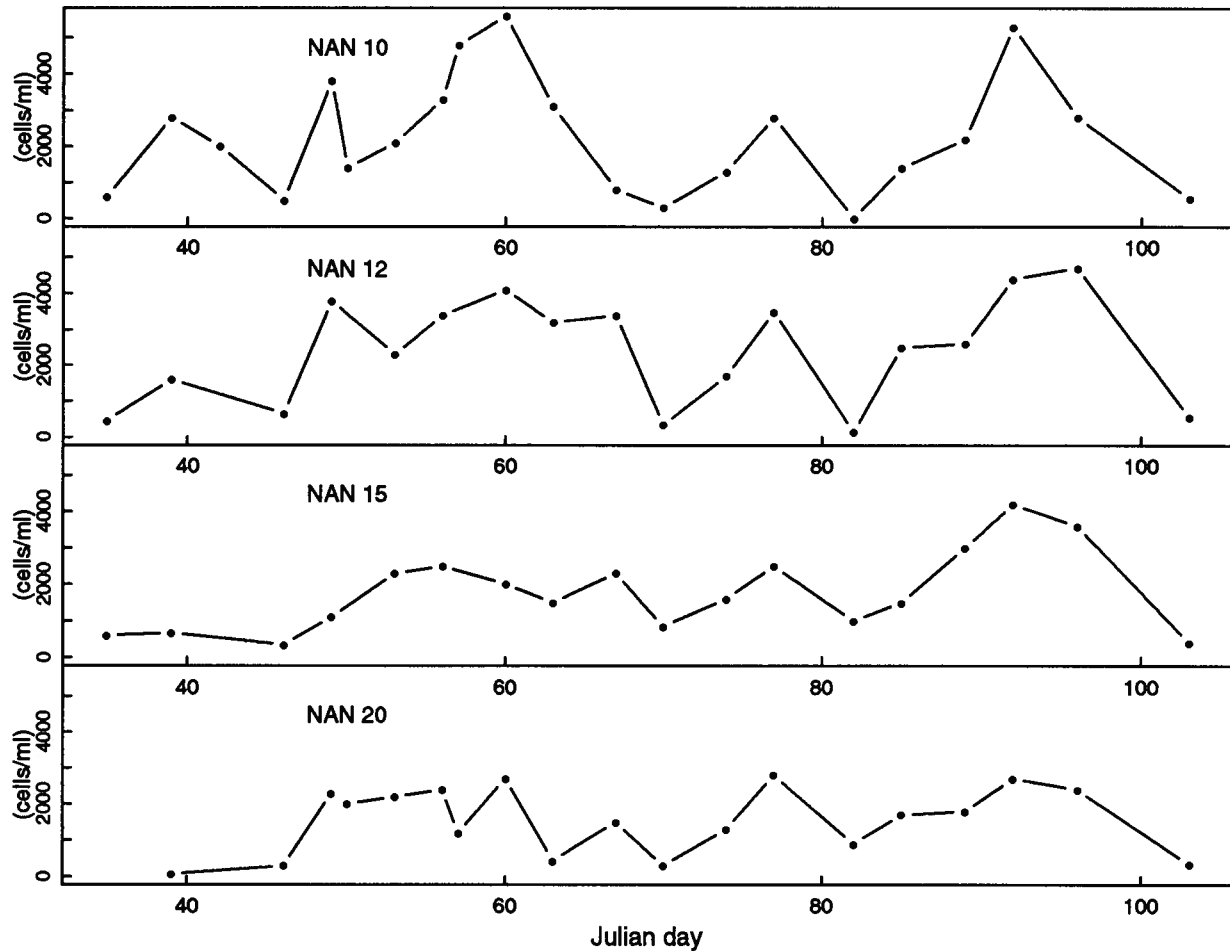


Figure 3.25: *Chaetoceros debilis* counts for 1993, inside stations.

spring bloom.

In 1993 samples the dominance of one species was overwhelming. The species was *Chaetoceros debilis* and a time series of its concentration is shown for each station. Figure 3.25 shows the series for stations from the inside to just outside the mouth of the bay (NAN 10 through 20). The results for the outside stations are shown starting at NAN 20 and progressing further from the bay to NAN 30 in figure 3.26.

At the inside stations *Chaetoceros debilis* was present and dominant from the first sampling date onwards. Concentrations rose between days 35 and 39 and subsequently

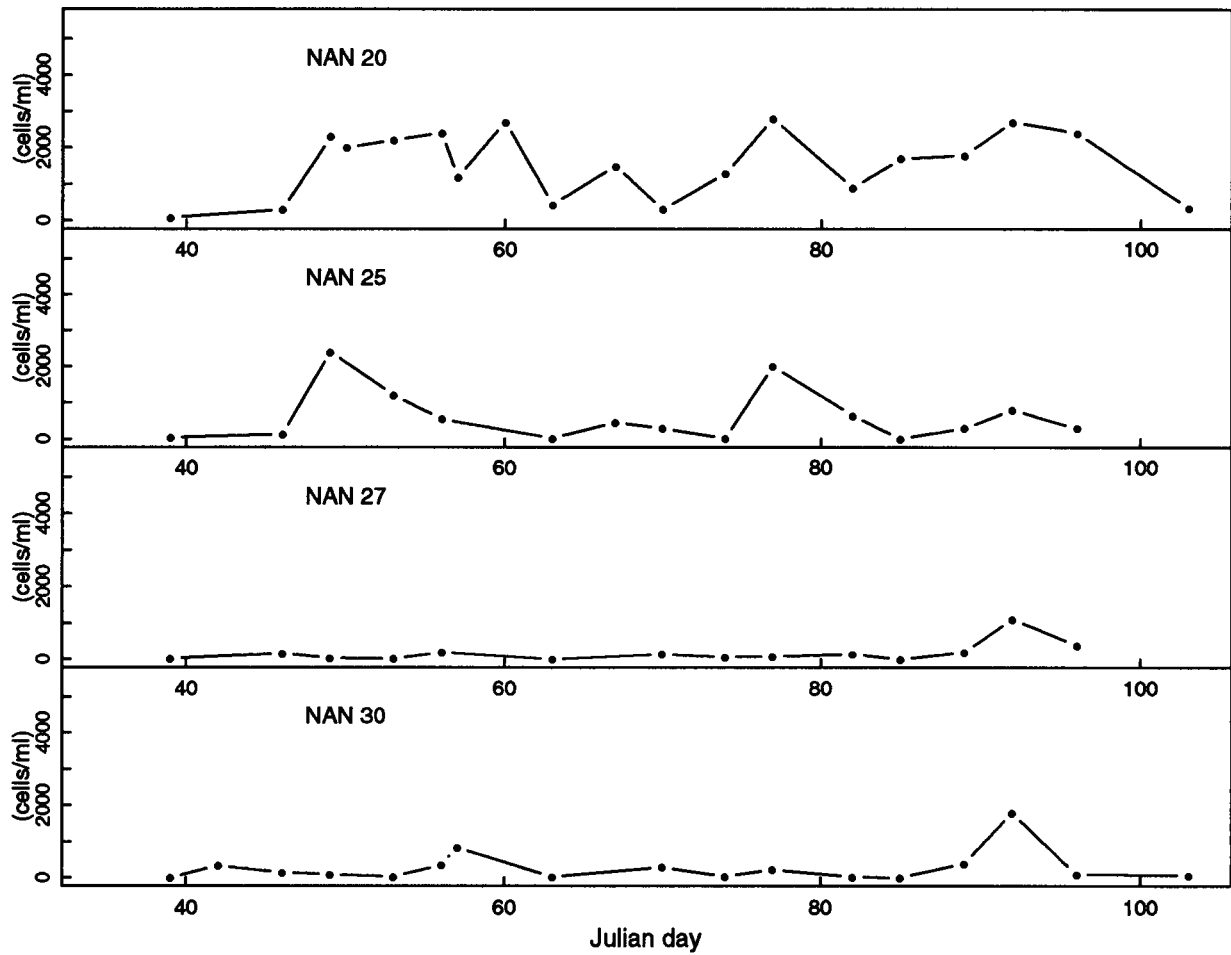


Figure 3.26: *Chaetoceros debilis* counts for 1993, outside stations.

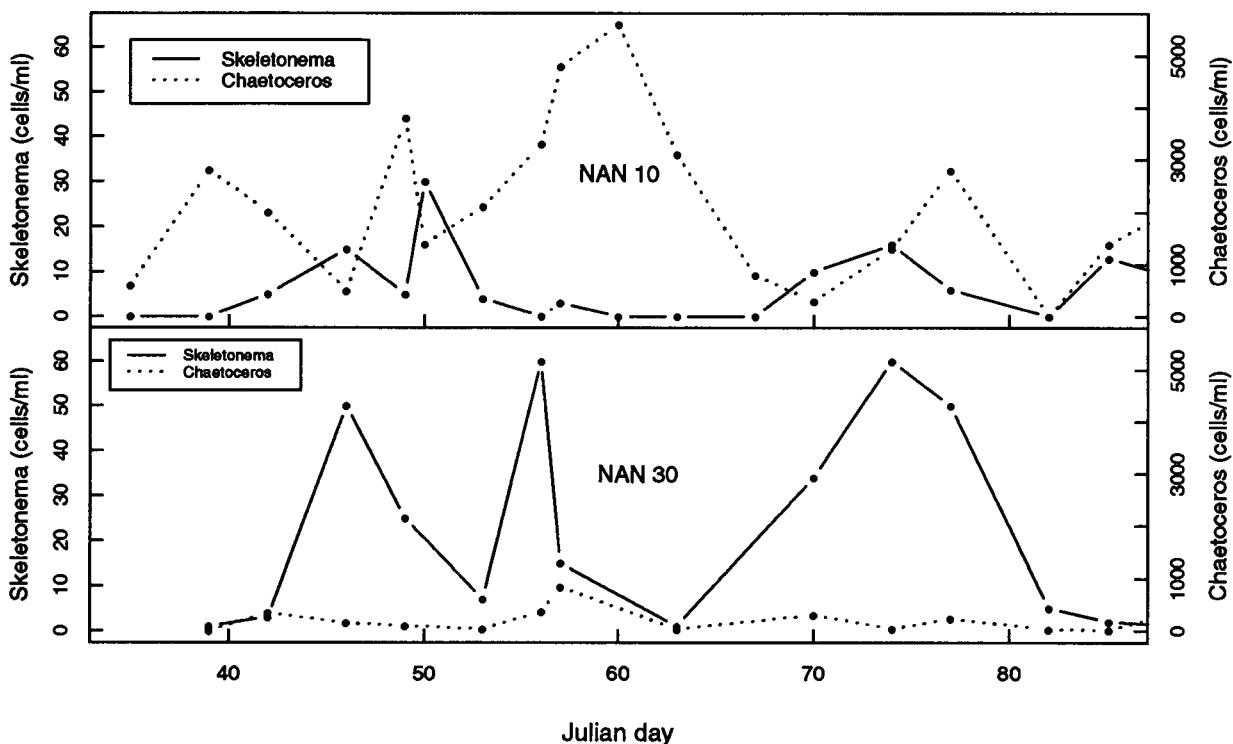


Figure 3.27: *Skeletonema costatum* and *Chaetoceros debilis* counts for 1993, NAN 10 and 30.

peaked several times broken up by intervals where numbers dropped.

On the outside, concentrations of *Chaetoceros debilis* were lower. Note that the same scale for vertical axes was used in both figures 3.25 and 3.26 so that a direct comparison is possible between all time series. Day 39 was the first day that the furthest outside station (NAN 30) was sampled. At this time no *Chaetoceros debilis* was found in the sample. By day 42 however *Chaetoceros debilis* appeared at all outside stations in much lower concentrations than on the inside and was present throughout the rest of the study period. A notable increase did not begin at NAN 27 and NAN 30 until day 89 and was suppressed within the week probably by strong southeasterly winds in the Strait.

Skeletonema costatum was present usually at very low numbers (0-10/ml) until day 96 when counts increased at the inside stations to concentrations > 1000/ml and on the

outside to $> 500/\text{ml}$. A time series of *Skeletonema costatum* and *Chaetoceros debilis* before the large increase in concentration is shown in figure 3.27. Concentrations of both species are shown on the same scales for each station. There were some higher counts of *S. costatum* on the outside compared to the inside, particularly at NAN 30, where concentrations were 40-60 cells/ml on days 46, 56 and 74 through 77. It is noted that *Skeletonema costatum* makes up a much larger portion of the total number of cells on the outside. On the inside concentrations of all other plankton are negligible compared to *Chaetoceros debilis*.

Thalassiosira spp. behaved much like *Skeletonema costatum*. Numbers did not increase above 10 cells/ml until the end of March and they reached the highest value of 200-500/ml at all stations on the last sampling date. Again there were some slightly higher counts at the outside stations during the same time periods.

3.6 Nutrients

Nutrients were sampled on each sampling day at each station. In 1992 nitrate, phosphate, ammonium and silicate analyses were done, while in 1993 only the first two concentrations were analyzed.

The main reason for sampling nutrients was to ensure that they were not limiting to phytoplankton before the spring bloom. Also a comparison was made between stations to consider the motion of different water masses by using nutrients as tracers. The latter proved unreasonable as nutrients were generally very high everywhere until phytoplankton began to bloom and then dropped quickly, with the exception of phosphate.

Nitrate concentrations from both years were high and typical for the Strait of Georgia during the winter and early spring (Harrison et al. [12]). Silicate concentrations were higher than expected in 1992, although the time series is consistent. Concentrations of

up to $60 \mu\text{M}$ are not uncommon in the Fraser River, which is high in silicate. Within the Strait around Nanosee bay however this concentration is expected to be more dilute around $20\text{--}30 \mu\text{M}$, [12]. Phosphate concentrations were expected to be within the $2\text{--}3 \mu\text{M}$ range, [12]. These data had intermittent spikes of up to $5 \mu\text{M}$ however which suggests that some of the samples were possibly contaminated. Ammonium samples also appear to have been contaminated, as concentrations far exceed the expected range for surface values (and ammonium is generally difficult to measure).

Nutrient data are summarized in figures 3.28 through 3.33. The 1992 phosphate and ammonium time series are excluded due to apparent contamination. 1993 phosphate values are shown although several suspiciously high concentrations are present in some of the series as well.

It is considered that nitrate becomes limiting at concentrations of $1 \mu\text{M}$, while phosphate concentrations are limiting at $1/16$ of that, given the Redfield ratio (Parsons, Takahashi and Hargrave [22]). Using these limits, nutrients were not limiting at any time throughout the experiment with the exception of nitrate at the inside stations at the very end of the 1993 record. Phytoplankton growth was therefore limited initially by light and the stability of the water column throughout the study period during both years. Also sinking rates in equation 1.13 will be assumed constant and unaffected by nutrient concentrations.

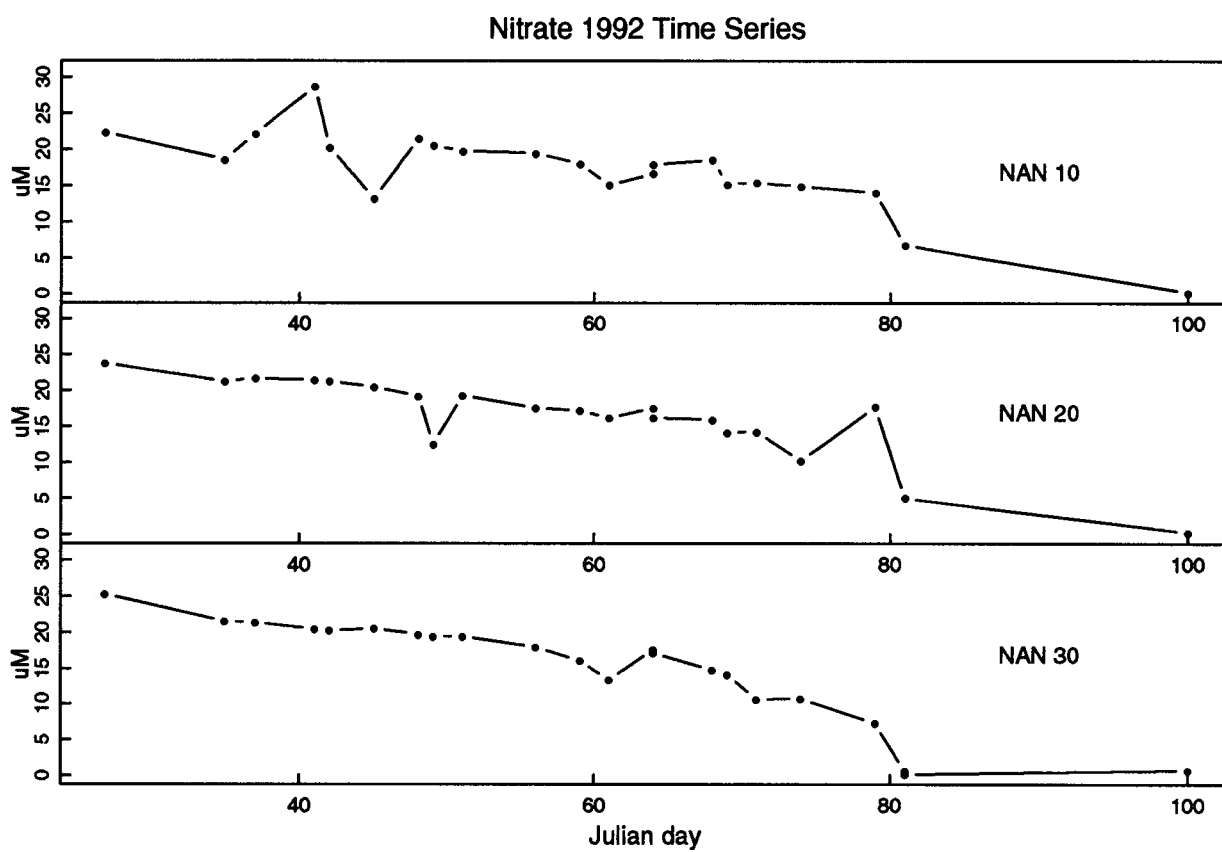


Figure 3.28: Time series of nitrate in 1992 for NAN 10, 20 and 30.

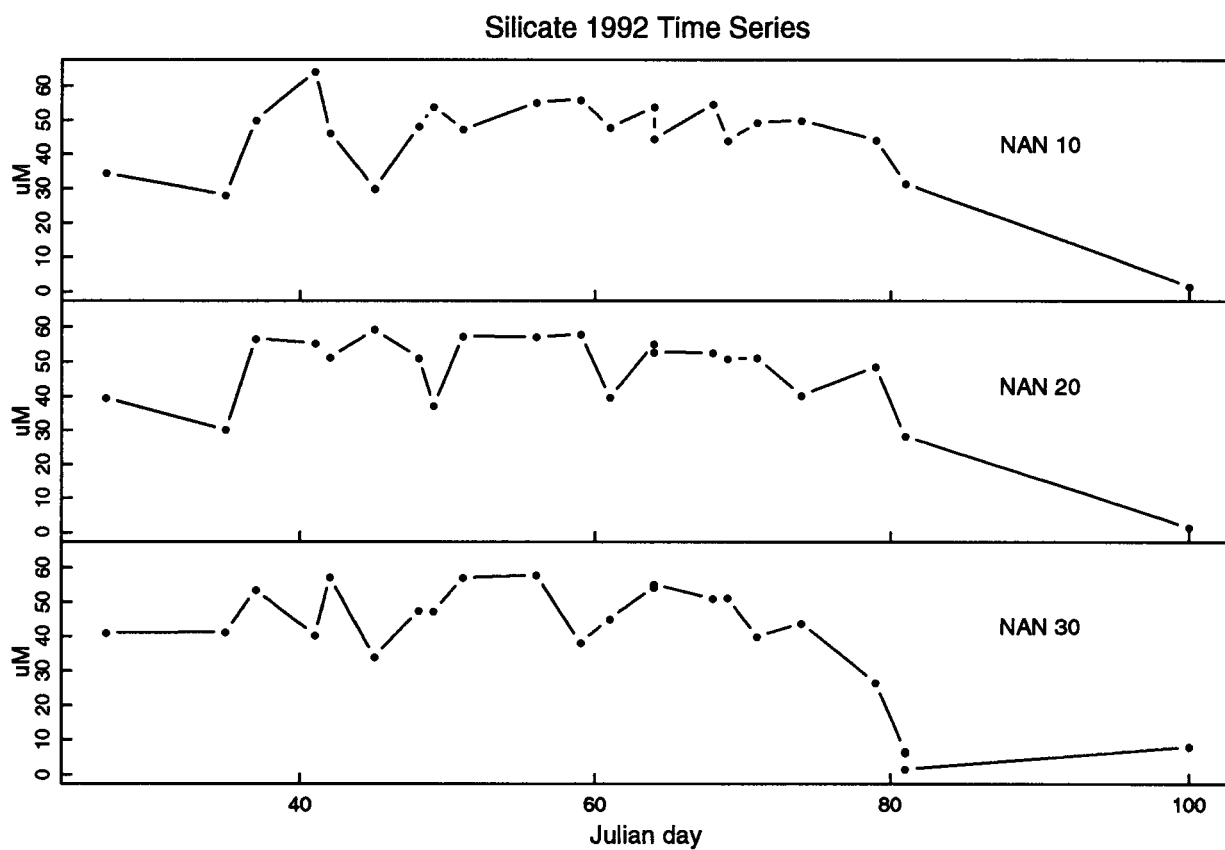


Figure 3.29: Time series of silicate in 1992 for NAN 10, 20 and 30.

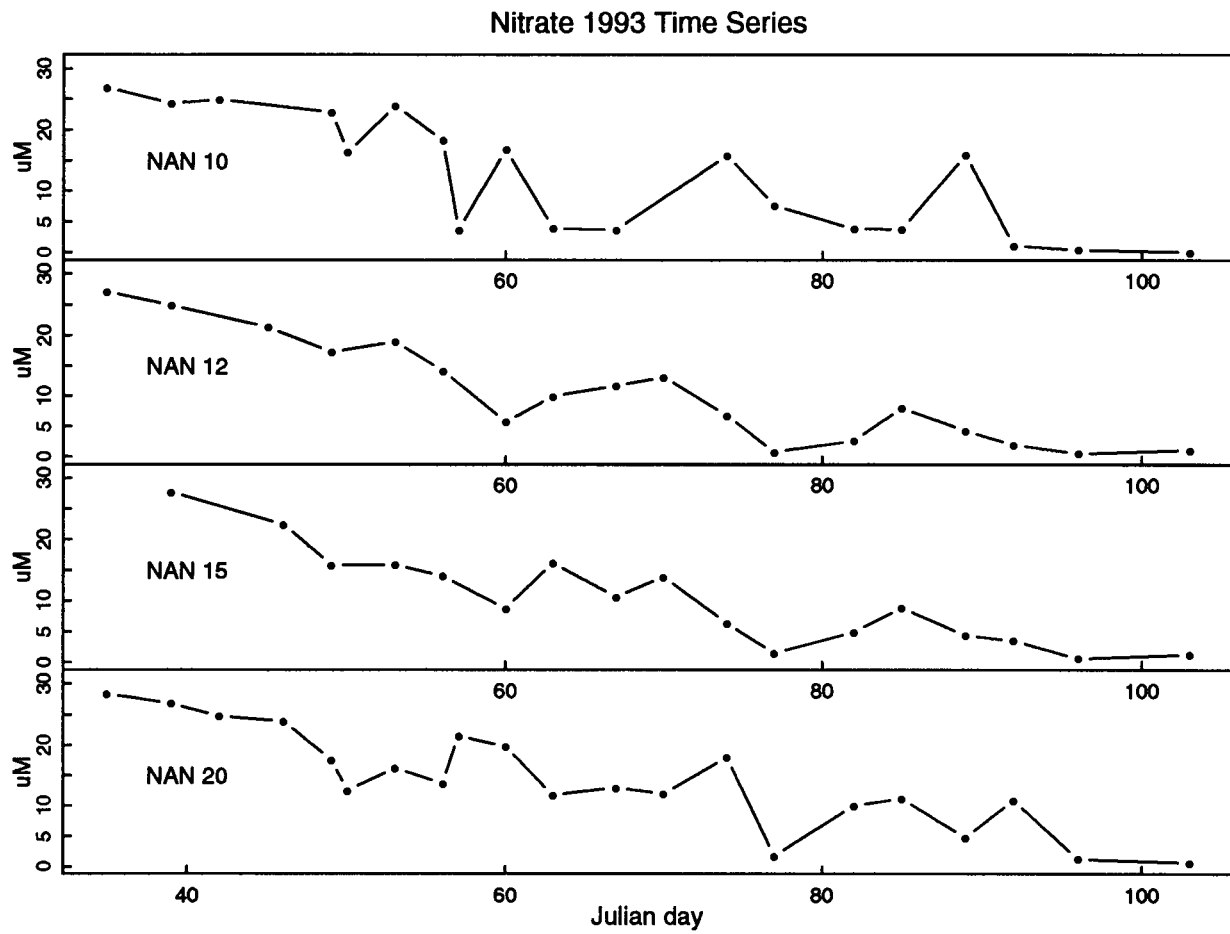


Figure 3.30: Time series of nitrate concentrations in 1993, inside stations.

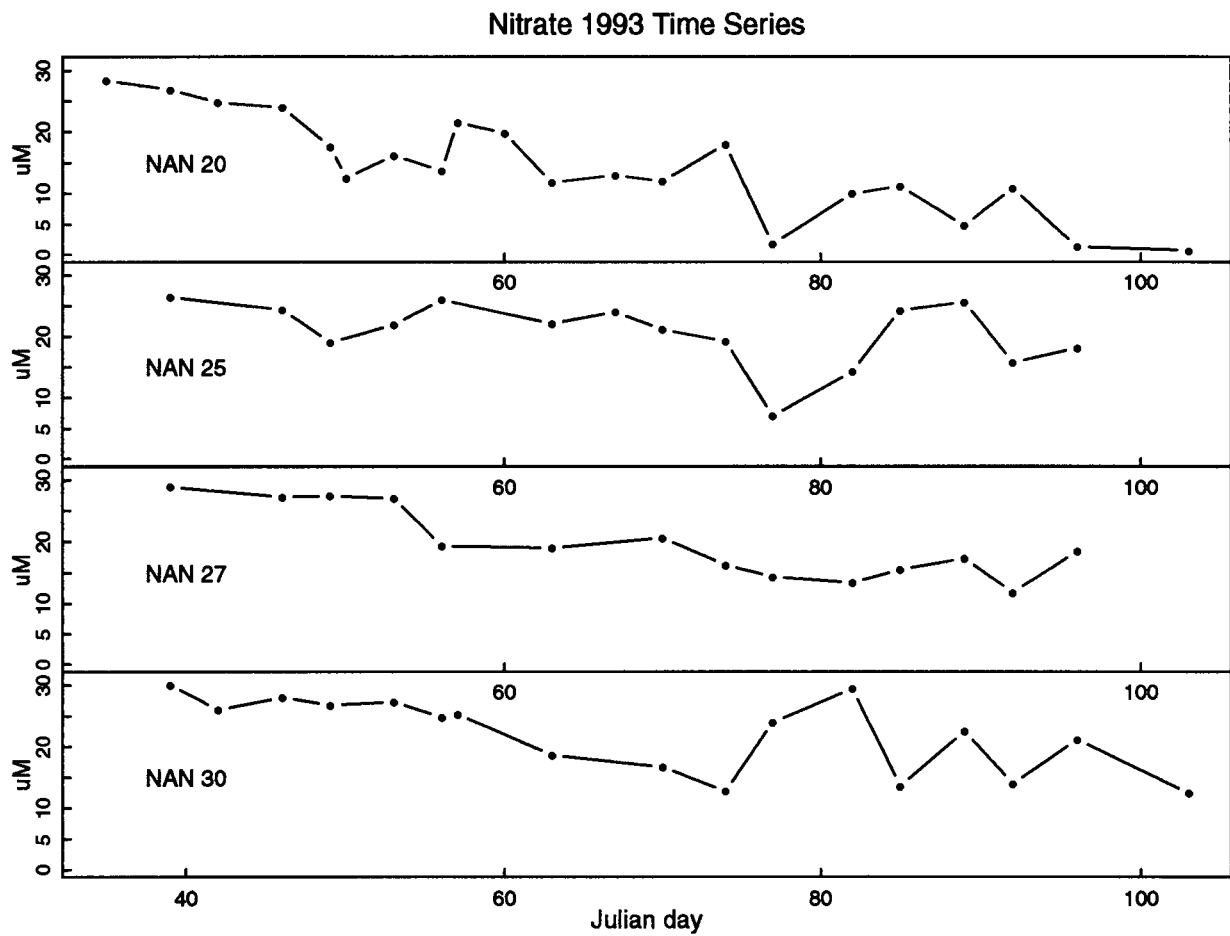


Figure 3.31: Time series of nitrate concentrations in 1993, outside stations.

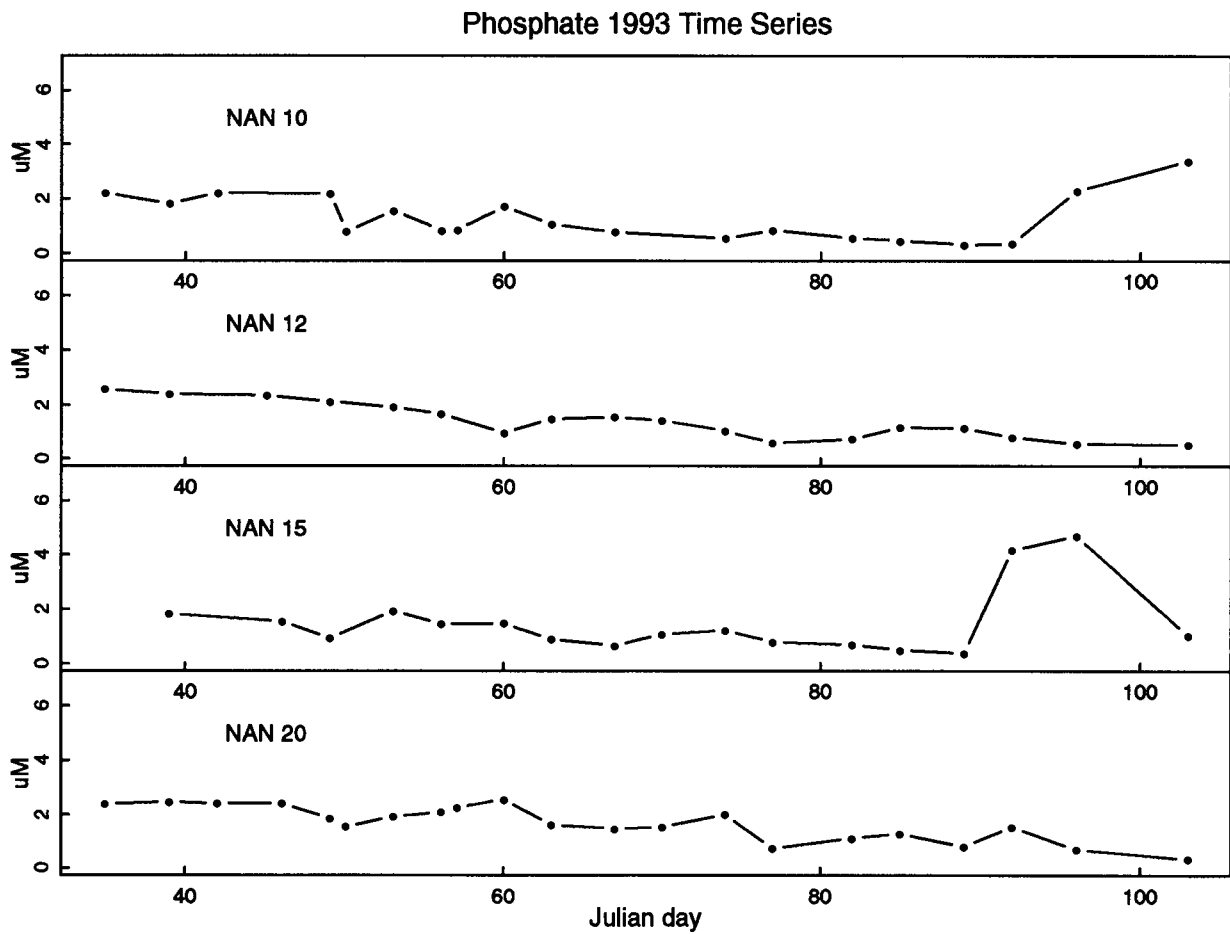


Figure 3.32: Time series of phosphate concentrations in 1993, inside stations.

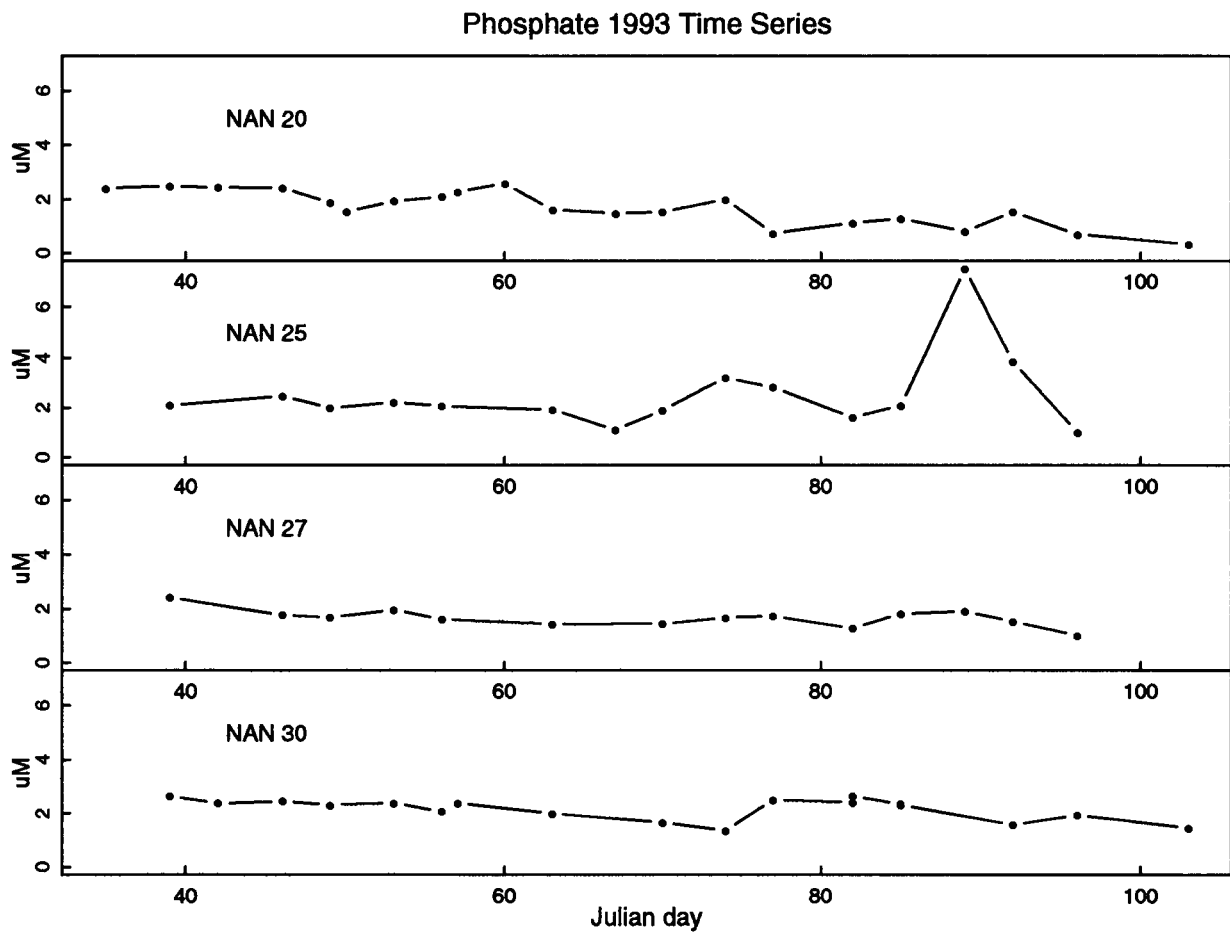


Figure 3.33: Time series of phosphate concentrations in 1993, outside stations.

Chapter 4

Discussion

The differences in the data between years made this experiment very interesting. Density structure, phytoplankton concentration and dominant species had little in common between years. Factors affecting phytoplankton growth are discussed as well as the possibility of seeding with reference to both the 1992 and 1993 situations. Terms in equation 1.13 are estimated where appropriate. Finally suggestions as to how to continue and improve experiments such as this one are made.

4.1 Limitations to phytoplankton growth during the onset of the spring bloom

The Sverdrup criterion as stated in chapter 1 is not suitable in balancing factors limiting phytoplankton growth to predict a spring bloom given these data. The mixed depth appears to have little meaning in the coastal environment. The critical depth, defined in equation 1.1 was calculated for these data as a minimum (see section 3.3.2). The estimated D_c still indicated that light was generally not limiting to phytoplankton growth throughout the study periods (at least when compared to vertical mixing). The following is a discussion of measured factors limiting phytoplankton growth in reference to the times when phytoplankton bloomed in each of 1992 and 1993, inside and outside of the bay.

4.1.1 1992

In 1992 light was not limiting at any time or location. D_c appears to be roughly the same for all stations. From day 45 onward the critical depth ranged from 20 to 40 m. D_c did not begin to drop until approximately one week after the bloom began when high concentrations of phytoplankton began to limit light penetration. During the entire period the density structure at all locations was reasonably well stratified. Mixed depths as calculated in section 3.2.1 were less than 12 m everywhere and often there was strong stratification at the surface as in the first example of figure 3.13. The velocity shear over this depth, $\frac{dU}{dz}$, necessary for turbulent mixing was large. Thus profiles indicated very limited vertical mixing of phytoplankton. Time variability in density structure appears to be a necessary consideration at least within the bay.

Figure 4.1 shows a time series of phytoplankton concentration at NAN 10 and NAN 30 with possible limiting factors. The critical depth and nitrate concentration are shown for both stations along with the flushing index as well as the principal component of the Ballenas wind. Concentrations of *Skeletonema costatum* are shown as *S. costatum* was present in the highest numbers during 1992 and was representative of all genera (see figures 3.23 and 3.24). This time series begins just before phytoplankton concentrations show a small increase and is truncated just after the apparent onset of the spring bloom. Note that at NAN 30 the concentrations of *S. costatum* after day 80 rise to 3900/ml, well outside the range shown on the plot.

The flushing index at 2 m indicates four periods of potentially favourable conditions for phytoplankton growth inside the bay. Between these intervals the top layer of the bay was flushed in a shorter time than that of phytoplankton generation. Note that both the 2 and 4 m flushing indices are shown as phytoplankton was sampled in the top 3 m. Also, the index was often very different at 4 m than at 2 m.

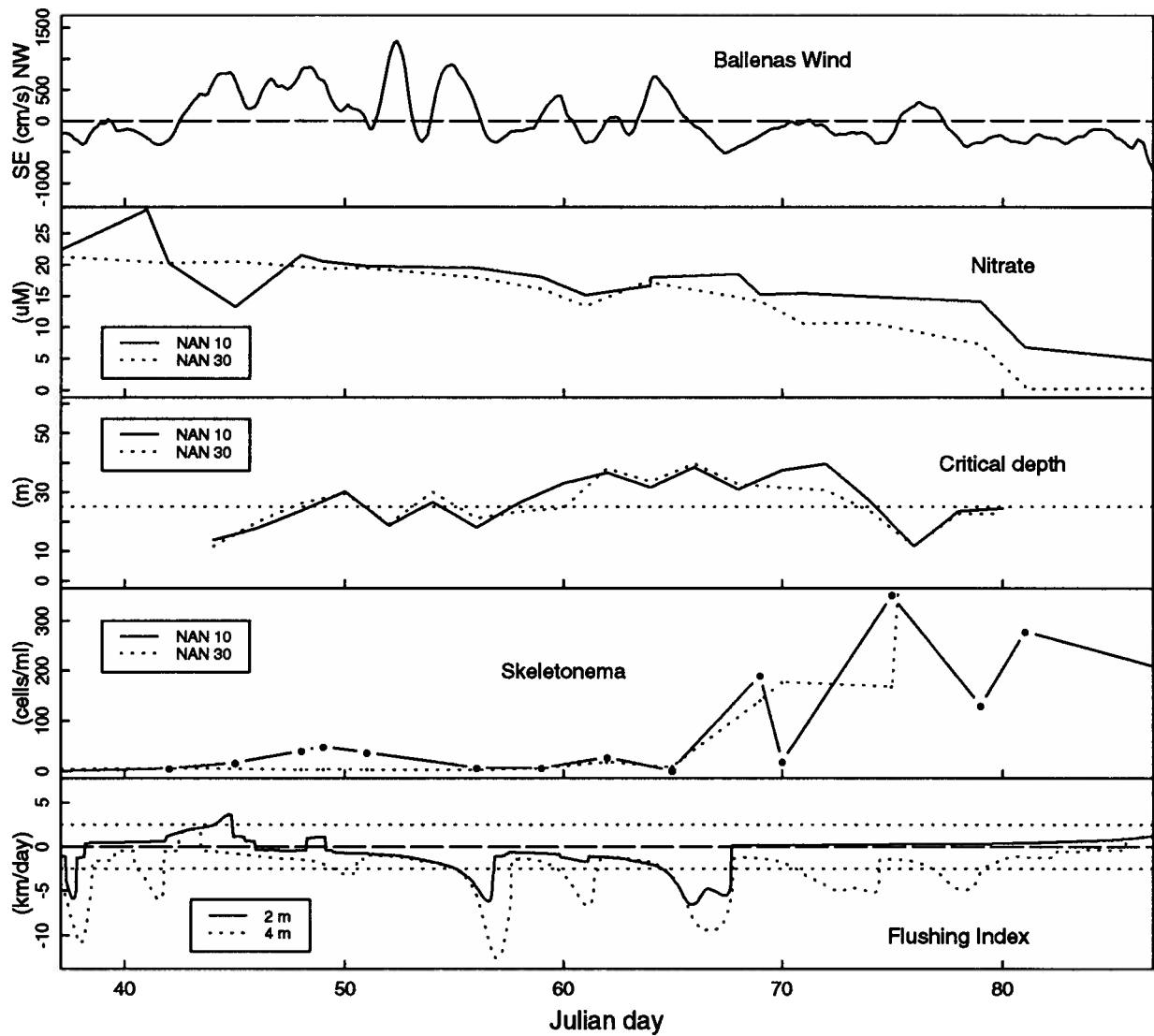


Figure 4.1: 1992 time series of phytoplankton concentration and factors possibly limiting its growth for stations NAN 10 and NAN 30. The dashed line at 25m on the critical depth plot is the maximum depth of the bay below datum.

NAN 10		
Time interval (Julian day)	$\frac{\Delta}{\Delta t}(\frac{\Delta \sigma_t}{\Delta z})$ (kg/m ⁴ /day)	$\frac{\Delta}{\Delta t}(\sigma_{t20})$ (kg/m ³ /day)
1992		
27-35	+0.71	-0.03
35-42	-1.5	-0.14
42-49	+0.03	+0.11
49-56	+0.30	0
56-65	-0.18	-0.03
65-70	-0.16	-0.03
70-75	0	+0.05
75-81	-0.05	+0.07
1993		
35-39	+0.40	0
39-46	-0.29	+0.004
46-49	+0.01	-0.007
49-53	-0.03	-0.05
53-56	-0.01	+0.03
56-60	+0.01	+0.008
60-63	+0.02	-0.01
63-67	0	+0.08
67-70	+0.07	-0.13
70-74	+0.02	+0.03
74-77	+0.28	+0.03
77-82	+0.90	+0.04
82-85	-1.6	-0.03
85-89	+0.03	-0.05
89-92	+0.01	-0.03
92-96	-0.09	0
96-103	+0.19	-0.01

Table 4.1: Phytoplankton growth parameters determined from CTD profiles for NAN 10, as described in section 3.2.3. For favourable growth conditions it is suggested that over the interval Δt , both $\frac{\Delta}{\Delta t}(\frac{\Delta \sigma_t}{\Delta z})$ must be positive and $|\frac{\Delta}{\Delta t}(\sigma_{t20})| < 0.05$. Favourable parameters are listed in bold. Parameters are shown for NAN 10 only as they do not seem applicable to the outside stations. Changes in density structure were small on the outside, thus parameters were small indicating potentially good growth conditions by these criteria.

During the first period, days 38 through 43, there was no increase in phytoplankton concentration. Note that at 4 m there was an inflow >2.5 km/day during this time. The parameters determined from density profiles (see table 4.1) were unfavourable, $\frac{\Delta}{\Delta t}(\frac{\Delta \sigma_t}{\Delta z})$ is negative and large suggesting that mixing has occurred during this period. Figure 3.14 shows the profiles near the beginning and end of this interval (days 35 and 42).

During the second period, day 45 through 55, there was a corresponding, but small, increase in phytoplankton concentration inside the bay. In this case the 4 m flushing index was also favourable for phytoplankton growth, as were the two parameters shown in table 4.1. Profiles taken during and just after this period are shown in figure 3.13 (day 49 and 56).

The third period was from day 57 through 64, during which a very small increase in *S. costatum* counts occurred. At this time the flushing index at 4 m showed an inflow >2.5 km/day for 2 days. The change in net stratification as measured from density profiles was also negative (although it was small), thus unfavourable to phytoplankton growth.

During the fourth period, days 68 through 89, the phytoplankton concentrations everywhere reached their highest values.

Note that the increase in *S. costatum* at NAN 10 around day 64 does not agree with either the flushing index or with the parameters in table 4.1. Concentrations began to increase at both NAN 10 and 30 around day 65, however within the bay the bloom seemed to be suppressed and then fully began after day 70. Any time lag between favourable conditions and an increase in phytoplankton concentration would be expected to be of the order of 2-3 days. In this case however the third favourable period defined by the 2 m flushing index leads the increase in phytoplankton concentration by almost a week. It is possible however that the decrease in *S. costatum* was in response to the inflow that occurred beginning on day 64.

In the Strait of Georgia conditions appear to be excellent for phytoplankton growth

throughout the study. From the beginning small numbers of phytoplankton were seen in the 25 ml samples, particularly *Skeletonema costatum*, thus a seed was present. The phytoplankton growth parameters determined from CTD profiles show favourable conditions at NAN 30 in 1992 with the exception of days 35 through 49. Changes in σ_{t20} were small after day 42, with magnitudes less than the upper limit of 0.05 kg/m^3 set in section 3.2.3. Likewise there were no large negative changes in net stratification. As noted D_c calculated as a minimum was large (over 20 m) and nutrient concentrations were high. Phytoplankton however did not begin to bloom until day 65. What limited phytoplankton growth earlier is unknown, perhaps a similar type of horizontal advection, that was flushing the bay and suppressing a bloom there, was responsible for horizontal transport in the Strait that also suppressed a bloom. The CTD profiles do not show large changes of density that would be indicative of advection. However if the density field is horizontally fairly homogeneous, advection can be occurring without causing appreciable density changes. The flushing index does show that after day 68, there was little exchange between the bay and the Strait. Perhaps the decreased exchange indicates less transport within the Strait as well and thus more favourable growth conditions. Examination of the principal component of the Ballenas wind record shows that, although winds were not particularly strong before day 65, after that they were weaker and the direction switched to predominantly from the northwest (figure 4.1).

4.1.2 1993

In 1993 the situation was very different. Density was less stratified than in 1992. Inside the bay phytoplankton concentrations were higher throughout the experiment, generally by at least an order of magnitude. In the Strait no large increase in phytoplankton occurred as it did in 1992. Concentrations were generally steady and moderately large compared to the early part of the 1992 record. Figure 4.2 shows nitrate concentrations,

critical depths, *C. debilis* concentrations (all at NAN 10 and 30), the principal component of the Ballenas wind and σ_{t7} at NAN 20 in place of the 1992 flushing indices. Recall that during the 1993 season *Chaetoceros debilis* dominated the phytoplankton community.

Inside the bay phytoplankton bloomed throughout the season. The bay was well mixed, generally to the bottom throughout the study period. Occasional decreases in concentration could be due to light limitation. Note periods in figure 4.2 where D_c drops below 25 m (the depth of the bay), which is shown on the plot, seem to correlate with subsequent decreases in *C. debilis* concentration. The parameters in table 4.1 indicate favourable conditions with the exception of days 39 through 46, days 49-53-56, days 63-67-70, days 82-85 and possibly days 92 through 96. During all of these intervals *C. debilis* counts decreased with the exception of days 53 through 56 where there was a small increase and days 82-85 where there was a strong increase. Note that these parameters were generally much smaller than in 1992 showing that changes in overall density structure tended to be small. All waters seemed to be much more homogeneous in 1993. Note that after day 96, although the parameters defined by the density profiles seem favourable, phytoplankton concentrations still continue to drop. It is suggested that nitrate became limiting at this point, as concentrations dropped below 1 μM to 0.4 μM on day 96 and then to 0.02 μM on the last sampling date.

A comparison between nitrate and *C. debilis* concentrations at NAN 10 is interesting. They seem related although it is difficult to tell if one signal leads the other. Earlier in the record it would appear that nitrate dropped in response to an increase in phytoplankton concentration. For example, the decrease in nitrate beginning on day 56 following the increase in *C. debilis*. Later however increasing nitrate may lead increasing *C. debilis* concentration. Note that after nitrate concentrations increased from days 82 and 89 *C. debilis* concentration rose until day 92 after which it decreased and nitrate became limiting.

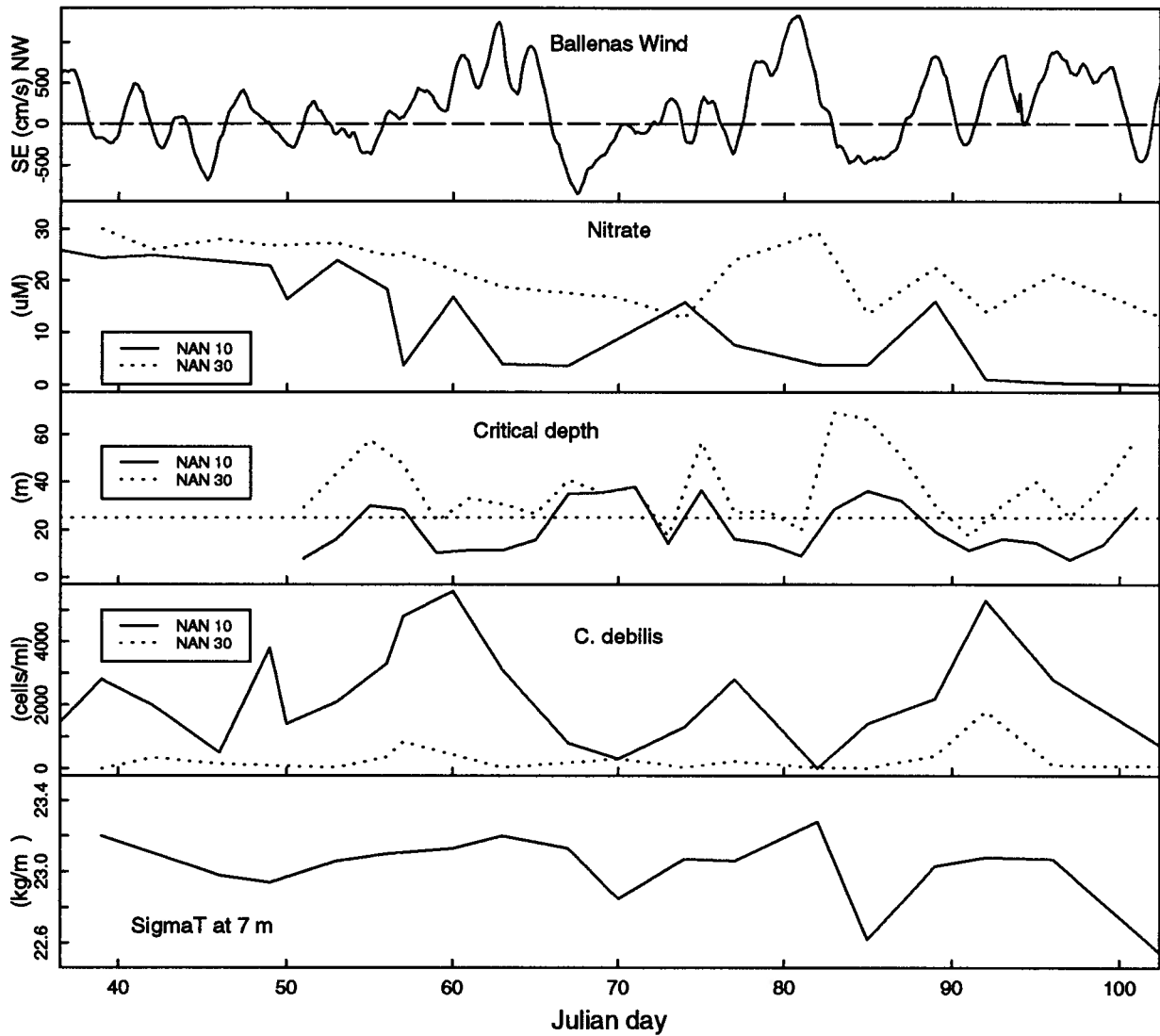


Figure 4.2: 1993 time series of phytoplankton concentration and factors possibly limiting its growth for stations NAN 10 and NAN 30. The dashed line at 25m on the critical depth plot is the maximum depth of the bay below datum.

In summary, conditions were favourable inside the bay during the 1993 season. It is not possible to determine what caused decreases in *C. debilis* concentration. It is suggested that a combination of mixing, flushing, light availability and towards the end nitrate limitation were responsible.

The outside stations during 1993 have comparatively low phytoplankton concentrations, although some phytoplankton was always present in the 25 ml samples which were counted. Nutrient concentrations were high and critical depths generally large, although the deeper CTD cast at NAN 30 indicated that the extent of vertical mixing in the Strait was often greater than 40 m (the depth of the cast). The small increases in phytoplankton concentration which occurred at NAN 30 around day 56 and then later on day 92 are difficult to explain. Note that only the latter increase was observed at NAN 27 (see figure 3.26). Conditions seem constant around day 56. Profiles were well mixed and the velocity shear necessary for turbulent mixing was low. The critical depth on day 57 was actually decreasing on the outside and was around 30 m. Profiles did not begin to show any noticeable structure until day 70. At this time the estimated mixed depths fluctuated from 20 m occasionally up to 6 m, until day 96 when profiles were mixed evenly to 40 m again. Changes in σ_{t20} were also small. Wind conditions were low before day 56 and may have allowed this small increase to occur. Stronger winds to the northwest following this time may have mixed the plankton downward. On day 92 however winds were moderately strong from the southeast.

In comparing the conditions at the inside and outside stations related to the large difference in phytoplankton concentrations, temperature was considered. It was suggested that perhaps higher temperatures in the bay led to excystment of phytoplankton and faster generation times than in the Strait. In general however temperature within the top 3 m were within 0.2 deg C of one another on the same days at all stations.

In summary phytoplankton concentrations inside the bay were much higher than

outside in 1993. Thus it appears that growth conditions in the Strait were poor although they were excellent in Nanoose bay. It is suggested that light was usually limiting on the outside due to vertical mixing, while on the inside, the depth of the bay limited mixing and as a result light was not limiting there. Outside concentrations were low and did not persist over any length of time. The source for the two small increases may have been advective transport rather than *in situ* growth.

Plankton communities differed between inside and outside stations. The proportion of *S. costatum* and *Thalassiosira* spp. to *Chaetoceros* spp. was higher on the outside (see figure 3.27). It is suggested that perhaps *S. costatum* and *Thalassiosira* spp. are able to use light more efficiently and thus did better than *Chaetoceros* spp. in the Strait where light may have been limiting. In the bay however where light was not limiting, *Chaetoceros* spp. dominated. Also filter feeders do not feed as well on *Chaetoceros* spp. due to their cetae (Jorgenson [15]). Another possibility as to why proportions of *S. costatum* and *Thalassiosira* spp. were low in the bay may therefore be because filter feeding bivalves are able to feed on them and not *Chaetoceros* spp.

C. debilis often dominates blooms in the Strait during the early summer (Harrison, Fulton, Taylor and Parsons [13]). It seems unusual that it bloomed in early February beginning the spring bloom. As *Chaetoceros* spp. frequently form resting spores [13] in the Strait of Georgia it is suggested that perhaps Nanoose bay had a high concentration of *C. debilis* cysts in 1993 and conditions for excystment became favourable yielding a strong *C. debilis* bloom.

4.2 Seeding by advection

To investigate possible seeding, the conservation equation of a scalar (equation 1.13) was used. Changes in phytoplankton concentration with respect to time were calculated and

accounted for by advection and/or the sources and sinks at that location. For seeding, advection from the potential seeding area was required.

4.2.1 1992

In 1992 (figure 4.1) there was really only one possible time interval, day 45 through 55, in which seeding could have occurred. During this interval the phytoplankton concentration increased inside the bay. This increase was the only appreciable one before a strong bloom in the Strait occurred. The current data showed that during this time there was a weak inflow, with the exception of a one day interval around day 48 at 2 m (at 4 m there was net inflow, throughout). This event was terminated by a negative flushing index indicating that net transport was into the bay at the surface. It is suggested that phytoplankton were grazed by oysters and flushed out of the bay at depth and did not provide the seed population for the bloom that occurred later outside.

The large increase in phytoplankton concentration at NAN 30 began on day 65 and was much stronger than in Nanoose bay. In the bay concentrations did not begin to rise until after day 65; an increase was found on day 69 (the next sampling date). Up to day 67 the flow at 2 and 4 m was into the bay. Thus in 1992 the bay did not seed the Strait. If any seeding occurred given the net transport, it is more likely that the Strait provided the seed for the bay.

4.2.2 1993

In 1993 the situation was very different. There were many intervals in which to investigate possible seeding. There was sufficient spatial resolution to calculate gradients, however no current data were available.

Use of the conservation equation

Equation 1.13 was evaluated by considering one dimension only, with derivatives calculated as averages over a single time interval. Thus equation 1.13 becomes:

$$\frac{dC}{dt} = -u \frac{dC}{dx} + C(t)(\mu - z - b - s) \quad (4.1)$$

Terms in equation 4.1 were evaluated as follows.

$$\left(\frac{\partial C}{\partial t}\right)_i = \frac{C_{i2} - C_{i1}}{t_2 - t_1} \quad (4.2)$$

$$\left(\frac{\partial C}{\partial x}\right)_i = \frac{1}{4} \left(\frac{C_{i1} - C_{(i-1)1} + C_{i2} - C_{(i-1)2}}{x_i - x_{i-1}} + \frac{C_{(i+1)1} - C_{i1} + C_{(i+1)2} - C_{i2}}{x_{i+1} - x_i} \right) \quad (4.3)$$

$$C_i(t) = \frac{C_{i2} + C_{i1}}{2} \quad (4.4)$$

The concentration of *Chaetoceros debilis* was used to represent the quantity C_{ij} . It was chosen as it was the dominant species at all locations and its numbers were very high. The indices i and j are used to denote location and time respectively. For locations, i was considered increasing in the positive x-direction. For example if NAN 12 were being considered then $(i + 1)$ would be NAN 15 and $(i - 1)$ NAN 10. As derivatives were calculated centred on one time interval j was 1 or 2, the beginning and end of that interval respectively. At end stations, such as NAN 10, the spatial gradient at the boundary was simply assumed to be zero.

Station 25 was used as an end point for calculations involving both inside and outside stations. For stations 10 through 25 the x-direction was east-west (positive moving out of the bay). For the outside stations 25 through 30, the x-direction was essentially northwest-southeast, increasing in the northwest direction. Note that at NAN 25 x and y terms could have been used, however it seemed that there were already a sufficient number of variables.

A range for the sum of the rates in the source and sink term ($\mu - b - z - s$) was chosen using reasonable estimates for each rate. Afterwards, the corresponding range of velocities required to satisfy equation 1.13 was calculated. Where possible, combinations of ($\mu - b - z - s$) and the velocity u were chosen to agree between stations. For example, the velocities at stations 12 and 15 were assumed to be equal because the stations were just less than 1 km apart and both were situated in a channel which is only 0.5 km wide. This assumption put another restriction on the equations. Likewise at the outside stations 27 and 30, where conditions for phytoplankton growth appeared to be similar (density profiles and Secchi disc depths agreed between the two and nutrients were high), a constant value for ($\mu - b - z - s$) was chosen.

Choice of biological rates

A reasonable range for generation times during the 1993 season was taken as (0.5-1.5) $days^{-1}$ (Parsons, Takahashi and Hargrave [22]).

For zooplankton grazing an upper limit for z was chosen using a maximum concentration of copepods and a maximum filtering rate for each animal of 200ml/day from Parsons, Takahashi and Hargrave [22]. The concentration used was 2/l as determined by LeBrasseur et al. [21] of the dominant copepod *Neocalanus plumchrus* during the spring in the Strait of Georgia. The calculated maximum rate (considering the time for 2 copepods to filter 1/e l) was 1 $days^{-1}$. A lower limit for z was assumed to be zero as for low phytoplankton concentrations zooplankton do not graze (Parsons [19]). Thus the range for z was (0-1) $days^{-1}$.

To determine b , the oyster concentration in the bay was assumed to be 30/ m^2 for the entire area of the bay. The value was chosen by observation of the shoreline and the shallows, and is hoped to represent an upper limit when used for all depths of the bay. This estimate suggests that there are 83 million oysters in Nanoose bay. Their filtering

rates were taken to be the same as that of mussels in 8.5 deg C water in Friday Harbour, (from Kine [5]). Oysters and mussels are classified in the same habitat group and have filtering rates which are of the same order of magnitude, [5]. The result was a range in b of $(0.2-0.5)days^{-1}$ within Nanoose bay. Note that the equation 1.13 requires that the oysters are being continually supplied with new water, and thus fresh phytoplankton. Given the density profiles in 1993 and the current data in 1992, this assumption seems reasonable. The upper limit of this rate suggests that the 83 million oysters in the bay could filter the entire volume of the bay in just under one week, which is within the estimated range of flushing times.

The sinking rate s was determined using Parsons, Takahashi and Hargrave [22], to be about $0.1days^{-1}$. Given the size of the other rates s was assumed to be zero for live phytoplankton. Where conditions were poor and phytoplankton were probably dying it is likely that s was larger, as dead phytoplankton sink an order of magnitude more quickly than live ones. Thus s was considered nonzero, ranging from $(0-0.1)days^{-1}$, outside the bay (where conditions for phytoplankton growth seemed to be poor) and inside towards the end of the study when nitrate became limiting.

Once a range of velocities was estimated for each location in a given interval, they were compared to those at adjacent stations, expecting them to be of the same order and direction. If the magnitude of the velocity was reasonable (also considering the time period over which it was maintained) its direction was considered. Two indicators for direction were used. For the inside station σ_{t7} at NAN 20 was used as described at the end of section 3.1. If σ_{t7} were decreasing with time (see figure 4.2) currents were expected to be into the bay. A constant or increasing σ_{t7} put no restriction on current direction. For the outside stations wind data were used. Note that the correlation between the principal component of the Ballenas wind and the v current velocity was 0.5 at 2 and 4 m. This is not a strong correlation, however it was used only to indicate direction.

The time series were investigated concentrating on times when numbers of *Chaetoceros debilis* at the outside stations increased. Because conditions for phytoplankton growth appear poor for *in situ* growth, as discussed in the previous section, advection is assumed to be responsible for the increases in phytoplankton concentrations seen there. For the inside stations special attention was paid to intervals with weak phytoplankton gradients and also to periods in which the change in C with time was close to zero. Where gradients were weak, current velocity became unimportant as the advective term was small and a direct estimate of $(\mu - b - z - s)$ could be made. Similarly where C was constant in time, one term was eliminated and advection was balanced by sources and sinks.

Application of the equation

A chronological summary of the results follows. All rates have units of days^{-1} and velocities are in km/day, (1 km/day = 1.16 cm/s).

Chaetoceros debilis was present inside the bay from the beginning of the experiment onward. The first time interval investigated was day 35-39, where information was available on both days only for the inside stations. It was found from stations 12 and 15 that a current of 0.6 km/day into the bay and total rates, $(\mu - b - z - s)$, of $+0.3 \text{ days}^{-1}$ at all stations provided a reasonable solution to the conservation equation 4.1. Assuming a growth rate μ of 0.7 days^{-1} , the sum of the sinks would be 0.4 days^{-1} , which seems reasonable expecting b to dominate and z and s to be small.

Note that NAN 30 was first sampled on day 39 and no *Chaetoceros debilis* was found in the 25 ml sample that was counted, although *C. debilis* was seen at NAN 27. On day 42 *Chaetoceros debilis* appeared at NAN 30 as well as NAN 27. For advective transport from NAN 25 a northwest current of approximately 1 km/day was necessary over the 3 day period to balance the increase in *C. debilis*. This current seems very reasonable as the wind was blowing predominantly from the southeast during this time. The total

rate $(\mu - b - z - s)$ was assumed to be zero in this case. Growth conditions were apparently poor and benthic grazing was not considered important in the Strait. Also phytoplankton concentrations were low so if zooplankton were present they were assumed not to be grazing. Note that there are no data from NAN 25 and 27 (only NAN 20 and 30) on day 42 so no comparison can be made.

The peak at NAN 25 on day 49 was investigated. The rate $(\mu - b - z - s)$ was assumed to be zero at this station as well. Using data from the inside stations a transport of 2 km/day out of the bay was necessary to balance this increase in phytoplankton given the gradient of C at the mouth of the bay. Over this time period however σ_{t7} became smaller suggesting that transport was into the bay. Using an optimistic positive growth rate of 0.5 still requires a small transport out of the bay. It appears in this case that the phytoplankton came from elsewhere, perhaps even the shallows on the south shore just outside the mouth of the bay.

The period from day 53 to 56 has small spatial gradients at the mouth of the bay. Rates were calculated from these data as they were not sensitive to changes in velocity. It appears that at stations 10 through 20 rates decreased to about $(0.1-0.2) \text{ days}^{-1}$. It is suggested that increased grazing by zooplankton at this time may be responsible.

The outside stations during the same interval and on to day 57 were investigated. On day 57 concentrations of *C. debilis* reached 670/ml. Assuming the source and sink term to be zero again, a transport rate of 0.3 km/day NW for both NAN 27 and NAN 30 was required from day 53 to 56. To account for the further increase in C at NAN 30 on day 57 a transport of 3-4 km/day would be required over one day. The later current is not excessive considering the 1992 current observations and that during the entire period the wind was blowing from the southeast. It is possible that the plankton was carried from station 25 up the Strait, although plankton at that location could easily have originated from the shallows outside Nanoose bay or elsewhere.

Later in the record total rates seemed to decrease at the inside stations. Using the interval from day 77 through 82, where again gradients were small, the total rate at NAN 10 was determined to be -0.4 days^{-1} and -0.2 days^{-1} at NAN 12 and 15. These values may be due to an increase in zooplankton and thus more intense grazing as well as a nonzero value of s as nutrients may be becoming more scarce.

Investigating the last increase in *C. debilis* observed at all of the outside stations suggests that NAN 25 was not the source of *C. debilis* in that case. Neglecting sources and sinks, a transport of -3 km/day at both NAN 27 and NAN 30 was required, which is from the opposite direction to NAN 25. For transport to occur from NAN 25 a growth rate of at least 0.6 days^{-1} would be required, which seems unlikely at this time. Likewise it appears that changes in C at NAN 25 over this period were balanced by currents going into Nanoose bay ($u = -0.1 \text{ km/day}$) as estimated from gradients at the mouth.

In summary it appears that it is possible for Nanoose bay to provide the seed phytoplankton population for the adjacent area of the Strait of Georgia at times. It is also possible that other areas may provide the seed and it is suggested that a combination is likely and seeding areas are different at different times. Terms in the conservation equation were difficult to evaluate, even with all of the assumptions, as there were many unknown variables. Also terms tend to be of the same order. Nonetheless the approximations seemed to yield reasonable values which agreed between adjacent stations, especially at the mouth of the bay where the spatial resolution was the highest. The first time *C. debilis* appeared at NAN 30 it could easily have originated from Nanoose bay, assuming that growth conditions at this time were poor in the Strait and advection was responsible.

4.3 Summary

The two seasons that were investigated were very different. In 1992 density structure was stratified with respect to 1993 with more brackish water, assumed to be the influence of the Fraser River. Net transport in 1992 was into the bay at upper and middle depths and it appears that the bay was flushed too rapidly to allow phytoplankton to bloom earlier in the season. Nutrients and light were not limiting at any time or location. In 1992 a strong phytoplankton bloom occurred in the bay and the Strait simultaneously beginning around day 65-70. Seeding was not possible in this year as transport was into the bay at the surface and middle depths and the bloom did not occur earlier in the bay than in the Strait.

In 1993 phytoplankton concentrations were appreciable in Nanoose bay from the first sampling day onward suggesting that growth conditions were good there. It appears that the bay was generally mixed to the bottom. It is suggested that phytoplankton concentrations were comparatively low in the Strait because light was limiting due to vertical mixing deeper than the critical depth. It is suggested that growth conditions at the inside stations were limited at different times by a combination of light, mixing, flushing and nitrate limitation toward the end of the study. Seeding from the bay during this season was possible although it is likely that different areas provided the seed at different times and in the absence of current measurements it is certainly not possible to be conclusive.

The differences in nature of phytoplankton growth (timing, concentrations, and species dominance at all locations) between both years suggests that while coastal environments are complicated they provide many different possibilities for phytoplankton blooms leading to biological diversity from year to year. In 1992 the bloom began later (day 65-70) than in 1993 apparently when phytoplankton growth conditions became favourable at all

sampling locations. During this year circulation was such that the bay was flushed in a shorter time than that of phytoplankton generation. In 1993 phytoplankton concentrations and growth conditions varied between the outside and inside stations. Phytoplankton bloomed in the bay much earlier than in 1992 (day 35 onward) and concentrations were higher in the Strait than they were preceding the bloom in 1992. It is likely that *in situ* growth conditions were poor on the outside and higher counts of phytoplankton were due to advection from areas such as Nanoose bay where concentrations were very high. Also the dominant species at all locations in 1993 was *Chaetoceros debilis*, which has the ability to form resting spores (Harrison et al. [13]). It appears that excystment of *C. debilis* in the bay led to a strong bloom which subsequently influenced species composition in the Strait. Thus in 1993 it was possible that the bay and other potential seeding areas had a major influence on phytoplankton concentration and composition in the Strait while in 1992 there was no influence from one area on the other.

4.4 Suggestions for improving or continuing this experiment

If this experiment were to continue there are several additions and changes that may improve results. Daily sampling is necessary as horizontal advection can play a major role. For example, the 1992 current record suggests that the bay can be flushed in less than one day. Note that the 1993 data showed a peak in *Chaetoceros debilis* on day 57 at NAN 30 while missing a possible increase at NAN 27 as it was not sampled on that day. Also, generation times may be as short as 18 hours during the spring bloom and phytoplankton disappear rapidly under adverse conditions.

Spatial resolution is necessary. Although there was much more energy spent analyzing the 1993 results due to the increased number of stations, the spatial resolution at

the mouth of the bay proved very useful in estimates made using the conservation equation 1.13. Ranges for parameters within the equations were narrowed significantly. For the outside stations estimates were vague and more difficult. If the total rate ($\mu - b - z - s$) had not been ignored the calculations would have become even more ambiguous.

Also in this experiment only phytoplankton and chlorophyll *a* concentrations were measured. The rates in the sum of biological sources and sinks (equation 1.13) were difficult to distinguish between as the measured *C* was the result of all influences (growth and grazing etc. as well as advection). Primary productivity rate measurements provide a measure of the true standing stock and thus μ could be separated from the sink terms in the sum of all of the rates. Although primary productivity rate measurements are difficult to make in the field (Parsons, Maita and Lalli [20]) they would be very useful in an experiment of this type.

Replicates in biological data can also improve results significantly, for example the chlorophyll *a* data.

Vertical turbulent diffusion has been neglected in this problem. It is recognized that it may be important. It is suggested that vertical profiles of biological parameters be taken, especially for nutrients and species composition.

The absence of current data in the 1993 data set is unfortunate. Without them nothing can be conclusively stated from this experiment. Current measurements are expensive and time consuming. It is suggested that since Lagrangian motion is of interest in this problem, drogues would be more appropriate than current meters. One could sample daily and when the first increase in phytoplankton concentration was observed, place a drogue at that location and track its motion. Sampling could be done following the drogue as well as at the other regular locations.

Appendix A

Dominant genera in species composition

1992						
J day	NAN 10		NAN 20		NAN 30	
27	<i>Melosira</i> sp.	0.5	<i>S. costatum</i>	0.3	<i>S. costatum</i>	0.5
37	<i>Thalassiosira</i> sp.	0.8	<i>Thalassionema</i> sp.	0.2	<i>S. costatum</i>	0.7
42	<i>S. costatum</i>	5	<i>S. costatum</i>	7	<i>S. costatum</i>	6
45	<i>S. costatum</i>	16	<i>S. costatum</i>	12	<i>S. costatum</i>	2
48	<i>S. costatum</i>	39	<i>S. costatum</i>	22	<i>S. costatum</i>	2
49	<i>S. costatum</i>	48	<i>S. costatum</i>	34	<i>S. costatum</i>	3
51	<i>S. costatum</i>	36	<i>S. costatum</i>	25	<i>Corethron</i> sp.	2
56	<i>Thalassiosira</i> sp.	2	<i>S. costatum</i>	8	<i>Thalassiosira</i> sp.	0.5
59	<i>Thalassiosira</i> sp.	5	<i>S. costatum</i>	2	<i>S. costatum</i>	5
62	<i>S. costatum</i>	24	<i>S. costatum</i>	12	<i>S. costatum</i>	7
65	<i>Chaetoceros</i> sp.	0.5	<i>S. costatum</i>	1.2	<i>S. costatum</i>	17
65	<i>S. costatum</i>	1.1	<i>S. costatum</i>	2	<i>S. costatum</i>	10
69	<i>S. costatum</i>	190	<i>S. costatum</i>	258	<i>S. costatum</i>	140
70	<i>S. costatum</i>	18	<i>S. costatum</i>	76	<i>S. costatum</i>	180
75	<i>S. costatum</i>	350	<i>S. costatum</i>	325	<i>S. costatum</i>	170
79	<i>Thalassiosira</i> sp.	750	<i>S. costatum</i>	900	<i>S. costatum</i>	3000
81	<i>Thalassiosira</i> sp.	360	<i>S. costatum</i>	670	<i>S. costatum</i>	3900
100	<i>Schrooderella</i> sp.	610	<i>Chaetoceros</i> sp.	330	<i>Chaetoceros</i> sp.	15

Table A.1: Dominant genera with abundance for 1992. All numbers have units of cells/ml. Note that on day 65 samples were drawn by the Nanoose personnel as well as myself. Both samples are included for comparison.

1993								
NAN								
Julian day	5	10	12	15	20	25	27	30
35		600	450	600				
39	340	2800	1000	660	80	40	30	<0.5
42		2000			700			340
46	60	500	650	350	300	130	170	150
49	160	3800	1600	1100	2300	2400	40	100
50		1400			2000			
53	270	2100	2300	2300	2200	1200	20	35
56	65	3300	3400	2500	2400	550	300	360
57		4800			1200			670
60	60	5600	4100	2000	1500			
63	<0.5	3100	3200	1500	440	25	1	30
67	330	800	3400	2300	1500	460		
70	1	300	340	850	300	300	300	140
74	500	1300	1700	1600	1300	30	60	70
77	<0.5	2800	3500	2500	2800	2000	80	230
82	<0.5	8	140	1000	900	650	30	150
86	830	1400	2500	1500	1700	12	6	14
89	230	2200	2600	3000	1800	300	200	400
92	300	5300	4400	4200	2700	800	1100	1800
96	85	2800	4700	3600	2400	300	400	100
103**	12	3000	2400	2200	1800			540

Table A.2: Dominant genera with abundance for 1993. Numbers are of *Chaetoceros debilis* cells/ml with the exception of day 103. Note that *C. debilis* was the dominant species throughout the experiment until day 103, when *Skeletonema costatum* became dominant (** *S. costatum* cells/ml). Missing counts correspond to stations that were not sampled on that day.

Bibliography

- [1] Baker, P. 1992. Low frequency residual circulation in Knight Inlet, a fjord of coastal British Columbia., Masters Thesis, The University of British Columbia. 184 pages.
- [2] Campbell J. and Aarup T. 1989. Photosynthetically available radiation at high latitudes. *Limnology and Oceanography*, **34** 1490–1499.
- [3] Cloern, J. E. 1991. Tidal stirring and phytoplankton bloom dynamics in an estuary. *Journal of Marine Research*, **49**, 203–221.
- [4] Cloern, J. E. 1982. Does Benthos Control Phytoplankton Biomass in South San Francisco Bay? *Marine Ecology Prog. Series*, **9** 191–202.
- [5] Conover, R. J. 1978. Transformation of organic matter. Vol 4 in *Marine Ecology: A Comprehensive, Integrated Treatise on Life in Oceans and Coastal Waters*. (ed. Otto Kine). John Wiley and Sons, New York. 277–288.
- [6] Cullen, J. J. 1982. The deep Chlorophyll Maximum: Comparing Vertical Profiles of Chlorophyll *a*. *Can. J. Fish. Aquat. Sci.*, **39** 791–802.
- [7] Cupp, E. E. 1943. *Marine Plankton Diatoms of the West Coast of North America*. University of California Press, Berkeley, California. 221 pages.
- [8] Falkowski, P. G. and Owens, T.G., 1978. Effects of Light Intensity on Photosynthesis and Dark Respiration in 6 species of Marine Phytoplankton. *Marine Biology*, **45**, 289–295.
- [9] Freeland, H. J. and Farmer, D. M., 1980. Circulation and Energetics of a Deep, Strongly Stratified Inlet *Can. J. Fish. Aquat. Sci.*, **37** 1398–1410.
- [10] Godin, G. 1972. *The Analysis of Tides*. University of Toronto Press, Toronto, Canada. 264 pages.
- [11] Hansen, D. V. and Rattray, M. Jr. 1966. New dimensions in estuary classification. *Limnology and Oceanography*, **11** 319–326.
- [12] Harrison, P. J., Clifford, P. J., Cochlan, W.P., Yin K., St John, M.A., Thompson, P.A., Sibbald and Albright, L. J. 1991. Nutrient and plankton dynamics in the Fraser River Plume, Strait of Georgia, British Columbia. *Marine Ecology Progress Series*, **70** 291–304.

- [13] Harrison P. J., Fulton J. D., Taylor F. J. R. and Parsons T.R. 1983. Review of the biological oceanography of the Strait of Georgia: pelagic environment. *Can. J. Fish. Aquat. Sci.*, **40** 1064–1094.
- [14] Harrison, P. J. and Turpin D. H. 1979. Limiting nutrient patchiness and its role in phytoplankton ecology. *J. exp. mar. Biol. Ecol.*, **39** 151–166.
- [15] Jorgenson, C. B. 1966. *Biology of Suspension Feeding*. International Series of Monographs in Pure and Applied Biology, Zoology Division. Volume 27. Pergamon Press, Oxford, U.K. 357 pages.
- [16] Kollstad, T. F. and Hansen, S. E. 1985. An Investigation of the Performance of 4 Different Current Meters When Applied in the Wave Zone. In: *Advances in Underwater Technology and Offshore Engineering Vol. 4: Evaluation, Comparison and Calibration of Oceanographic Instruments*. Proceedings of an International Conference (Ocean Data). Society for Underwater Technology, London, England. 223–245.
- [17] Lawson, K. D. et al. 1983. The Development of a Spherical, Electromagnetic Current Meter. In: *Proceedings of Oceans 1983, Vol. 1 Technical Papers*. Institute of Electrical and Electronics Engineers, Piscataway, New Jersey. 187–193.
- [18] LeBlond, P. H. and Mysak, L. A. 1978. *Waves in the Ocean*. Elsevier Science Publishers B. V., Amsterdam, The Netherlands. 602 pages.
- [19] Parsons, T. R. and LeBrasseur R. J. 1970. The availability of food to different trophic levels in the marine food chain. in *Marine Food Chains*. (ed. J. H. Steele). Oliver and Boyd, Edinburgh, U. K. 325–343.
- [20] Parsons, T. R., Maita, Y. and Lalli, C. M. 1984. *A Manual of Chemical and Biological Methods for Seawater Analysis*. Pergamon Press, Oxford, U.K. 173 pages.
- [21] Parsons, T. R., Stephens K. and LeBrasseur R. J. 1969. Production studies in the Strait of Georgia. Part 1. Primary production under the Fraser River plume, February to May, 1967. *J. exp. mar. Biol. Ecol.*, **3** 51–61.
- [22] Parsons, T. R., Takahashi, M. and Hargrave B. 1973. *Biological Oceanographic Processes*. Pergamon Press, Oxford, U.K. 332 pages.
- [23] Pond, S. and Pickard, G. L. 1983. *Introductory Dynamical Oceanography*, 2nd edition. Pergamon Press, Oxford, U.K. 329 pages.
- [24] Press, W. H., Flannery, B. P., Teukolsky, S. A. and Vetterling, V. T. 1988. *Numerical Recipes in C, The Art of Scientific Computing*. Cambridge University Press. 735 pages.

- [25] Stacey, M. W., Pond, S., LeBlond, P. H., Freeland, H. J. and Farmer D. M. 1987. An Analysis of the Low-Frequency Current Fluctuations in the Strait of Georgia, from June 1984 until January 1985. *Journal of Physical Oceanography*. **17**, No. 3, 326-342.
- [26] Statistical Sciences, Inc. *S-PLUS User's Manual, Version 3.1 Supplement*, Seattle: Statistical Sciences, Inc., 1992.
- [27] Sutherland, T. and C. Leonard, 1992. A segmented pipe sampler for integrated profiling of the upper water column. *J. Plankton Res.*, (in press).
- [28] Sverdrup, H. U., 1953. On conditions for the vernal blooming of phytoplankton. *J. Cons. Explor. Mer*, **18**, 287-295.
- [29] Thompson, R. 1981. *Oceanography of the British Columbia Coast*. Canadian Special Publication of Fisheries and Aquatic Sciences **56**, Ottawa. 139-185.
- [30] de Young, B. 1986. The circulation and internal tide of Indian Arm, B. C. PhD Thesis, University of British Columbia. 175 pages.